A Study on the Influence of Asphalt Layer Temperature on TSDD-Measured Deflection Slopes and Deflections

April 2026

Publication No. FHWA-HRT-26-057

U.S. Department of Transportation
Federal Highway Administration

Research, Development, and Technology
Turner-Fairbank Highway Research Center
6300 Georgetown Pike McLean, VA 22101-2296

Turner-Fairbank
Highway Research Center

FOREWORD

Reliable assessment of pavement structural conditions is essential for effective pavement management. Traffic speed deflection devices (TSDDs) have emerged as efficient tools for network-level pavement monitoring, enabling near-continuous measurements of structural response at traffic speeds. However, asphalt concrete (AC) is temperature sensitive and variability in temperature within the AC layer of the pavement structure can significantly influence TSDD measurements, making it challenging to analyze and compare structural condition across locations and times.

To overcome this challenge, the research team developed practical temperature adjustment models for deflection and deflection slope data collected along the midline of dual tires under moving loads—a configuration used by many TSDDs. The research team developed the models through an extensive simulation effort comprising more than 250,000 synthetic cases, covering a wide range of pavement structures based on the Federal Highway Administration's (FHWA) Long-Term Pavement Performance (LTPP) database. These models were then validated using field data. The team utilized advanced viscoelastic modeling techniques to accurately capture the effects of temperature across various structural configurations.

The resulting models offer a scalable, device-independent framework for normalizing TSDD data across various temperature conditions. Although validation was performed using data from a single type of TSDD, the traffic speed deflectometer (TSD), the development of the models did not depend on any device-specific characteristics. As a result, these models are broadly applicable to any TSDD that measures the midline deflection or slope under dual-tire moving loads.

The research team expects these models to assist transportation agencies, researchers, and practitioners in more effectively utilizing TSDD technologies to inform pavement management decisions, improve maintenance planning, and enhance network-level performance. Additionally, highway data collection service providers and consultants involved in pavement structural assessment and analysis may find this information valuable.

Jean Nehme, Ph.D., P.E.
Director, FHWA Office of Infrastructure
Research and Development

Notice

This document is disseminated under the sponsorship of the U.S. Department of Transportation (USDOT) in the interest of information exchange. The U.S. Government assumes no liability for the use of the information contained in this document.

The U.S. Government does not endorse products or manufacturers. Trademarks or manufacturers' names appear in this report only because they are considered essential to the objective of the document.

Non-Binding Contents

Except for the statutes and regulations cited, the contents of this document do not have the force and effect of law and are not meant to bind the States or the public in any way. This document is intended only to provide information regarding existing requirements under the law or agency policies.

Quality Assurance Statement

The Federal Highway Administration (FHWA) provides high-quality information to serve Government, industry, and the public in a manner that promotes public understanding. Standards and policies are used to ensure and maximize the quality, objectivity, utility, and integrity of its information. FHWA periodically reviews quality issues and adjusts its programs and processes to ensure continuous quality improvement.

Disclaimer for Product Names and Manufacturers

The U.S. Government does not endorse products or manufacturers. Trademarks or manufacturers' names appear in this document only because they are considered essential to the objective of the document. They are included for informational purposes only and are not intended to reflect a preference, approval, or endorsement of any one product or entity.

TECHNICAL REPORT DOCUMENTATION PAGE

1. Report No. FHWA-HRT-26-057	2. Government Accession No.	3. Recipient's Catalog No.	
4. Title and Subtitle A Study on the Influence of Asphalt Layer Temperature on TSDD-Measured Deflection Slopes and Deflections		5. Report Date April 2026	
		6. Performing Organization Code:	
7. Author(s) Mahdi Nasimifar (ORCID: 0000-0002-3604-3681) and Atish Nadkarni (ORCID: 0000-0002-7931-1965)		8. Performing Organization Report No.	
9. Performing Organization Name and Address Engineering & Software Consultants, LLC. 11921 Freedom Drive, Suite 550 Reston, VA 20190		10. Work Unit No.	
		11. Contract or Grant No. 693JJ324D000006	
12. Sponsoring Agency Name and Address Office of Infrastructure Research and Development Federal Highway Administration 6300 Georgetown Pike McLean, VA 22101-2296		13. Type of Report and Period Covered Final report; August 2023—November 2024	
		14. Sponsoring Agency Code HRDI-1	
15. Supplementary Notes The contracting officer's representative was Nadarajah Sivaneswaran (ORCID: 0000-0003-0287-664).			

16. Abstract

Pavement condition assessment is crucial for devising effective maintenance strategies. Traffic speed deflection devices (TSDDs) are increasingly being adopted worldwide for collecting pavement structural data at traffic speed. However, the temperature of the asphalt concrete layer during measurements can significantly affect TSDD readings, necessitating temperature adjustment for proper data interpretation. While previous research has addressed temperature adjustments for certain deflection-based indices, such as the surface curvature index obtained from specific devices such as the traffic speed deflectometer (TSD), many other deflection and deflection slope parameters remain unexplored. This study addresses that gap by investigating the effect of temperature on deflections and deflection slopes collected along the midline of dual tires under a moving load. The methodology involves creating a comprehensive dataset through simulated TSDD measurements across a range of pavement structures and temperatures. For this study, the research team used the Long-Term Pavement Performance database to develop a range of representative pavement structures and analyzed more than 250,000 unique cases under simulated TSDD moving load in various temperatures. The researchers then used the database to study the temperature influence zones and develop temperature adjustment models for measured deflection slopes and deflections. Importantly, while the model development was independent of any particular TSDD device, the team evaluated the developed models with the collected field data from a TSD, due to its wide availability and adoption. However, the developed temperature adjustment models are generally applicable to any TSDD that collects midline deflection or slope data from dual tire loading while moving. Additionally, the researchers included an open-source script to automate the adjustment process for practical implementation.

17. Key Words TSDD, deflection slopes, deflection, temperature adjustment	18. Distribution Statement No restrictions. This document is available to the public through the National Technical Information Service, Springfield, VA 22161. https://www.ntis.gov

19. Security Classif. (of this report) Unclassified	20. Security Classif. (of this page) Unclassified	21. No. of Pages 99	22. Price N/A

Form DOT F 1700.7 (8-72) Reproduction of completed page authorized.

SI* (MODERN METRIC) CONVERSION FACTORS

APPROXIMATE CONVERSIONS TO SI UNITS

Symbol	When You Know	Multiply By	To Find	Symbol
		LENGTH		
in	inches	25.4	millimeters	mm
ft	feet	0.305	meters	m
yd	yards	0.914	meters	m
mi	miles	1.61	kilometers	km
		AREA		
in^2	square inches	645.2	square millimeters	mm^2
ft^2	square feet	0.093	square meters	m^2
yd^2	square yard	0.836	square meters	m^2
ac	acres	0.405	hectares	ha
mi^2	square miles	2.59	square kilometers	km^2
		VOLUME		
fl oz	fluid ounces	29.57	milliliters	mL
gal	gallons	3.785	liters	L
ft^3	cubic feet	0.028	cubic meters	m^3
yd^3	cubic yards	0.765	cubic meters	m^3
	NOTE: volumes greater than 1,000 L shall be shown in m^3			
		MASS		
oz	ounces	28.35	grams	g
lb	pounds	0.454	kilograms	kg
T	short tons (2,000 lb)	0.907	megagrams (or "metric ton")	Mg (or "t")
		TEMPERATURE (exact degrees)		
°F	Fahrenheit	5 (F-32)/9 or (F-32)/1.8	Celsius	°C
		ILLUMINATION		
fc	foot-candles	10.76	lux	lx
fl	foot-Lamberts	3.426	$candela/m^2$	cd/m^2
		FORCE and PRESSURE or STRESS		
lbf	poundforce	4.45	newtons	N
lbf/in^2	poundforce per square inch	6.89	kilopascals	kPa

APPROXIMATE CONVERSIONS FROM SI UNITS

Symbol	When You Know	Multiply By	To Find	Symbol
		LENGTH		
mm	millimeters	0.039	inches	in
m	meters	3.28	feet	ft
m	meters	1.09	yards	yd
km	kilometers	0.621	miles	mi
		AREA		
mm^2	square millimeters	0.0016	square inches	in^2
m^2	square meters	10.764	square feet	ft^2
m^2	square meters	1.195	square yards	yd^2
ha	hectares	2.47	acres	ac
km^2	square kilometers	0.386	square miles	mi^2
		VOLUME		
mL	milliliters	0.034	fluid ounces	fl oz
L	liters	0.264	gallons	gal
m^3	cubic meters	35.314	cubic feet	ft^3
m^3	cubic meters	1.307	cubic yards	yd^3
		MASS		
g	grams	0.035	ounces	oz
kg	kilograms	2.202	pounds	lb
Mg (or "t")	megagrams (or "metric ton")	1.103	short tons (2,000 lb)	T
		TEMPERATURE (exact degrees)		
°C	Celsius	1.8C+32	Fahrenheit	°F
		ILLUMINATION		
lx	lux	0.0929	foot-candles	fc
cd/m^2	candela/m2	0.2919	foot-Lamberts	fl
		FORCE and PRESSURE or STRESS		
N	newtons	2.225	poundforce	lbf
kPa	kilopascals	0.145	poundforce per square inch	lbf/in^2

*SI is the symbol for International System of Units. Appropriate rounding should be made to comply with Section 4 of ASTM E380. (Revised March 2003)

TABLE OF CONTENTS

LIST OF FIGURES

LIST OF TABLES

LIST OF ABBREVIATIONS

AASHTO	American Association of State Highway Transportation Officials
AC	asphalt concrete
FHWA	Federal Highway Administration
FWD	falling weight deflectometer
GPR	ground-penetrating radar
GUI	graphical user interface
IQR	interquartile range
LTPP	Long-Term Pavement Performance
Q1	first quartile
Q3	third quartile
RMSE	root mean square error
SCI	surface curvature index
TSDD	traffic speed deflection device
TSD	traffic speed deflectometer

EXECUTIVE SUMMARY

Pavement condition assessment is crucial for devising effective maintenance strategies. Traffic speed deflection devices (TSDDs) are increasingly being adopted worldwide for collecting pavement structural data at traffic speed. However, the temperature of the asphalt concrete layer during measurements can significantly affect TSDD readings, necessitating temperature adjustment for proper data interpretation. While previous research has addressed temperature adjustments for certain deflection-based indices, such as the surface curvature index obtained from specific devices such as the traffic speed deflectometer (TSD), many other deflection and deflection slope parameters remain unexplored. This study addresses that gap by investigating the effect of temperature on deflections and deflection slopes collected along the midline of dual tires under a moving load. The methodology involves creating a comprehensive dataset through simulated TSDD measurements across a range of pavement structures and temperatures. For this study, the research team used the Long-Term Pavement Performance database (FHWA. n.d.) to develop a range of representative pavement structures and analyze more than 250,000 unique cases under simulated TSDD moving load in various temperatures. The researchers then used the database to study the temperature influence zones and develop temperature adjustment models for measured deflection slopes and deflections. Importantly, while the model development was independent of any particular TSDD device, the team evaluated the developed models with the collected field data from a TSD, due to its wide availability and adoption. However, the developed temperature adjustment models are generally applicable to any TSDD that collects midline deflection or slope data from dual tire loading while moving. Additionally, the researchers included a Python® script to automate the adjustment process for practical implementation.

CHAPTER 1. INTRODUCTION

BACKGROUND

Assessing an in-service pavement's structural condition is crucial for determining effective pavement maintenance strategies. Typically, structural condition is evaluated by interpreting pavement responses under a stationary loading from nondestructive testing devices, such as the falling weight deflectometer (FWD), at the project level. The use of moving deflectometers that can measure pavement responses at traffic speed—collectively referred to as traffic speed deflection devices (TSDDs), including the traffic speed deflectometer (TSD)—is growing worldwide. Leveraging TSDDs facilitates the integration of structural data into network-level pavement management. This integration enables the effective planning of maintenance and rehabilitation strategies. Such optimization enhances fund allocation efficacy and strengthens network performance by enabling timely interventions through proactive maintenance. As a result, asset lifespans are prolonged, and costly reactive actions are mitigated.

Pavement surface deflections and deflection slopes are key structural response measurements collected by TSDDs under moving loads. Among the various TSDDs in use, the TSD is one of the most widely implemented and documented devices. The TSD is equipped with multiple Doppler lasers mounted on a beam, which allows for the measurement of surface vertical deflection velocities, and reports at intervals as low as several centimeters using the Doppler effect. These sensors are positioned both in front of and behind the center of the dual tires on the rear axle. TSD data include Doppler laser deflection velocity; deflection slopes (calculated by dividing the deflection velocity at each measurement point by the device's instantaneous speed); vehicle speed; and strain gauge load measurements illustrating instantaneous dynamic load, air temperature, and asphalt pavement surface temperature. Surface deflections are not directly measured but are instead calculated and reported by applying a deflection algorithm to the measured deflection slopes.

In flexible pavements, the stiffness or modulus of the asphalt concrete (AC) layer is significantly influenced by temperature. Consequently, pavement responses obtained from TSDDs—such as measured deflection slopes and deflections—are also affected by temperature variations. Temperature within the AC layer fluctuates with factors such as surface temperature, time of day, and average air temperature from the previous day (Lukanen, Stubstad, and Briggs 2000). In practical terms, the temperature at the middepth of the AC layer usually serves as the temperature for AC modulus estimation. To ensure consistency and comparability of measurements across a network and over time, adjusting the measurements to reflect those readings obtained at a reference middepth temperature is essential.

Nasimifar et al. (2020) previously developed a temperature adjustment factor for one of the most commonly used TSD deflection indices, the surface curvature index (SCI). SCI is defined as the difference between D_0 and D_{300}, the deflection at a distance of 300 mm from center point of the applied load. Some researchers have also used the temperature models in the American Association of State Highway Transportation Officials (AASHTO) *Guide for Design of Pavement Structures* (AASHTO 1993), which was originally developed for use with the maximum deflection at the center of the FWD loading plate (D_{0_FWD}), to adjust the reported D_0

deflection from TSDD data. However, to the research team's knowledge, no studies regarding the temperature adjustment of deflection slopes or the temperature normalization of other TSDD-reported deflections have been conducted. Therefore, developing temperature adjustment factors for deflection slopes as well as calculated deflections is essential to fully benefit from using TSDDs for pavement management.

OBJECTIVE

The primary objective of this study is to investigate the effect of AC layer temperature on pavement deflection slopes and deflections obtained from TSDD measurements. The study aims to determine the temperature influence zones for deflection slopes and deflections. Additionally, the goal is to develop temperature adjustment factors for all temperature-affected deflection slopes and deflections collected by TSDDs, to enable adjustments of these measurements to a reference middepth AC layer temperature.

METHODOLOGY

Empirical models, which rely on field studies or laboratory experiments, are common in pavement engineering. They are generally easier to develop than mechanistic models because empirical models are derived from fitting experimental data and simplify complex systems. However, they are also limited to the representativeness of the data used to develop them. To develop empirical models for temperature adjustment of TSDD measurements, reliable experimental data covering a range of pavement structures and measurement temperatures must be available. These data should include TSDD measurements at various pavement layer temperatures on known pavement structures, encompassing different types of structures with varying layer thicknesses and properties. Currently, to the research team's knowledge, such a comprehensive dataset is not available for developing empirical models.

As a result, the research team implemented the methodology outlined in figure 1 to formulate the temperature adjustment models. They constructed a comprehensive dataset by simulating deflection and slope measurements from TSDD for actual pavement structures. For structural selection, the research team used the Long-Term Pavement Performance (LTPP) database (FHWA n.d.), targeting 408 pavement sections across 44 U.S. States and 8 Canadian provinces, where back-calculated unbound layer moduli from FWD data were available.

The study team used 6 distinct performance-graded (PG) binders (AASHTO 1998) in the analyses, estimating the dynamic moduli of AC at 5 damage levels for each binder across 21 different AC layer temperatures, ranging from 10 to 50 °C in 2 °C intervals. In total, the team created 257,040 cases, each representing a unique combination of parameters. They conducted the simulation of TSDD measurements by using ELLVA (Levenberg 2016), a viscoelastic analytical tool. The assembled database facilitated the development of temperature adjustment models for measured TSDD deflection slopes and deflections. Further details of this methodology are provided in subsequent sections.

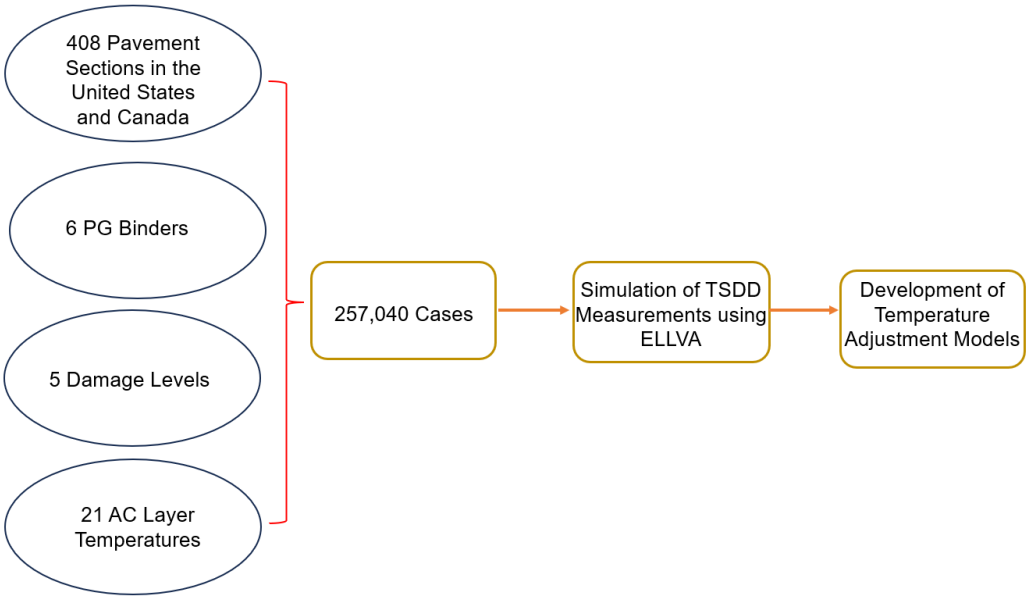

Source: FHWA.

Figure 1. Graph. Model development methodology.

CHAPTER 2. DATABASE DESCRIPTION

Developing a robust model requires a database that encompasses a wide range of pavement structures with varying material types and stiffnesses. The most effective approach to achieving this objective is by using actual pavement structure data that accurately represent real-world conditions.

SELECTION OF PAVEMENT LAYER STRUCTURES

The Federal Highway Administration's (FHWA) LTTP InfoPave™ Web portal (FHWA n.d.) provides comprehensive information on pavement structures included in LTPP studies. Among the required parameters for simulation, layer thicknesses and moduli are of particular importance. After thoroughly reviewing the available sections, the researchers selected those sections containing these two essential parameters. The research team used 408 pavement sections, spanning 44 U.S. States and 8 Canadian provinces, as depicted in figure 2, in this study. The team extracted detailed information regarding these sections from the InfoPave Web portal.

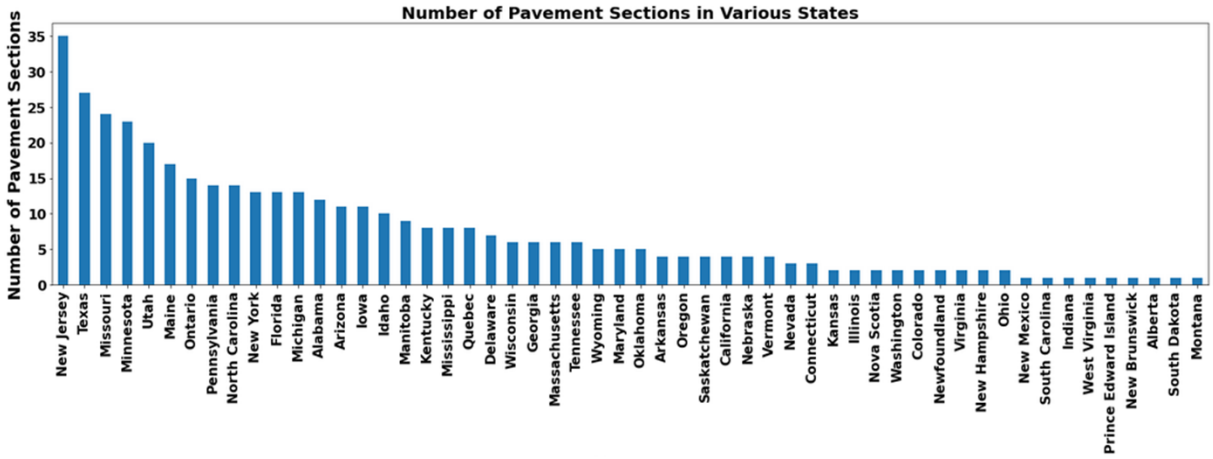

Source: FHWA.

Figure 2. Graph. Distribution of pavement sections used in database creation across U.S. States and Canadian provinces.

Layer Thickness and Underlying Layer Moduli

Out of the 408 pavement sections, 314 were constructed with a regular base, while 94 sections had a treated base. The extracted information for these sections from the LTPP database is displayed in table 1 and table 2. These tables include ranges for AC thickness, base thickness, and subbase thickness, as well as back-calculated moduli values for the base, subbase, and subgrade layers from FWD data.

Table 1. Range of layer thicknesses and unbound layer moduli for pavement sections included in the database with granular base.

Granular base (314 Sections)											
AC Thickness		Base Thickness		Subbase Thickness		Base Modulus		Subbase Modulus		Subgrade Modulus	
Range (mm)	No. Cases	Range (mm)	No. Cases	Range (mm)	No. Cases	Range (MPa)	No. Cases	Range (MPa)	No. Cases	Range (MPa)	No. Cases
25–50	10	75–125	52	0	160	40–150	95	40–150	30	35–50	2
50–100	41	125–175	72	50–150	22	150–250	95	150–250	57	50–75	38
100–150	47	175–225	54	150–250	22	250–350	68	250–350	23	75–100	58
150–200	43	225–275	52	250–350	25	350–450	25	350–450	22	100–125	57
200–250	52	275–325	41	350–450	18	450–550	18	450–550	8	125–150	53
250–300	49	325–375	6	450–550	24	550–650	9	550–650	3	150–175	42
300–350	39	375–425	23	550–650	23	650–750	1	650–750	7	175–200	24
350–400	17	425–475	5	650–750	6	750–850	1	750–850	3	200–225	19
400–450	9	475–525	4	750–850	2	850–950	1	—	—	225–250	9
>450	7	>525	5	>850	11	>950	1	—	—	>250	11

—Not applicable.
MPa = megapascal.

Table 2. Range of layer thicknesses and unbound layer moduli for pavement sections included in the database with treated base.

Treated base (94 Sections)											
AC Thickness		Base Thickness		Subbase Thickness		Base Modulus		Subbase Modulus		Subgrade Modulus	
Range (mm)	No. Cases	Range (mm)	No. Cases	Range (mm)	No. Cases	Range (MPa)	No. Cases	Range (MPa)	No. Cases	Range (MPa)	No. Cases
25–50	6	50–125	29	0	38	200–1,000	15	40–150	30	50–75	2
50–100	25	125–175	23	50–150	9	1,000–1,800	8	150–250	15	75–100	5
100–150	31	175–225	22	150–250	16	1,800–2,600	18	250–350	7	100–125	3
150–200	16	225–275	4	250–350	8	2,600–3,400	14	350–450	3	125–150	7
200–250	5	275–325	9	350–450	3	3,400–4,200	13	450–550	1	150–175	10
250–300	8	325–375	3	450–550	3	4,200–5,000	7	—	—	175–200	17
300–350	2	375–425	4	550–650	8	5,000–5,800	6	—	—	200–225	12
350–400	1	—	—	650–750	1	5,800–6,400	5	—	—	225–250	15
—	—	—	—	750–850	0	6,400–7,200	5	—	—	>250	23
—	—	—	—	>850	7	>7,200	3	—	—	—	—

—Not applicable.

Asphalt Layer Properties

AC is highly temperature dependent. Selecting appropriate asphalt properties is important for establishing a robust database for temperature adjustment model development. Given that the research team planned to conduct a viscoelastic analysis for the cases created in the database, determining the required asphalt binder properties for viscoelastic simulation was essential.

The viscosity of asphalt binder is dependent on temperature. The ASTM International viscosity–temperature relationship (ASTM International 1998) is commonly employed to determine the viscosity of the binder at the temperature of interest, as shown in figure 3.

$$loglog\eta = A + VTSlogT_R$$

Figure 3. Equation. Viscosity–temperature relationship for binders.

Where:

η = viscosity in (centipoise).
TR = temperature in Rankine.
A = regression intercept.
VTS = regression slope of viscosity–temperature susceptibility.

The dynamic shear rheometer test data, as described in AASHTO T315 (AASHTO 2012), can be used to estimate the A and VTS parameters for each type of binder. Table 3 shows the viscosity regression parameters for various asphalt binder PGs (AASHTO 1998).

Table 3. *A* and *VTS* Parameters based on asphalt PG grade (AASHTO 1998).

Asphalt Binder Grade	*A*	*VTS*	Asphalt Binder Grade	*A*	*VTS*
46–34	11.504	−3.901	64–28	10.312	−3.44
46–40	10.101	−3.393	64–34	9.461	−3.134
46–46	8.755	−2.905	64–40	8.524	−2.798
52–10*	13.386	−4.57	70–10	10.69	−3.566
52–16	13.305	−4.541	70–16*	10.641	−3.548
52–22	12.755	−4.342	70–22	10.299	−3.426
52–28	11.84	−4.012	70–28	9.715	−3.217
52–34	10.707	−3.602	70–34	8.965	−2.948
52–40	9.496	−3.164	70–40*	8.129	−2.648
52–46	8.31	−2.736	76–10	10.059	−3.331
58–10	12.316	−4.172	76–16*	10.015	−3.315
58–16	12.248	−4.147	76–22	9.715	−3.208
58–22*	11.787	−3.981	76–28	9.2	−3.024
58–28	11.01	−3.701	76–34	8.532	−2.785
58–34	10.035	−3.35	82–10	9.514	−3.128
58–40	8.976	−2.968	82–16	9.475	−3.114
64–10	11.432	−3.842	82–22	9.209	−3.019
64–16	11.375	−3.822	82–28	8.75	−2.856
64–22*	10.98	−3.68	82–34	8.151	−2.642

*Selected PG binder types for the analyses.

By using the *A* and *VTS* parameters detailed in table 3 for various PG binders, alongside the relationship presented in figure 3, the researchers delineated the viscosity–temperature susceptibility curves, as depicted in figure 4-A through figure 4-G. Binders with steeper curves exhibit higher sensitivity to temperature variations, whereas binders with flatter curves show less sensitivity. To encompass a broad range of variations while streamlining analyses and considering commonly used binder types, the research team chose the six PG binders—identified with an asterisk in table 3—for analysis. Figure 5 shows the temperature susceptibility curves for these selected binder types.

It is important to note that the viscosity parameters presented in table 3 were derived from testing data on RTFO (rolling thin-film oven) residue, which effectively represent the viscosity of a specific binder type during short-term aging in production and paving operations. Even if the type of binder is identified for a specific road section, the viscosity susceptibility parameters at the time of TSDD testing may differ from those at the time of construction. However, incorporating multiple binder types in the dataset can be advantageous for developing a more comprehensive model that encompasses the properties of various binder types, as will be further explained in this report.

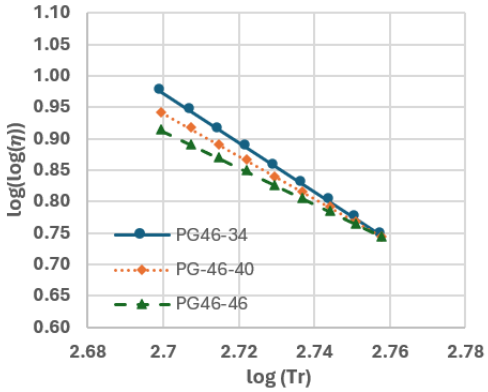

A. Temperature susceptibility curves for PG46-xx binders.

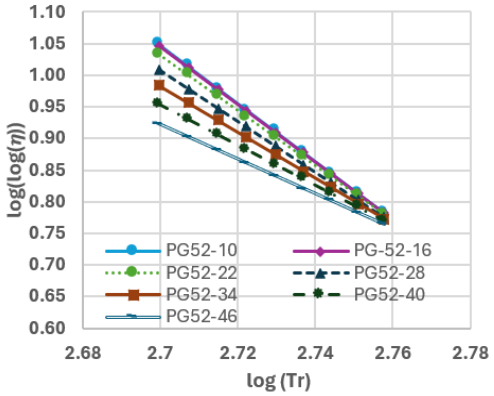

B. Temperature susceptibility curves for PG52-xx binders.

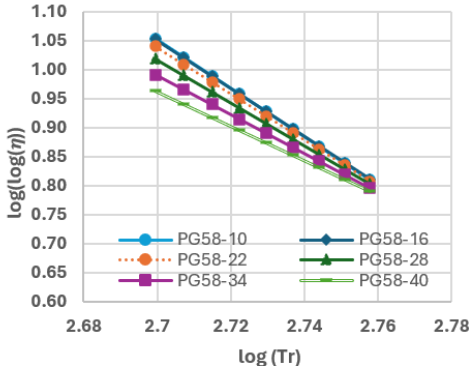

C. Temperature susceptibility curves for PG58-xx binders.

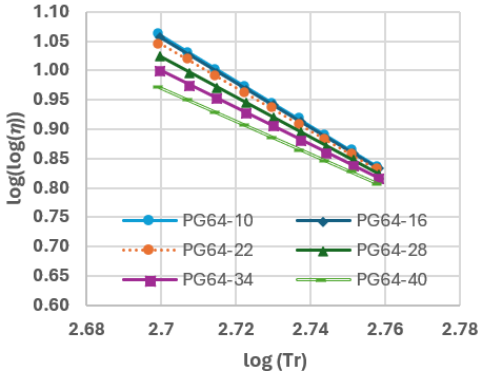

D. Temperature susceptibility curves for PG64-xx binders.

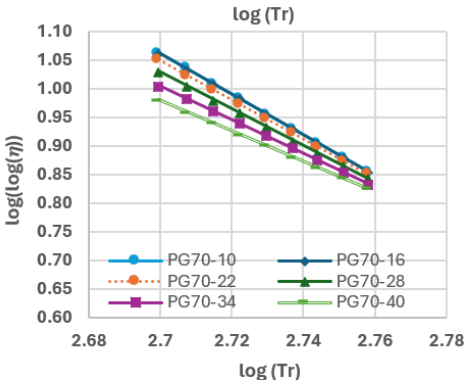

E. Temperature susceptibility curves for PG70-xx binders.

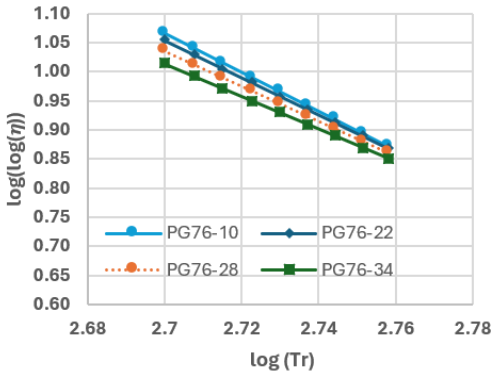

F. Temperature susceptibility curves for PG76-xx binders.

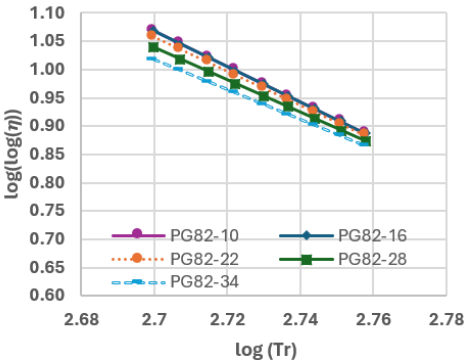

G. Temperature susceptibility curves for PG82-xx binders.

All images source: FHWA.

Figure 4. Graphs. Viscosity–temperature susceptibility curves for various PG binders.

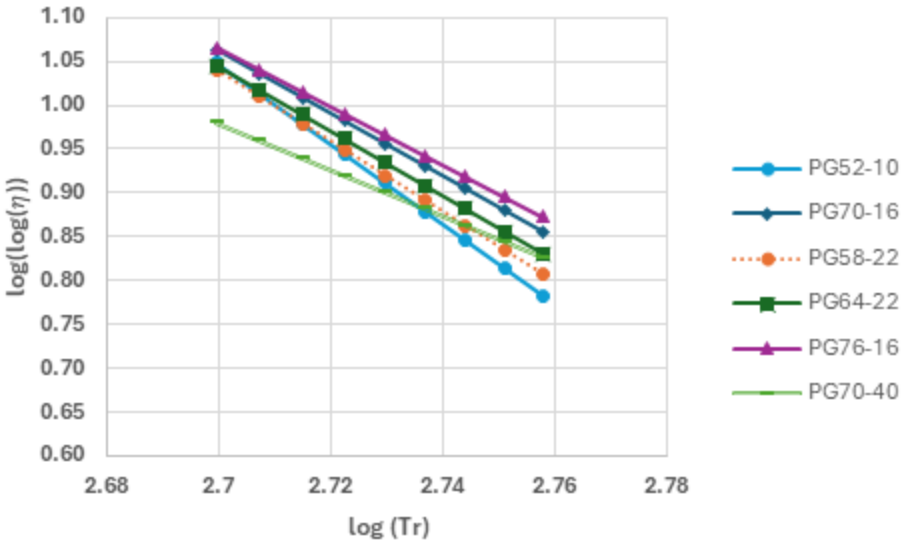

Source: FHWA.

Figure 5. Graph. Viscosity–temperature susceptibility curves for selected PG binders for analyses.

Next, for each selected binder type, the research team calculated the dynamic modulus over 21 analysis temperatures at various loading frequencies using the Witczak predictive equation (Kim et al. 2011), as depicted in figure 6.

$$\log E^* = 3.750063 + 0.02932\rho_{200} - 0.001767(\rho_{200})^2 - 0.002841\rho_4 - 0.058097V_a - 0.802208\frac{V_{beff}}{V_{beff}+V_a} + \frac{3.871977 - 0.0021\rho_4 + 0.003958(\rho_{38}) - 0.000017(\rho_{38})^2 + 0.005470\rho_{34}}{1 + e^{(-0.603313 - 0.313351\log(f) - 0.393532\log(\eta))}}$$

Figure 6. Equation. Witczak predictive formula for dynamic modulus.

Where:

E^* = dynamic modulus in psi.
η = binder viscosity in 10^6 poise (calculated for each binder type and analysis temperature).
f = loading frequency in Hz.
V_a = air void content in percentage (assumed 4 percent).
V_{beff} = effective binder content in percentage by volume (assumed 6 percent).
ρ_{34} = cumulative percentage retained on the 3/4 inch sieve (assumed 6 percent).
ρ_{38} = cumulative percentage retained on the 3/8 inch sieve (assumed 28 percent).
ρ_4 = cumulative percentage retained on the no. 4 sieve (assumed 49 percent).
ρ_{200} = percentage passing the no. 200 sieve (assumed 4 percent).

To account for the influence of damage on the dynamic modulus, the researchers adjusted the predictive undamaged dynamic moduli for five damage levels (0, 0.3, 0.6,1, and 1.5) using the figure 7 equation (Habbouche et al. 2018).

$$E_{Damaged} = 10^{\delta} + \frac{E^* - 10^{\delta}}{1 + e^{-0.3+5log\, d_{AC}}}$$

Figure 7. Equation. Damaged dynamic modulus.

Where:

$E_{Damaged}$ = damaged modulus.
E^* = predicted AC layer modulus from the predictive equation.
δ = minimum modulus taken from figure 8.
d_{AC} = fatigue damage.

$$\delta = 3.750063 + 0.02932\rho_{200} - 0.001767(\rho_{200})^2 - 0.002841\rho_4 - 0.058097V_a - 0.802208\frac{V_{beff}}{V_{beff} + V_a}$$

Figure 8. Equation. Minimum modulus from predictive formula.

Thus, the team constructed five dynamic modulus curves for each binder type at each analysis temperature. For example, figure 9 illustrates the dynamic modulus curves for PG 70-16 at 20 °C at various damage levels.

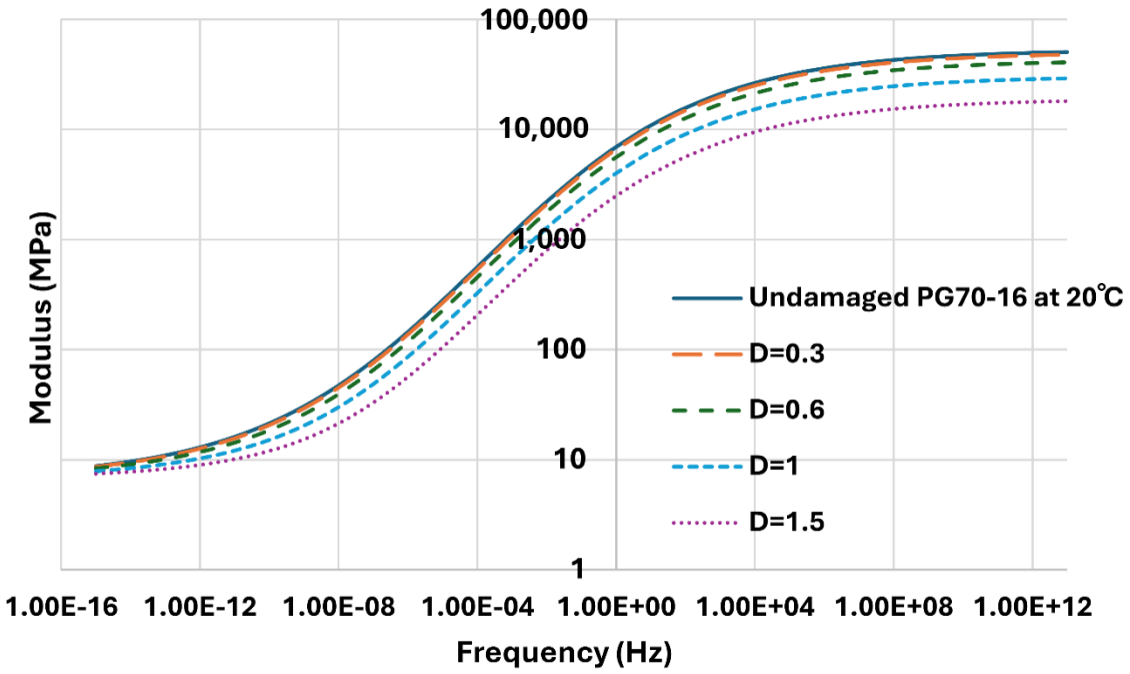

Source: FHWA.

Figure 9. Graph. Dynamic modulus curves for PG 70-16 at different damage levels at 20 °C.

The methodology involved simulating TSDD measurements on pavement structures generated from the dataset using a viscoelastic tool. Characterizing the viscoelastic behavior of asphalt material required the creep compliance parameters, as shown in figure 10 (Smith 1971).

$$D(t) = D_\infty + \frac{D_0 - D_\infty}{1 + \left(\frac{t}{\tau_D}\right)^{n_D}}$$

Figure 10. Equation. Creep compliance formula.

Where:

D_0 and D_∞ = short- and long-term compliances, respectively.
τ_D is characteristic retardation time, and n_D is shape parameter.

The previously obtained damaged dynamic modulus can be converted to creep compliance form using interconversion methods. For this purpose, the research team employed the Prony series (Park and Schapery 1999). Subsequently, the team extracted the creep compliance parameters for each binder type at every temperature and damage level for analysis purposes.

Summary of Dataset Characteristics

In the absence of a representative set of field data covering a broad range of pavement structures and testing temperatures to develop a temperature adjustment model, the research team created a comprehensive simulation of TSDD measurements on a range of representative pavement structures and temperatures. Previous sections provide detailed descriptions of selected pavement structures and asphalt layer characteristics.

Table 4 summarizes the structure of the dataset, which includes 408 unique pavement structures. Among these, 314 sections feature a regular base, while 94 sections have a treated base, sourced from the LTPP database. The analyses encompass six PG binders, representing a wide range of viscosity variations across different temperatures. The research team computed the AC moduli for the analysis cases at five damage levels. They calculated these AC moduli at 21 temperatures, ranging from 10 to 50 °C, with intervals of 2 °C. Given these parameters, the database comprises 257,040 case studies. The analysis of this dataset serves as a robust foundation for developing temperature adjustment models because it covers a wide range of pavement structures and critical parameters affecting the temperature's impact on TSDD measurements.

Table 4. The structure of the created dataset used for TSDD simulations.

Unique Pavement Structures	Asphalt Binder Types	Damage Levels	AC Layer Temperatures	Total Number of Case Studies
408 LTPP sections: 314 with a regular base 94 with a treated base	6 PG binders: PG52-10 PG58-22 PG64-22 PG70-16 PG76-16 PG70-40	5 damage levels: 0 0.3 0.6 1 1.5	21 AC layer temperatures: From 10 to 50 ℃ at intervals of 2 ℃	257,040

In the literature, a single reference temperature at the middepth of the AC layer is commonly used for temperature adjustment purposes (AASHTO 1993; Lukanen, Stubstad, and Briggs 2000). For the simulations in this study, the team assumed that the temperature gradient is uniform throughout the thickness of the AC layer, with a constant temperature representing the middepth temperature of the AC layer. The effect of the temperature gradient on the results is discussed in Appendix A.

Notably, the research team assumed that certain material properties would remain constant across all cases. These properties include the thickness of the subgrade (2,500 mm); the modulus of the bedrock (10,000 MPa); and the Poisson ratios of asphalt (0.3), base (0.35), subbase (0.4), subgrade (0.4), and bedrock (0.25).

CHAPTER 3. SIMULATION OF TSDD MEASUREMENTS IN VARIOUS AC LAYER TEMPERATURES

VISCOELASTIC SIMULATION

The goal of this phase of the study was to simulate pavement surface deflections and deflection slopes along the midline of the dual tires under a moving load—the typical response measurements collected by TSDDs. These simulated responses formed the foundation for developing temperature adjustment models. To perform these simulations, the research team used the ELLVA viscoelastic tool. Developed as a spreadsheet software, ELLVA provides an analytical model capable of computing pavement responses, including stresses, strains, and displacements, for layered viscoelastic half-spaces under a moving load with constant speed (Levenberg 2013). In this model, the asphalt mixtures in the surface layer are represented as viscoelastic materials, characterized by their creep compliance, while the unbound layers are treated as elastic materials. Figure 11 shows a snapshot of this tool. Levenberg (2016) verified the model's accuracy by comparing the computed pavement responses with those derived from a benchmark solution for a traveling load on a homogenous isotropic viscoelastic half-space.

To conduct analyses, inputs are required for three main sections: system, loading, and response. In the system section, essential data such as layer thicknesses and viscoelastic creep compliance are entered for each case in the dataset. The research team used consistent loading parameters throughout the analyses, including a loading stress of 0.8 MPa, a loading area radius of 89.2 mm, and a constant speed of 16,666.7 mm/s (60 kph).

To simulate deflection and deflection slope responses consistent with typical TSDD measurements, the researchers defined the evaluation point at the midline of the dual tires, where pavement surface deflection responses are commonly recorded. For this study, the spacing of the dual tires was based on the standard configuration, with $y = 171.45$ mm representing the lateral midpoint between the tires, and $z = 0$ representing the pavement surface. Because the ELLVA tool models the effect of a single circular load, the team applied the principle of superposition to calculate the response from dual tires by doubling the computed values. Since deflection slopes represent the first derivative of deflections in the distance domain, the research team used a Python® script to calculate them individually for each analysis case. Figure 12 provides a clear depiction, showcasing the calculated asymmetric surface deflections under TSDD load using ELLVA, alongside estimated deflection slopes derived from the first derivative of the deflection curve.

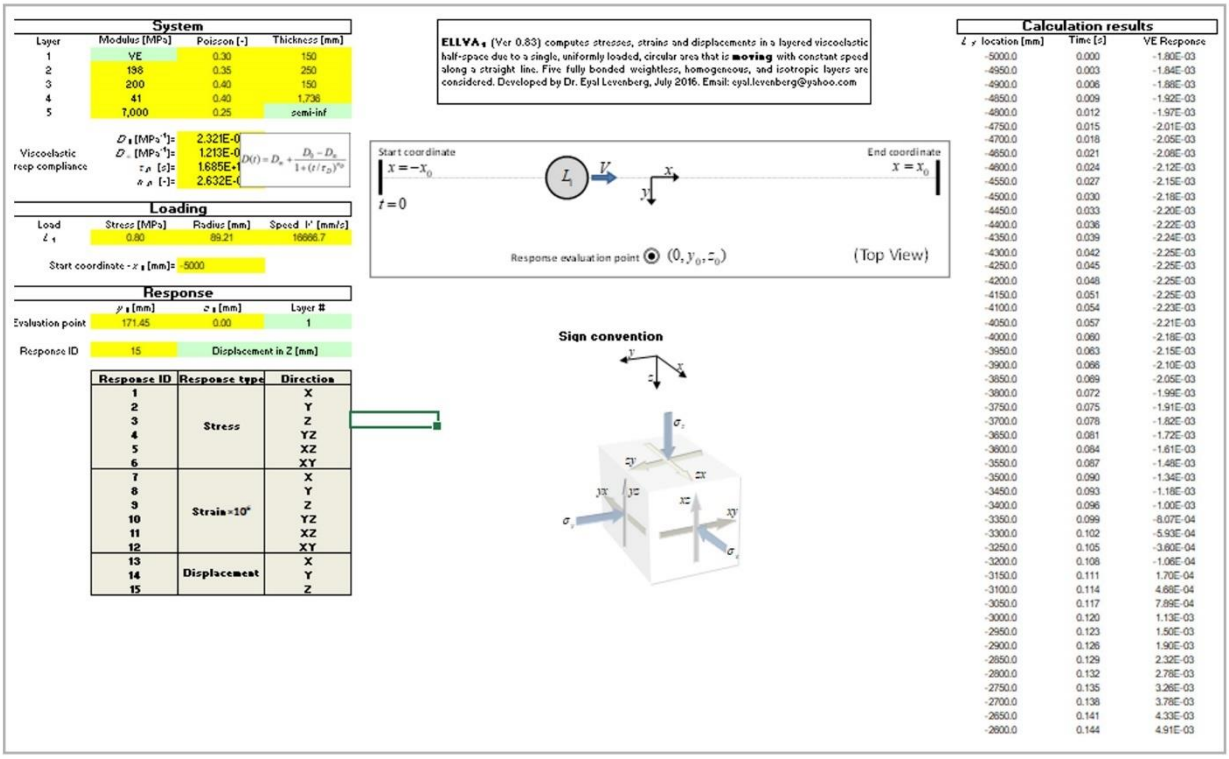

Source: FHWA.
ID = identification.

Figure 11. Screenshot. ELLVA program interface.

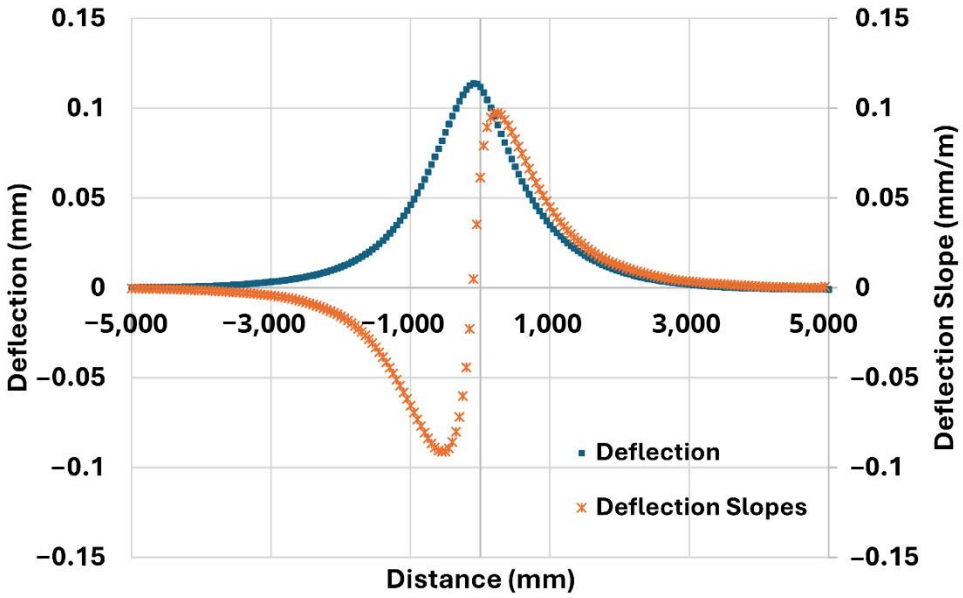

Source: FHWA.

Figure 12. Graph. Calculated TSDD surface deflections in one analysis case using ELLVA alongside extracted deflection slopes from the first derivative of the deflection curve.

CHARACTERIZATION OF DEFLECTION SLOPES AND DEFLECTION BOWLS IN THE DATABASE

The researchers extracted 257,040 asymmetric deflection bowls under TSDD loading from the ELLVA analyses. Subsequently, they calculated the deflection slope curves for these bowls and incorporated them into the simulated TSDD measurement database. Figure 13-A through figure 13-E illustrate deflection bowls at 5 distinct AC layer temperatures: 10, 20, 30, 40, and 50 °C, respectively, with each comprising 12,240 cases. The team conducted similar analyses for other AC layer temperatures. Generally, with increasing temperatures, deflection bowls tend to become thinner and taller due to the softer AC layer stiffness.

Table 5 presents the average vertical surface deflections at various distances for the five AC layer temperatures within the simulated TSDD database. While these values represent averages and may not fully reflect the actual sensitivity to temperature variations, they do reveal discernible trends. Notably, deflections closer to the center of the dual tires show an apparent increase with rising temperatures, whereas deflections farther from the load exhibit less sensitivity to temperature variations. The research team observed similar trends in the calculated deflection slope curves at these five AC layer temperatures, as illustrated in figure 14-A though figure 14-E and table 6. A detailed analysis of the impact of temperature on deflection bowls and deflection slope curves is presented in the following section.

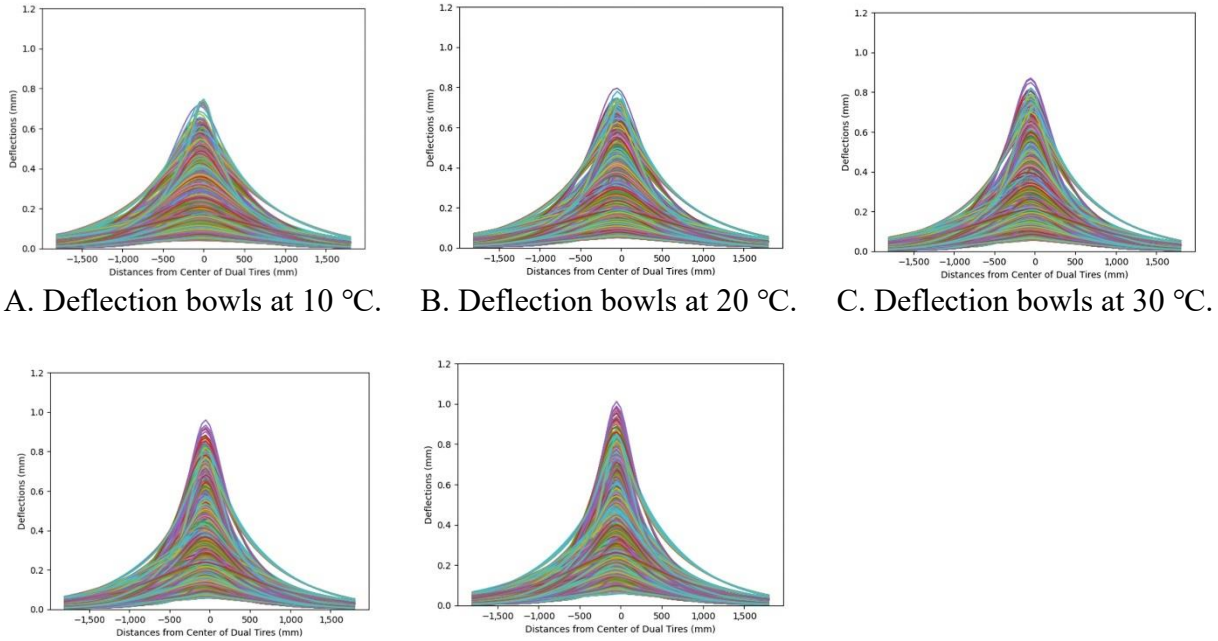

A. Deflection bowls at 10 °C. B. Deflection bowls at 20 °C. C. Deflection bowls at 30 °C.

D. Deflection bowls at 40 °C. E. Deflection bowls at 50 °C.

All images source: FHWA.
Note: Each subplot includes 12,240 deflection bowls.

Figure 13. Graphs. Deflection bowls included in the TSDD simulated database for five AC layer temperatures.

Table 5. Average vertical surface deflections at various distances for five AC layer temperatures in a simulated TSDD database.

Vertical Surface Deflections at Various Distances (mm)	AC Layer Temperature				
	10 ℃	20 ℃	30 ℃	40 ℃	50 ℃
$D_{-1,800}$	0.02026	0.01917	0.01774	0.01679	0.01653
$D_{-1,200}$	0.04458	0.04479	0.04337	0.04177	0.04091
D_{-900}	0.06569	0.06861	0.06887	0.06791	0.06713
D_{-600}	0.09618	0.10503	0.11062	0.11342	0.11488
D_{-300}	0.13801	0.15796	0.17674	0.19262	0.20550
D_0	0.16572	0.19226	0.22132	0.25024	0.27767
D_{300}	0.12218	0.13455	0.14605	0.15519	0.16171
D_{600}	0.08178	0.08621	0.08941	0.09118	0.09194
D_{900}	0.05461	0.05561	0.05584	0.05554	0.05508
$D_{1,200}$	0.03643	0.03603	0.03531	0.03453	0.03391
$D_{1,500}$	0.02419	0.02336	0.02250	0.02179	0.02129
$D_{1,800}$	0.01583	0.01493	0.01416	0.01358	0.01320

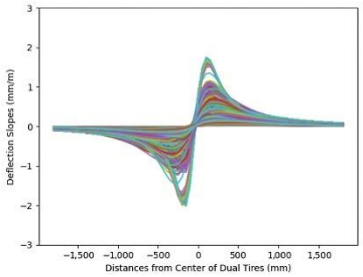

A. Deflection slopes at 10 ℃.

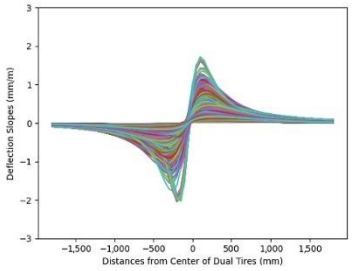

B. Deflection slopes at 20 ℃.

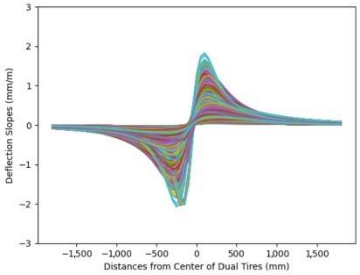

C. Deflection slopes at 30 ℃.

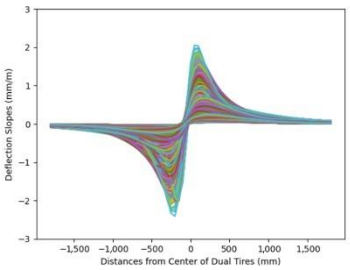

D. Deflection slopes at 40 ℃.

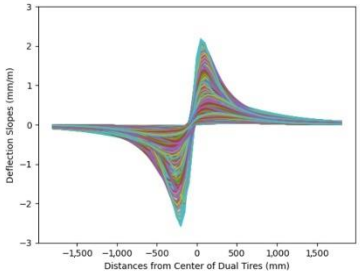

E. Deflection slopes at 50 ℃.

All images source: FHWA.
Note: Each subplot includes 12,240 deflection slope.

Figure 14.Graphs. Deflection slopes included in the TSDD simulated database for five AC layer temperatures.

Table 6. Average vertical surface deflection slopes at various distances for five AC layer temperatures in a simulated TSDD database.

Deflection Slopes at Various Distances (mm/m)	AC Layer Temperature				
	10 °C	20 °C	30 °C	40 °C	50 °C
$S_{-1,800}$	−0.02804	−0.02833	−0.02733	−0.02613	−0.02541
$S_{-1,200}$	−0.05987	−0.06600	−0.06894	−0.06927	−0.06859
S_{-900}	−0.08697	−0.10107	−0.11194	−0.11806	−0.12069
S_{-600}	−0.12385	−0.15299	−0.18355	−0.20941	−0.22834
S_{-300}	−0.15284	−0.19856	−0.26099	−0.33376	−0.40935
S_0	0.08450	0.12806	0.18512	0.25619	0.34147
S_{300}	0.15583	0.19159	0.23150	0.26973	0.30215
S_{600}	0.10652	0.12249	0.13719	0.14828	0.15542
S_{900}	0.07104	0.07769	0.08266	0.08551	0.08680
$S_{1,200}$	0.04774	0.05010	0.05129	0.05149	0.05128
$S_{1,500}$	0.03244	0.03300	0.03289	0.03244	0.03199
$S_{1,800}$	0.02225	0.02208	0.02161	0.02113	0.02079

CHAPTER 4. DETERMINATION OF TEMPERATURE INFLUENCE ZONE OF TSDD MEASUREMENTS

Temperature directly affects the properties of the asphalt layer, consequently impacting its response to moving loads and resulting in alterations in the shape and magnitude of deflection bowls and slopes. Asphalt layer properties are known to influence deflections near the loading area, but to the research team's knowledge, a comprehensive evaluation of the temperature's influence zone on deflection bowls and slopes remains unexplored in existing literature.

DEFINITION OF TEMPERATURE ADJUSTMENT FACTORS

To delineate the temperature influence zone, the researchers extracted the deflections and deflection slopes for all cases analyzed. Subsequently, they calculated the temperature adjustment factors for each of these parameters by using the equations shown in figure 15 and figure 16.

$$\lambda_d = \frac{D_{d_{Ref-T}}}{D_{d_T}}$$

Figure 15. Equation. Definition of deflection temperature adjustment factor.

Where:

λ_d = deflection temperature adjustment factor for the deflection at distance "*d*" from the center of the dual tire.

$D_{d_{Ref-T}}$ = deflection at distance "*d*" from the center of the dual tire at the reference temperature (e.g., 20 °C).

D_{d_T} = deflection at distance "*d*" from the center of the dual tire at the AC layer temperature used for each case.

$$\delta_d = \frac{S_{d_{Ref-T}}}{S_{d_T}}$$

Figure 16. Equation. Definition of deflection slope temperature adjustment factor.

Where:

δ_d = deflection slope temperature adjustment factor for the deflection slope at distance "*d*" from the center of the dual tire.

$S_{d_{Ref-T}}$ = deflection slope at distance "*d*" from the center of the dual tire at the reference temperature (e.g., 20 °C).

S_{d_T} = deflection slope at distance "*d*" from the center of the dual tire at the AC layer temperature used for each case.

The research team set the reference temperature at 20 ℃ in this study; however, the results remain independent of the selected reference temperatures. To compute deflection and deflection slope temperature adjustment factors, the researchers initially categorized the analysis cases based on unique input parameters, such as pavement layer thicknesses, modulus, PG binder, and damage level at the selected reference temperature, resulting in a total of 12,240 cases. Then, they derived adjustment factors for all analysis cases by using the aforementioned equations.

TEMPERATURE INFLUENCE ZONE FOR TSDD DEFLECTION BOWLS

Delineating the influence zones where responses are highly sensitive to temperature fluctuations is essential. Considering asphalt rheology, asphalt stiffness decreases with increasing AC layer temperatures and conversely increases with decreasing temperatures. While exceptions may exist within the dataset, generally, adjustment factors for deflection and deflection slopes, governed by asphalt properties, tend to be greater than 1.0 when the AC layer temperature is lower than the chosen reference temperature, and they tend to be less than 1.0 when the temperatures exceeds the reference temperature. Thus, to provide clarity, the distribution of adjustment factors is presented separately for cases with AC layer temperatures below and above the reference temperature (in this study, set at 20 ℃).

Variation of Temperature Adjustment Factors for Deflections

Figure 17-A through figure 17-E and figure 18-A through figure 18-E illustrate the distributions of deflection adjustment factors for cases with AC layer temperatures above and below the reference temperature (20 ℃), respectively. These figures present separate plots representing various ranges of AC layer thickness.

The distribution of analysis cases across different ranges of AC thickness is as follows:

- AC thicknesses between 25 and 100 mm: 51,660 cases.
- AC thicknesses between 100 and 200 mm: 86,310 cases.
- AC thicknesses between 200 and 300 mm: 71,820 cases.
- AC thicknesses between 300 and 400 mm: 37,170 cases.
- AC thicknesses between 400 and 500 mm: 9,450 cases.

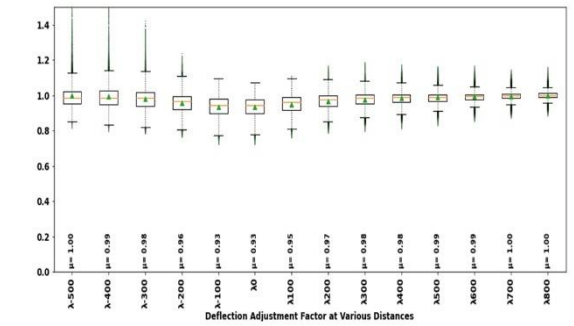

A. AC thicknesses between 25 and 100 mm.

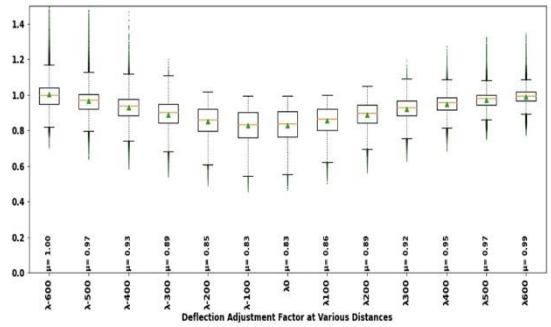

B. AC thicknesses between 100 and 200 mm.

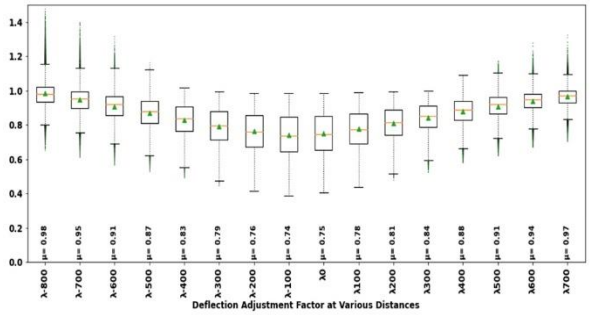

C. AC thicknesses between 200 and 300 mm.

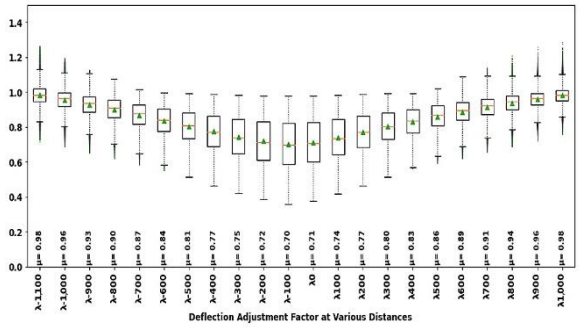

D. AC thicknesses between 300 and 400 mm.

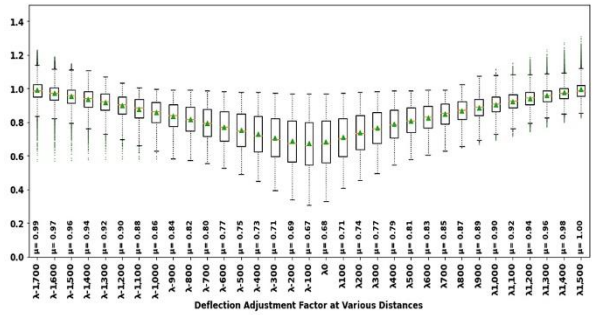

E. AC thicknesses between 400 and 500 mm.

All images source: FHWA.

Figure 17. Graphs. Deflection adjustment factor distributions for cases with AC layer temperatures higher than 20 °C for various AC layer thicknesses.

Given the significant influence of AC layer thickness on the contribution of the asphalt layer to both deflection and deflection slope, the temperature influence zone varies across these different thickness ranges.

The research team used box-and-whisker plots to visually represent the distribution of deflection adjustment factors within the database. The box signifies the interquartile range (IQR), spanning from the first quartile (Q1) to the third quartile (Q3) of the dataset, thereby encompassing the middle 50 percent of the data. Within the box, a line denotes the median of the data.

Additionally, the mean (μ) of the data is displayed on the plot. The whiskers extend from the edges of the box, indicating the variability of the data outside the upper (Q3) and lower (Q1) quartiles. These whiskers extend to 1.5 times the IQR from the edges of the box. Any data points lying beyond the whiskers are considered outliers, signifying data points that are unusually high or low compared with the rest of the dataset.

Taller box plots indicate larger IQRs, suggesting heightened variability to temperature changes within the dataset. Since the researchers separated the temperature adjustment factors for temperatures below or above the reference values, a mean value close to 1 represents diminished sensitivity to temperature variations at those specific distances.

The plots extend up to distances where adjustment factors reach a mean value of 1, delineating the temperature's influence zone on deflection. While some cases may exist where adjustment factors at distances beyond those shown here exhibit temperature sensitivity, the zones depicted in the figures generally represent a higher likelihood of temperature influence zones on deflection bowls in the analysis cases.

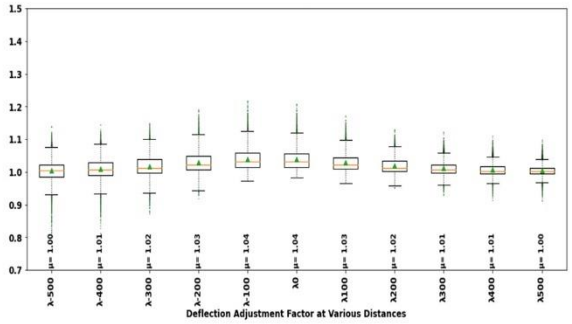

A. AC thicknesses between 25 and 100 mm.

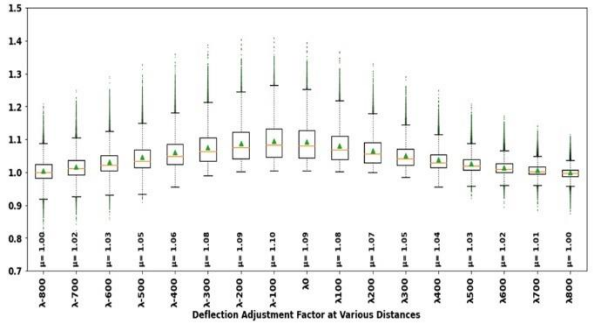

B. AC thicknesses between 100 and 200 mm.

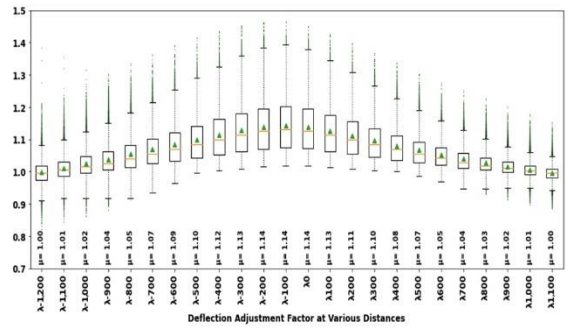

C. AC thicknesses between 200 and 300 mm.

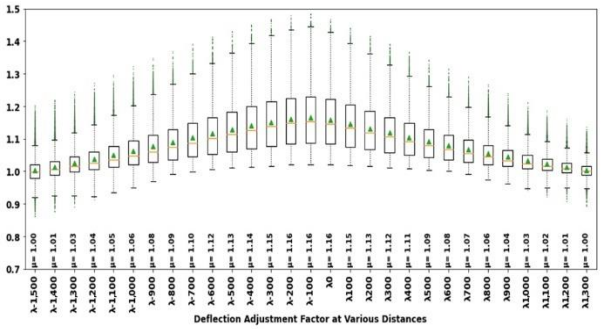

D. AC thicknesses between 300 and 400 mm.

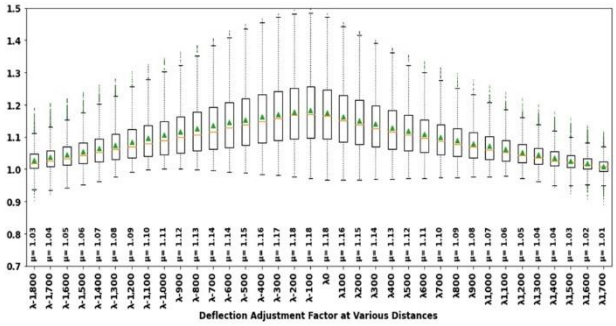

E. AC thicknesses between 400 and 500 mm.

All images source: FHWA.

Figure 18. Graphs. Deflection adjustment factor distributions for cases with AC layer temperatures lower than 20 °C for various AC layer thicknesses.

The research team derived the following observations from figure 17 and figure 18:

- Within the dataset, as the AC layer thickness increases, the box plots become taller, indicating a greater variability of deflection temperature adjustment factor values within the IQR.

- The mean values of deflection temperature adjustment factors, representing the central tendency of the data, vary with AC layer thicknesses. For instance, focusing on the deflection adjustment factor at the center of the dual tire (λ_0), for cases with temperatures above the reference temperature, the values vary with AC layer thicknesses (from thinner to thicker) as follows: 0.93, 0.83, 0.75, 0.71, and 0.68. Similarly, for cases with temperatures lower than the reference temperature, the respective values for differing AC layer thicknesses (from thinner to thicker) are 1.04, 1.09, 1.14, 1.16, and 1.18.

- The temperature influence zones expand proportionally with increasing AC layer thickness. For instance, while the temperature influence zone for cases with AC layer thicknesses in the range of 25–100 mm spans approximately 500 mm on either side of the center of dual tires, it widens to 1,400 mm for cases with AC layer thicknesses between 400 and 500 mm.

- The sensitivity of deflection to temperature, along with the extension of the influence zone on either side of the load center, varies due to the asymmetric nature of deflection bowls and the occurrence of maximum deflections behind the load owing to response lag. Notably, deflection adjustment factors for deflections behind the center of dual tires are relatively higher, resulting in taller boxes and a broader influence zone. This phenomenon is particularly pronounced in thicker asphalt layers.

- Outliers are data points that fall significantly above or below the whiskers of the plot, indicating unusual values. The occurrence of outliers decreases for deflections exhibiting higher sensitivity to temperatures, as well as in plots depicting thicker AC layer thicknesses, which are also more susceptible to temperature changes.

Temperature-Influenced Deflections

Figure 19 provides a detailed depiction of temperature influence zones on deflection bowls. The figure shows deflection bowls for various AC layer thicknesses at five distinct temperatures: 10, 20, 30, 40, and 50 °C. These temperatures encompass the range of analysis temperatures employed in the database for illustrative purposes. The corresponding number of analysis cases for each temperature, used in figure 19-A through figure 19-E, are as follows: 2,460; 4,110; 3,420; 1,770; and 450, respectively. The researchers averaged these deflection bowls across cases for each temperature to enhance clarity in the plot.

Similar observations to those mentioned in the previous section are evident here. As the AC layer thicknesses increase, the temperature influence zone also expands. Additionally, a higher sensitivity of deflection bowls for deflections occurs behind the load compared with those in front at the same distance from the center of dual tires. Table 7 offers a comprehensive overview of the most probable temperature influence zones for surface deflection, accounting for different AC layer thicknesses.

Table 7. Likely temperature influence zones for surface deflection under TSDD load for various pavement structures.

AC Thickness Range (mm)	Temperature Influence Zones	
	Distance Behind the Center of the Load (mm)	Distance in Front of the Load Center (mm)
25–100	400	400
100–200	600	500
200–300	900	800
300–400	1,100	900
400–500	1,400	1,100

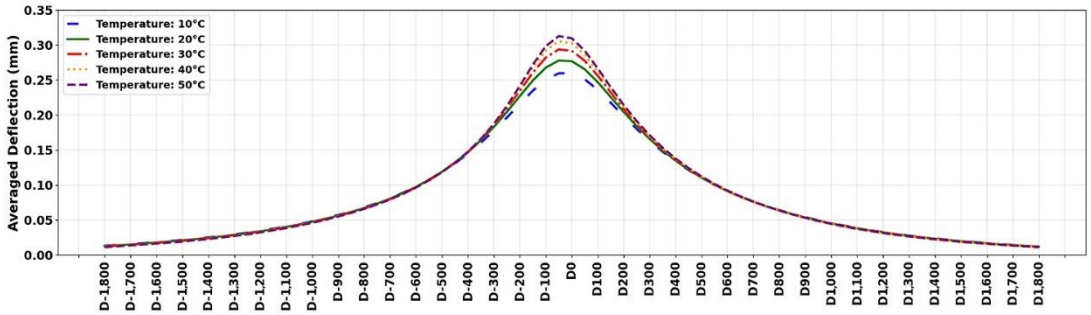

A. AC thickness between 25 and 100 mm.

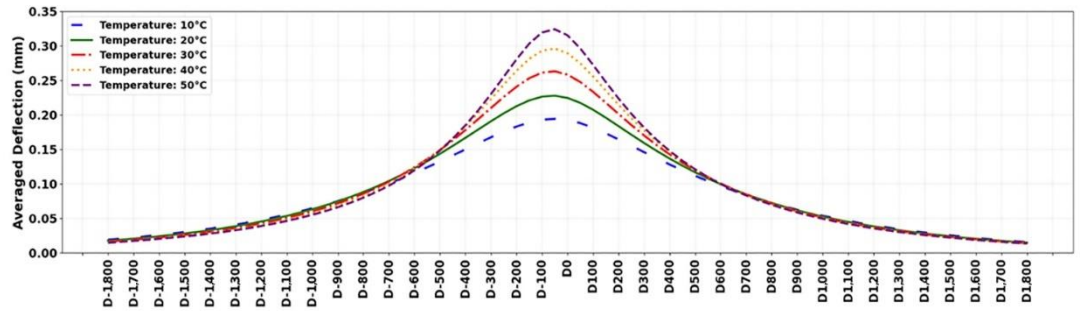

B. AC thickness between 100 and 200 mm.

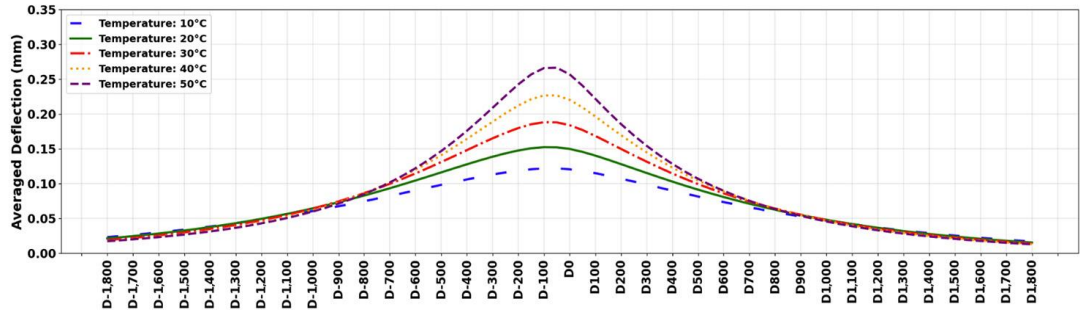

C. AC thickness between 200 and 300 mm.

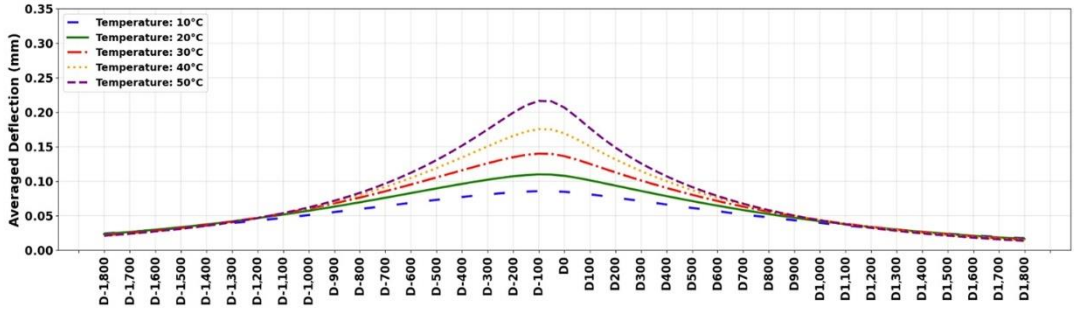

D. AC thickness between 300 and 400 mm.

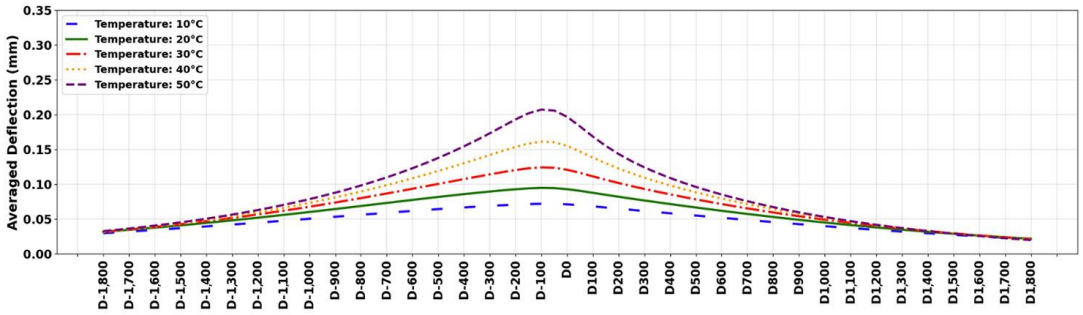

E. AC thickness between 400 and 500 mm.

All images source: FHWA.

Figure 19. Graphs. Demonstration of temperature influence zone on deflection bowls for various AC layer thicknesses.

TEMPERATURE INFLUENCE ZONE FOR TSDD DEFLECTION SLOPES

As with surface deflections, deflection slopes are influenced by temperature variations due to the viscoelastic nature of asphalt materials. The following sections provide a detailed assessment of the temperature sensitivity of deflection slope measurements, highlighting trends observed across various pavement configurations. Understanding these sensitivities is essential for developing temperature adjustment models.

Variation of Temperature Adjustment Factors for Deflection Slopes

Figure 20 and figure 21 show box-and-whisker plots illustrating the distributions of deflection slope temperature adjustment factors. Figure 20 focuses on cases with AC layer temperatures above the reference temperature (20 °C), whereas figure 21 examines cases with temperatures below the reference. Like deflection temperature adjustment factors, the box plots for deflection slope temperature adjustment factors exhibit increasing heights with the thickness of the AC layer, indicating greater variability of data in response to temperature fluctuations. Moreover, the mean values of deflection slope temperature adjustment factors within the influence zones deviate further from 1.0 as the layer thickness increases. Additionally, the temperature influence zones on deflection slopes expand as the AC layer thickness increases.

The values of deflection slope temperature adjustment factors are higher than those of deflection temperature adjustment factors, and the temperature influence zones are wider. This observation suggests that slopes exhibit greater sensitivity to temperature variations compared with deflections.

The asymmetrical impact of temperature is apparent in the analysis. Deflection slope temperature adjustment factors for positions situated behind the center of dual tires display relatively greater variations, leading to taller boxes, and an extended influence zone. This asymmetry becomes more pronounced in thicker asphalt layers. Moreover, the occurrence of outliers diminishes for deflection slopes in plots representing thicker AC layer thicknesses, which are also more responsive to temperature changes.

Figure 20-A through figure 20-E and figure 21-A through figure 21-E show that deflection slope temperature adjustment factors for slopes located approximately 100 mm behind the center of the dual tire exhibit some uncommon values compared to the rest. This anomaly can be attributed to the proximity of this position to the zero-slope location, where slope values change signs. Consequently, this position corresponds to small slope values, which significantly affect the sensitivity of this parameter to temperature. The researchers observed a high number of outliers in the vicinity of this position.

Temperature-Influenced Deflection Slopes

Figure 22-A through figure 22-E present averaged deflection slope values for various AC layer thicknesses across five distinct temperatures: 10, 20, 30, 40, and 50 °C, respectively. The figure corroborates that slopes at thicker AC layers are more sensitive to temperature, and that the temperature influence zone for deflection slope is wider than that for deflection. Additionally, table 8 provides a comprehensive overview of the most likely temperature influence zones for deflection slopes, considering various AC layer thicknesses.

Table 8. Likely temperature influence zones for surface deflection slopes under TSDD load for various pavement structures.

AC Thickness Range (mm)	Temperature Influence Zones	
	Distance Behind the Center of the Load (mm)	Distance in Front of the Load Center (mm)
25–100	500	500
100–200	800	700
200–300	1,100	900
300–400	1,200	900
400–500	1,500	1,100

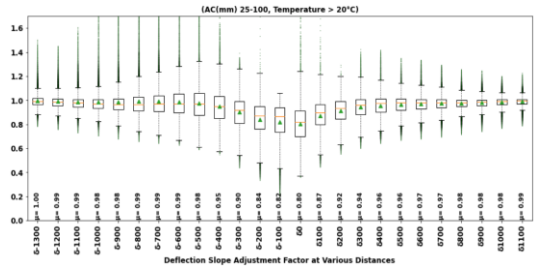

A. AC thicknesses between 25 and 100 mm.

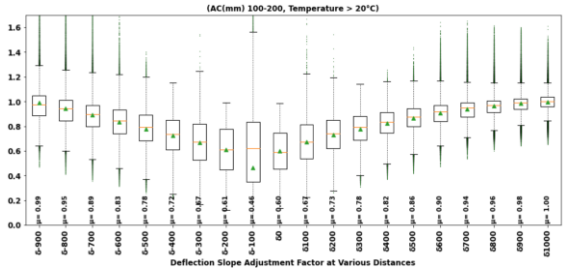

B. AC thicknesses between 100 and 200 mm.

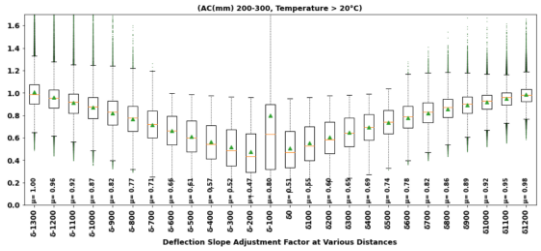

C. AC thicknesses between 200 and 300 mm.

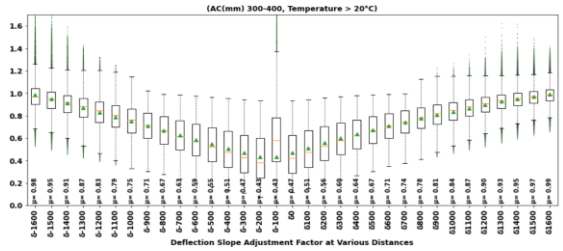

D. AC thicknesses between 300 and 400 mm.

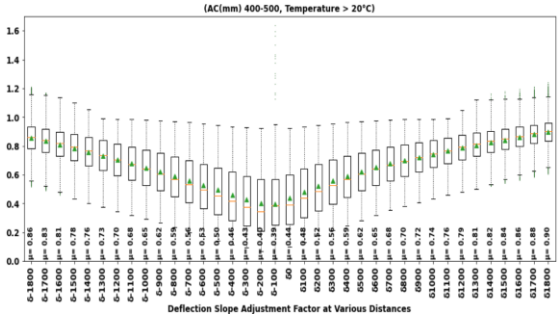

E. AC thicknesses between 400 and 500 mm.

All figures source: FHWA.

Figure 20. Graphs. Deflection slope adjustment factor distributions for cases with AC layer temperatures higher than 20 °C for various AC layer thicknesses.

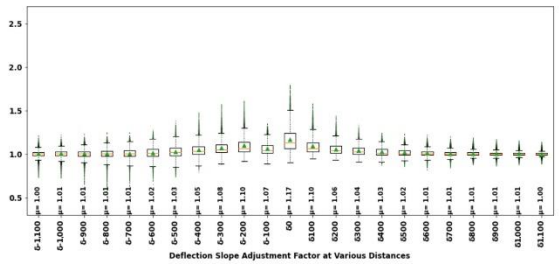

A. AC thicknesses between 25 and 100 mm.

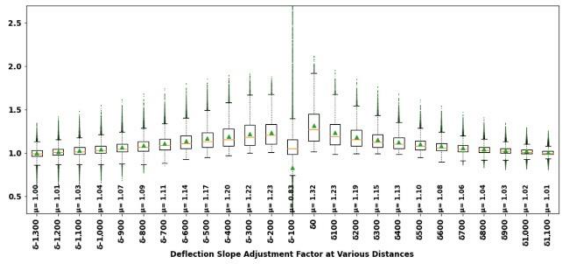

B. AC thicknesses between 100 and 200 mm.

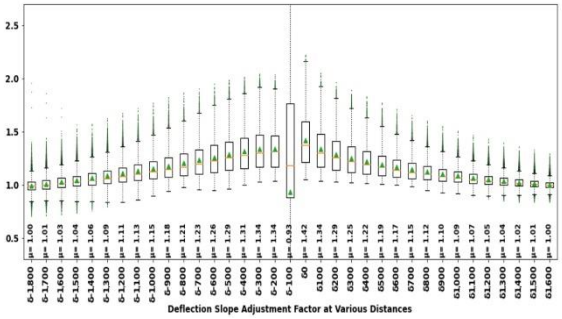

C. AC thicknesses between 200 and 300 mm.

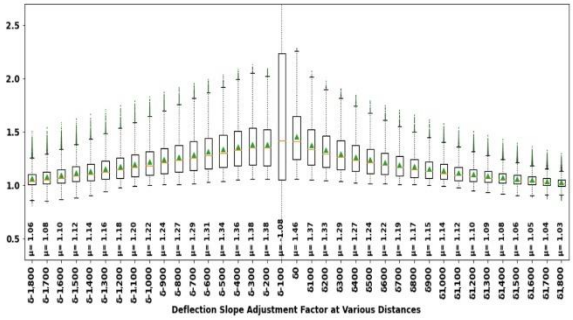

D. AC thicknesses between 300 and 400 mm.

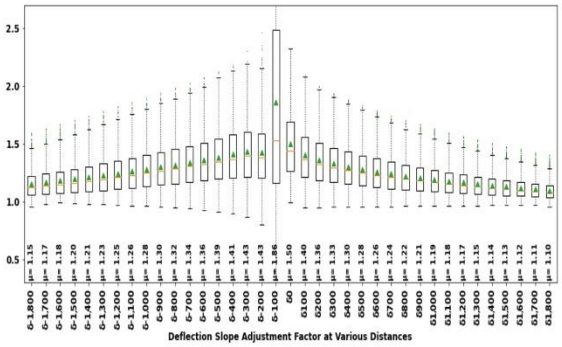

E. AC thicknesses between 400 and 500 mm.

All images source: FHWA.

Figure 21. Graphs. Deflection slope adjustment factor distributions for cases with AC layer temperatures lower than 20 °C for various AC layer thicknesses.

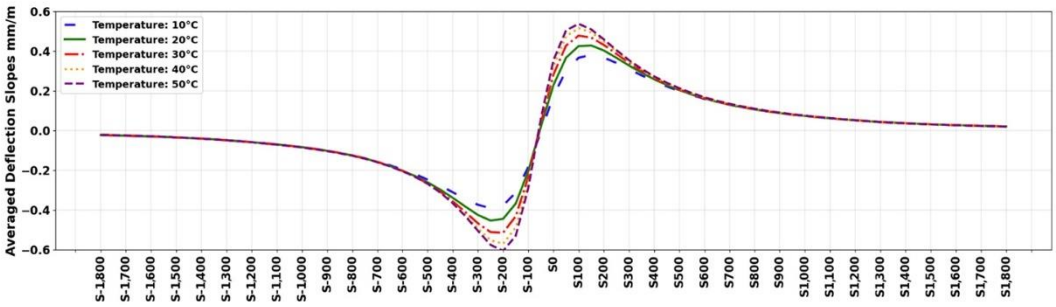

A. AC thickness between 25 and 100 mm.

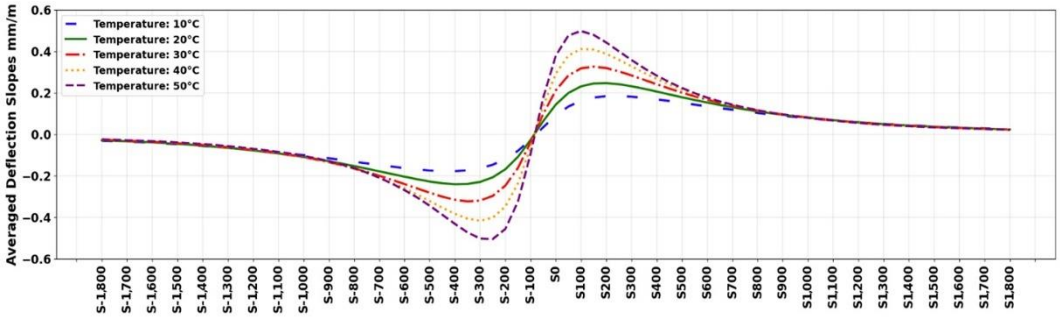

B. AC thickness between 100 and 200 mm.

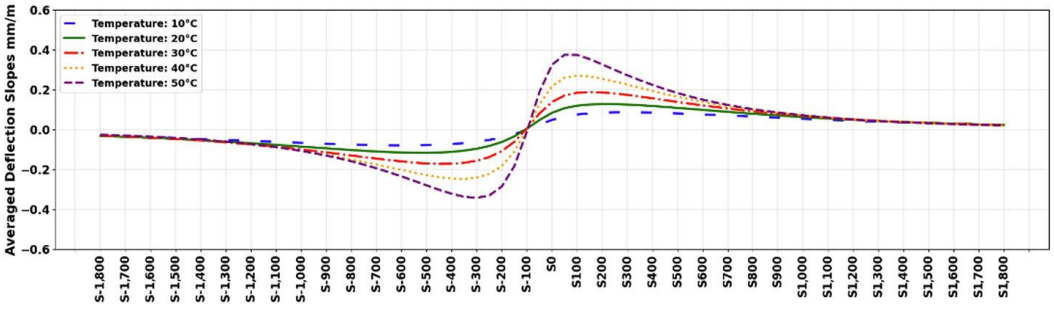

C. AC thickness between 200 and 300 mm.

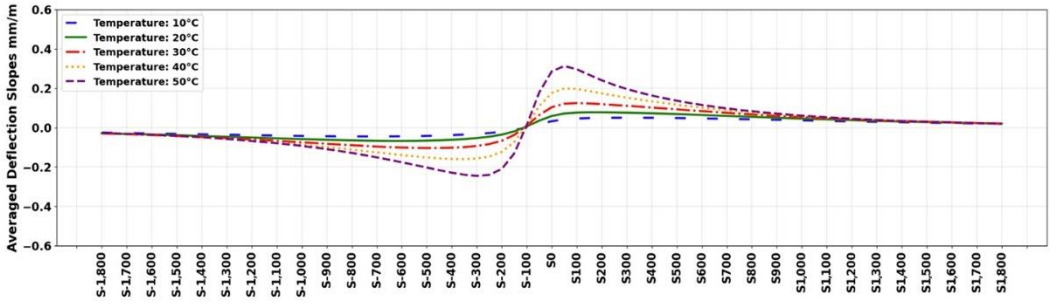

D. AC thickness between 300 and 400 mm.

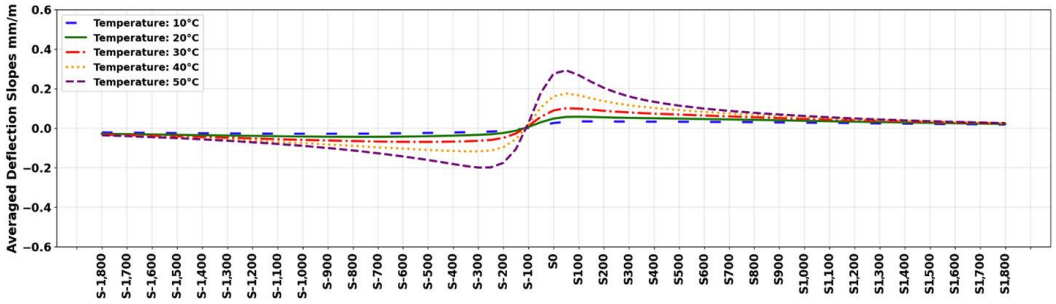

E. AC thickness between 400 and 500 mm.

All images source: FHWA.

Figure 22. Graphs. Demonstration of temperature influence zone on deflection slope curves for various AC layer thicknesses.

CHAPTER 5. SENSITIVITY ANALYSES OF TEMPERATURE ADJUSTMENT FACTORS

Before developing temperature adjustment models, comprehending the sensitivity of temperature adjustment factors to various parameters is beneficial for selecting the most effective parameters for use in the models. Due to the similarity in sensitivity analyses of deflection and deflection slope temperature adjustment factors, this section exclusively presents the sensitivity of deflection temperature adjustment factors for brevity. The researchers used the complete database, which comprises more than 250,000 analyzed cases, in this section.

The research team used Spearman's rank correlation coefficient (Spearman 1904) to evaluate the strength and direction of the monotonic relationship between variables for sensitivity analyses. In Spearman's correlation, the data values of the two variables are initially ranked, and then the correlation coefficient is computed based on the ranks rather than the original values. The coefficient ranges from −1 to 1, where a coefficient of 1 signifies a perfect positive monotonic relationship (as one variable increases, the other also increases); a coefficient of −1 indicates a perfect negative monotonic relationship (as one variable increases, the other decreases); and a coefficient of 0 indicates no monotonic relationship between the variables.

In the preceding section, the researchers demonstrated that responses in the vicinity of the loading area are more sensitive to temperature changes. Figure 23 illustrates the Spearman correlation coefficients between deflection temperature adjustment factors and temperature at various positions. Notably, the adjustment factor at 50 mm behind the load (which is close to the maximum deflections) exhibits the highest correlation, with correlations decreasing for factors farther from the center of the dual tires. Consequently, the distance from the loading area emerges as a significant parameter that plays a pivotal role in the development of temperature adjustment models.

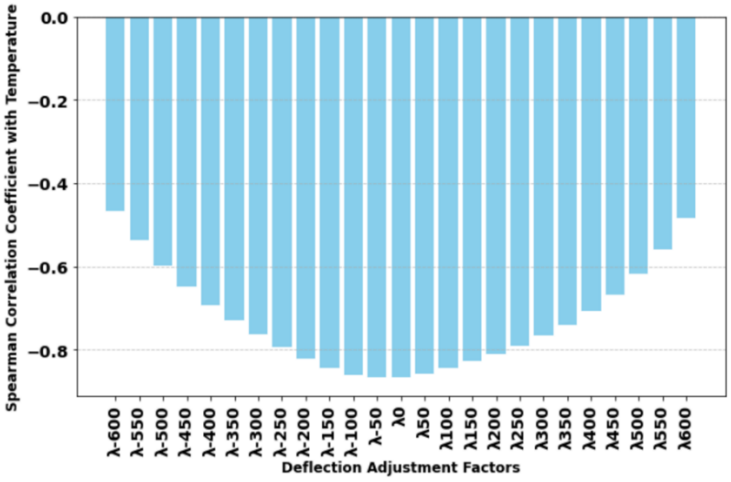

Source: FHWA.

Figure 23. Graph. Spearman correlation coefficients between temperatures and deflection adjustment factors.

To explore the effects of other parameters, the researchers calculated Spearman coefficients between the most sensitive deflection adjustment factor (λ_{-50}) and other parameters within the database. As anticipated and as figure 24 shows, the AC layer thickness exhibits the highest correlation, indicating its significant involvement in temperature adjustments. The underlying layers serve as a foundation for the AC layer, and their properties (thickness and modulus) have affect surface responses under varying temperatures. However, as depicted in the figure, the correlations with these parameters are minimal, and their use is impractical since they are commonly unknown at the time of TSDD measurements. Nevertheless, the database encompasses a variety of pavement structures, indirectly considering the effect of underlying layers on temperature adjustments through the developed model.

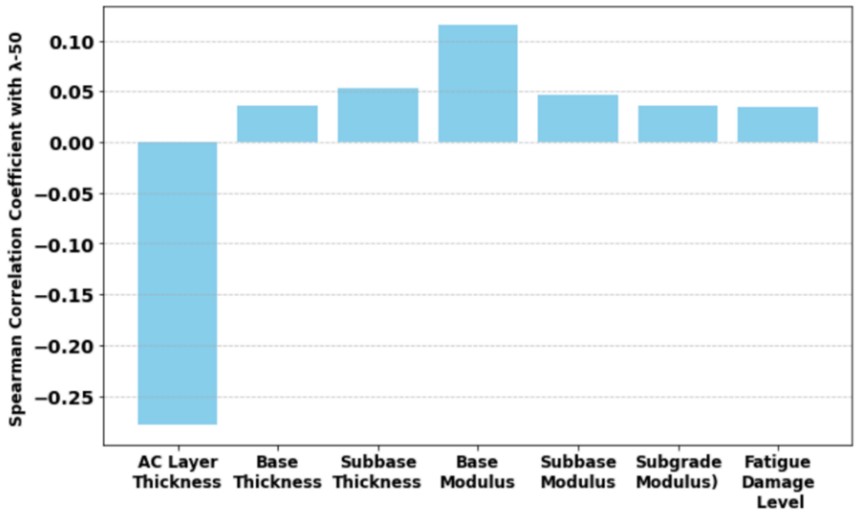

Source: FHWA.

Figure 24. Graph. Spearman correlation coefficients between λ_{-50} and material properties.

The SCI is a widely used deflection index, computed as the difference between the deflection at the center of the dual tire (D_0) and the deflection 300 mm in front of it (D_{300}). Figure 25 depicts the variation of the SCI temperature adjustment factor (λ_{SCI}) across different temperatures within the research team's database. To improve clarity and facilitate the assessment of case distribution, the research team rounded and grouped the values to the nearest 0.05. While a clear decreasing trend in λ_{SCI} values with increasing AC layer temperature may be anticipated, the presence of noteworthy outliers is notable. These outliers stem from the intrinsic variation within the dataset, encompassing a broad spectrum of pavement structures that exhibit distinct responses to temperature changes. Despite inherent variability, a consistent trend is observed across most of the dataset, as shown in the graph in figure 25, representing the distribution of cases within temperature bins. Particularly, figure 26-A through figure 26-E show the occurrence of outliers diminishes for pavement structures with thicker AC layers. Consequently, a more pronounced pattern is observable for thicker asphalt layers.

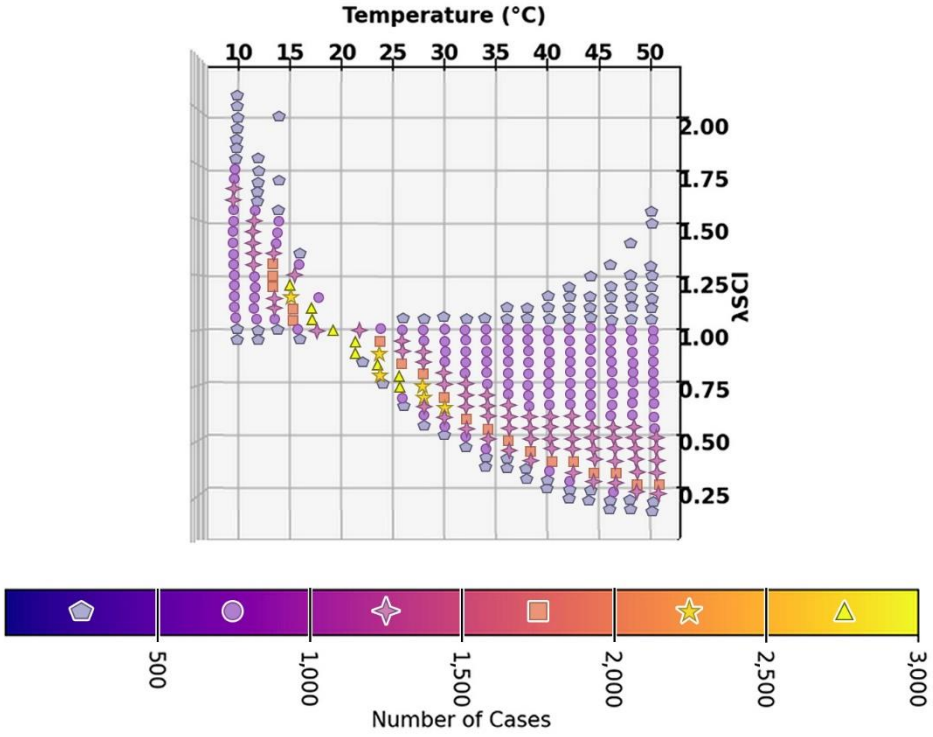

Source: FHWA.

Figure 25. Graph. Variation of SCI temperature adjustment factor in the database.

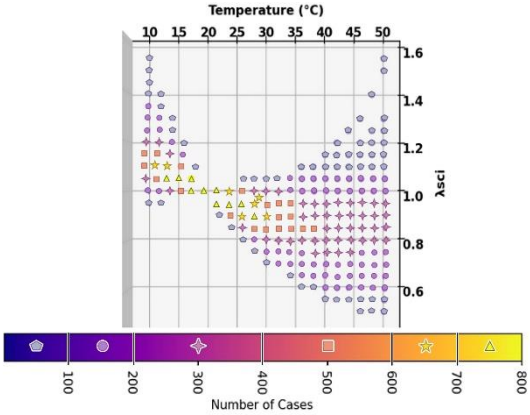

A. AC thickness between 25 and 100 mm.

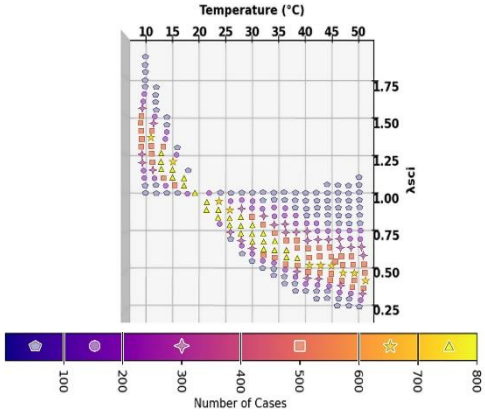

B. AC thickness between 100 and 200 mm.

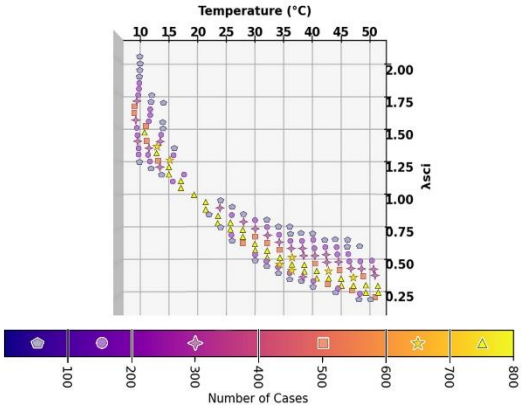

C. AC thickness between 200 and 300 mm.

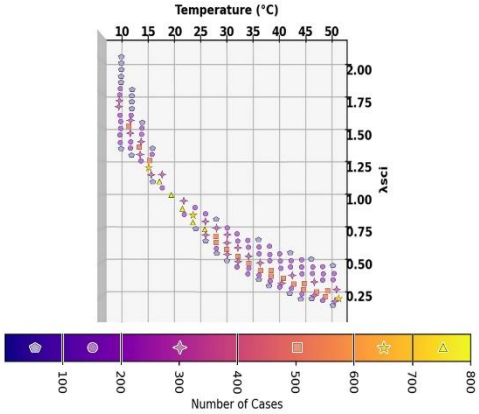

D. AC thickness between 300 and 400 mm.

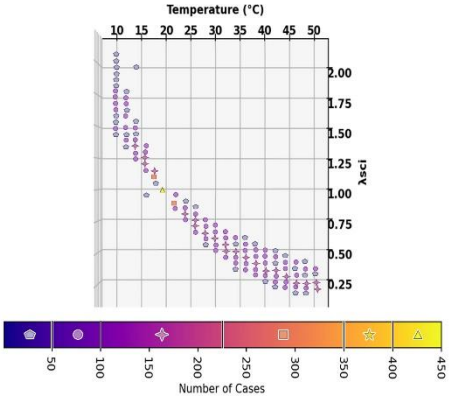

E. AC thickness between 400 and 500 mm.

All images source: FHWA.

Figure 26. Graphs. Variation of SCI temperature adjustment factor in the database for different AC layer thicknesses.

CHAPTER 6. TEMPERATURE ADJUSTMENT MODELS FOR SURFACE DEFLECTIONS UNDER TSDD LOADING

In accordance with the preceding discussion, deflection temperature adjustment factors are predominantly influenced by temperature variations, the thickness of the AC layers, and the distance from the center of dual tires. Consequently, any temperature adjustment models should comprehensively incorporate these influential parameters. The research team used the formula shown in figure 27 to evaluate multiple functional forms for temperature adjustments and found that the equation demonstrated superior performance within the database, thus serving as the cornerstone for subsequent model development in this study.

$$\lambda_d = 10^{(a_{d1} + a_{d2} \log(h_{AC}))(T_{Ref} - T)}$$

Figure 27. Equation. Deflection temperature adjustment factor formula.

Where:

λ_d = temperature adjustment factor for deflection at a distance "*d*" from the center of the dual tire.
T_{Ref} = reference middepth AC layer temperature (e.g., 20 °C).
T = middepth AC layer temperature (°C) at the time of measurement.
h_{AC} = AC layer thickness (mm).
a_{d1} and a_{d2} = model constants and are a function of distance "*d.*"

The research team employed the deflection temperature adjustment factors for all 257,040 analysis cases to compute the model constants, as delineated in figure 27, for temperature-sensitive deflections within the influence zone at 50 mm intervals. The team outlines these model constants in table 9.

The researchers performed the optimization of the model constants by minimizing the root mean square error (RMSE) between the temperature adjustment factors in the database and those factors calculated using the formula in figure 27. The team accomplished this optimization process by using the Nelder-Mead algorithm, which is also known as the downhill simplex method (Nelder and Mead 1965), available in Python libraries.

The research team computed the RMSE by using the formula in figure 28:

$$RMSE = \sqrt{\frac{\sum_1^N \left(\left(\lambda_{Model} - \lambda_{database} \right) / \left(\lambda_{database} \right) \right)^2}{N}}$$

Figure 28. Equation. The RMSE formula.

Where:

λ_{Model} = deflection temperature adjustment factor for each case obtained using the equation in figure 27.

$\lambda_{database}$ = deflection temperature adjustment factor for each case in the database.

N = number of analysis cases (257,040).

Table 9. Model constants and associated RMSE for temperature adjustment models for surface deflections under TSDD loading.

Deflection Temperature Adjustment Factor	a_{d1}	a_{d2}	RMSE	Deflection Temperature Adjustment Factor	a_{d1}	a_{d2}	RMSE
$\lambda_{-1,400}$	−2.2469E-03	2.5452E-04	0.0838	λ_{0}	−1.7501E-02	1.0731E-02	0.0577
$\lambda_{-1,350}$	−2.5034E-03	4.2317E-04	0.0837	λ_{50}	−1.6951E-02	1.0287E-02	0.0567
$\lambda_{-1,300}$	−2.9720E-03	6.8735E-04	0.0836	λ_{100}	−1.6299E-02	9.7614E-03	0.0562
$\lambda_{-1,250}$	−3.3635E-03	9.3340E-04	0.0834	λ_{150}	−1.5428E-02	9.1384E-03	0.0561
$\lambda_{-1,200}$	−3.8429E-03	1.2169E-03	0.0832	λ_{200}	−1.4629E-02	8.5622E-03	0.0562
$\lambda_{-1,150}$	−4.3149E-03	1.5105E-03	0.0831	λ_{250}	−1.3859E-02	8.0024E-03	0.0565
$\lambda_{-1,100}$	−4.9304E-03	1.8719E-03	0.0830	λ_{300}	−1.2937E-02	7.3995E-03	0.0568
$\lambda_{-1,050}$	−5.5004E-03	2.2194E-03	0.0830	λ_{350}	−1.2085E-02	6.8341E-03	0.0570
$\lambda_{-1,000}$	−6.1425E-03	2.6081E-03	0.0833	λ_{400}	−1.1322E-02	6.3230E-03	0.0572
λ_{-950}	−6.7711E-03	2.9925E-03	0.0835	λ_{450}	−1.0550E-02	5.8150E-03	0.0573
λ_{-900}	−7.5154E-03	3.4448E-03	0.0838	λ_{500}	−9.7270E-03	5.2972E-03	0.0573
λ_{-850}	−8.2180E-03	3.8815E-03	0.0839	λ_{550}	−9.0180E-03	4.8375E-03	0.0572
λ_{-800}	−8.9693E-03	4.3538E-03	0.0840	λ_{600}	−8.2870E-03	4.3790E-03	0.0568
λ_{-750}	−9.7362E-03	4.8387E-03	0.0839	λ_{650}	−7.5268E-03	3.9173E-03	0.0563
λ_{-700}	−1.0615E-02	5.3810E-03	0.0836	λ_{700}	−6.8584E-03	3.5058E-03	0.0557
λ_{-650}	−1.1441E-02	5.9162E-03	0.0829	λ_{750}	−6.1934E-03	3.0995E-03	0.0552
λ_{-600}	−1.2354E-02	6.4964E-03	0.0817	λ_{800}	−5.5882E-03	2.7306E-03	0.0547
λ_{-550}	−1.3222E-02	7.0637E-03	0.0801	λ_{850}	−4.9644E-03	2.3554E-03	0.0542
λ_{-500}	−1.4217E-02	7.6999E-03	0.0783	λ_{900}	−4.3461E-03	1.9850E-03	0.0537
λ_{-450}	−1.5165E-02	8.3219E-03	0.0760	λ_{950}	−3.7084E-03	1.6209E-03	0.0533
λ_{-400}	−1.6082E-02	8.9438E-03	0.0734	λ_{1000}	−3.2392E-03	1.3369E-03	0.0531
λ_{-350}	−1.6998E-02	9.5658E-03	0.0705	λ_{1050}	−2.5709E-03	9.5774E-04	0.0531
λ_{-300}	−1.7809E-02	1.0152E-02	0.0676	λ_{1100}	−2.1164E-03	6.8621E-04	0.0532
λ_{-250}	−1.8419E-02	1.0656E-02	0.0647	—	—	—	—
λ_{-200}	−1.8742E-02	1.1025E-02	0.0624	—	—	—	—
λ_{-150}	−1.8842E-02	1.1272E-02	0.0607	—	—	—	—
λ_{-100}	−1.8559E-02	1.1284E-02	0.0596	—	—	—	—
λ_{-50}	−1.8063E-02	1.1087E-02	0.0587	—	—	—	—

—Not applicable.

The research team determined the absolute error between the temperature adjustment factors calculated from the model and those factors in the database for some TSDD-reported deflections by using the formula in figure 29. Figure 30 presents box plots depicting the calculated errors, including the mean and standard deviation. The range of errors and associated statistical parameters validate the appropriateness of the optimized parameters for the temperature adjustment model and their ability to predict reasonable adjustment factors.

$$Absolute\ Error = \left| \frac{\lambda_{d_m} - \lambda_d}{\lambda_d} \right| \times 100$$

Figure 29. Equation. The absolute error formula.

Where:

λ_{d_m} = temperature adjustment factor at distance "*d*" using the equation in figure 27 with the corresponding parameters listed in table 9.

λ_d = temperature adjustment factor at distance "*d*" in the database.

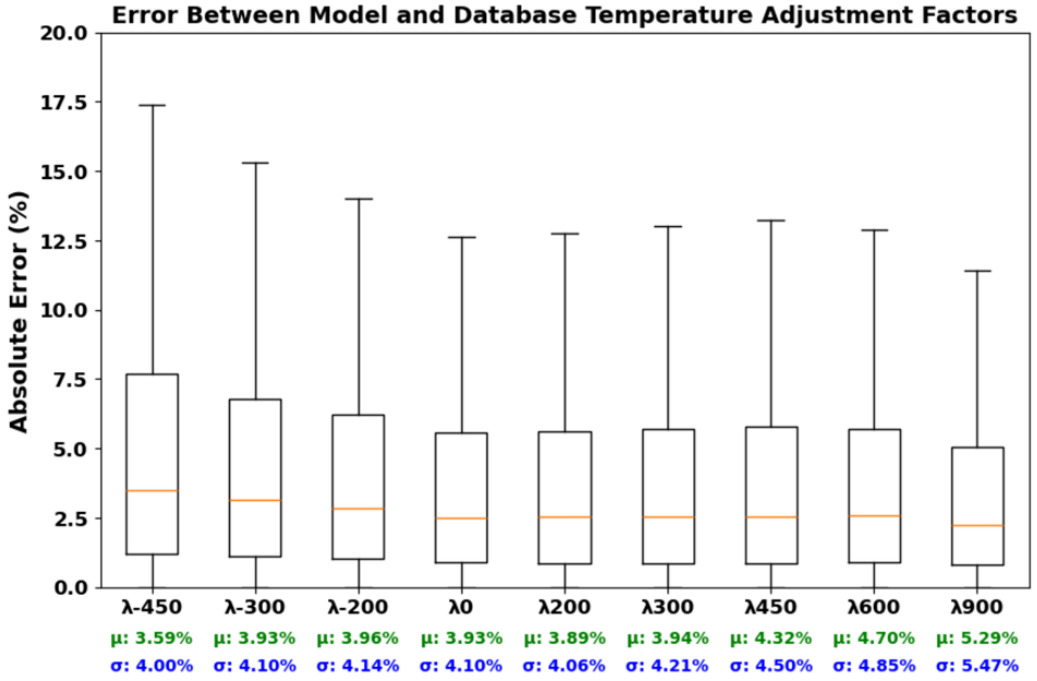

Source: FHWA.

Figure 30. Graph. The box plot illustrating the absolute error between model and database temperature adjustment factors for TSDD-reported deflections.

The research team visualized the temperature adjustment factors for some TSDD-reported deflections, which are most affected by temperature, as shown in figure 31-A thorough figure 31-F. The team derived these adjustment factor curves by using the formula in figure 27 with constants detailed in table 9 and accounting for various temperatures and AC layer thicknesses. The diagram illustrates consistent trends the researchers observed in the database, indicating that thicker asphalt layers exhibit heightened sensitivity to temperature changes, particularly in

deflections occurring behind the loading. Conversely, deflections in thinner asphalt layers (75 mm and below) demonstrate minimal sensitivity to temperature variations.

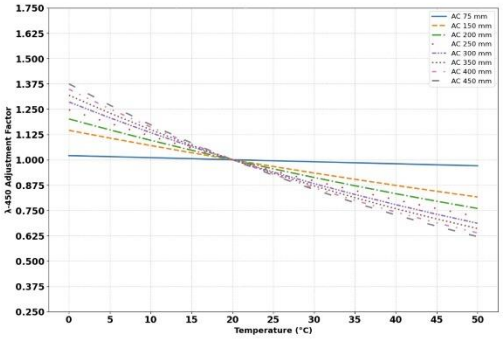

A. Temperature adjustment factor for D_{-450}.

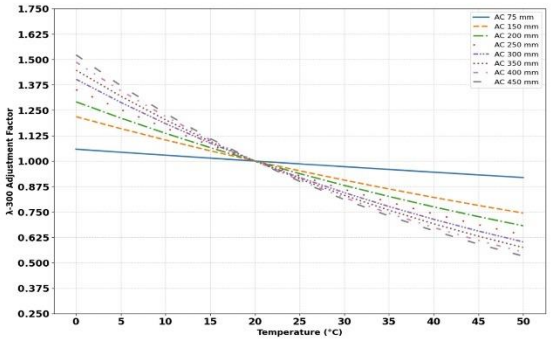

B. Temperature adjustment factor for D_{-300}.

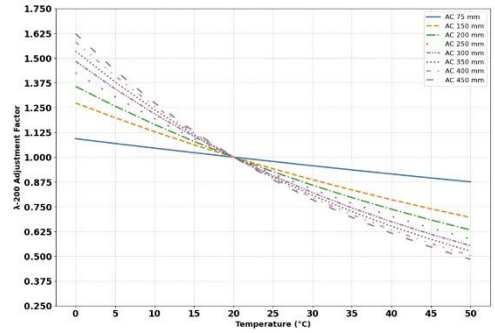

C. Temperature adjustment factor for D_{-200}.

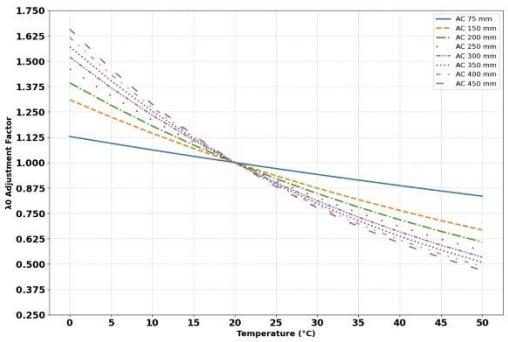

D. Temperature adjustment factor for D_0.

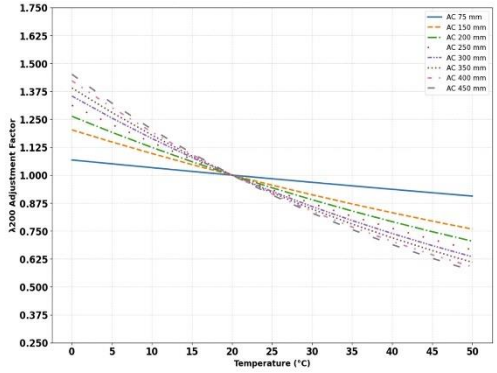

E. Temperature adjustment factor for D_{200}.

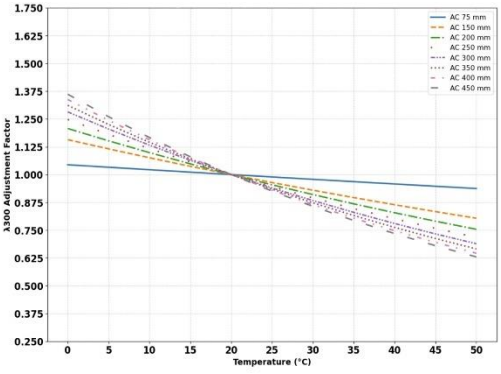

F. Temperature adjustment factor for D_{300}.

All images source: FHWA.

Figure 31. Graphs. The temperature adjustment factor curves for various surface deflections under TSDD loading in different AC layer ranges.

Figure 32 shows the temperature adjustment factor was computed separately for SCI, given its frequent use with TSDD data. Although this equation is provided for convenience, SCI can also be temperature adjusted using temperature-corrected D_0 and D_{300} by employing the formula in figure 27 and the corresponding model constants outlined in table 9.

$$\lambda_{SCI} = 10^{(-0.03514445+0.02180329\log(h_{AC}))(T_{Ref}-T)}$$

Figure 32. Equation. SCI temperature adjustment factor formula.

Figure 33 presents the SCI temperature adjustment curves for various AC layer thicknesses. Compared with the deflection diagrams in figure 31, the SCI adjustment factors exhibit higher values. This observation can be attributed to the nature of the SCI as a deflection index primarily correlated with asphalt layer properties, making it more sensitive to temperature variations.

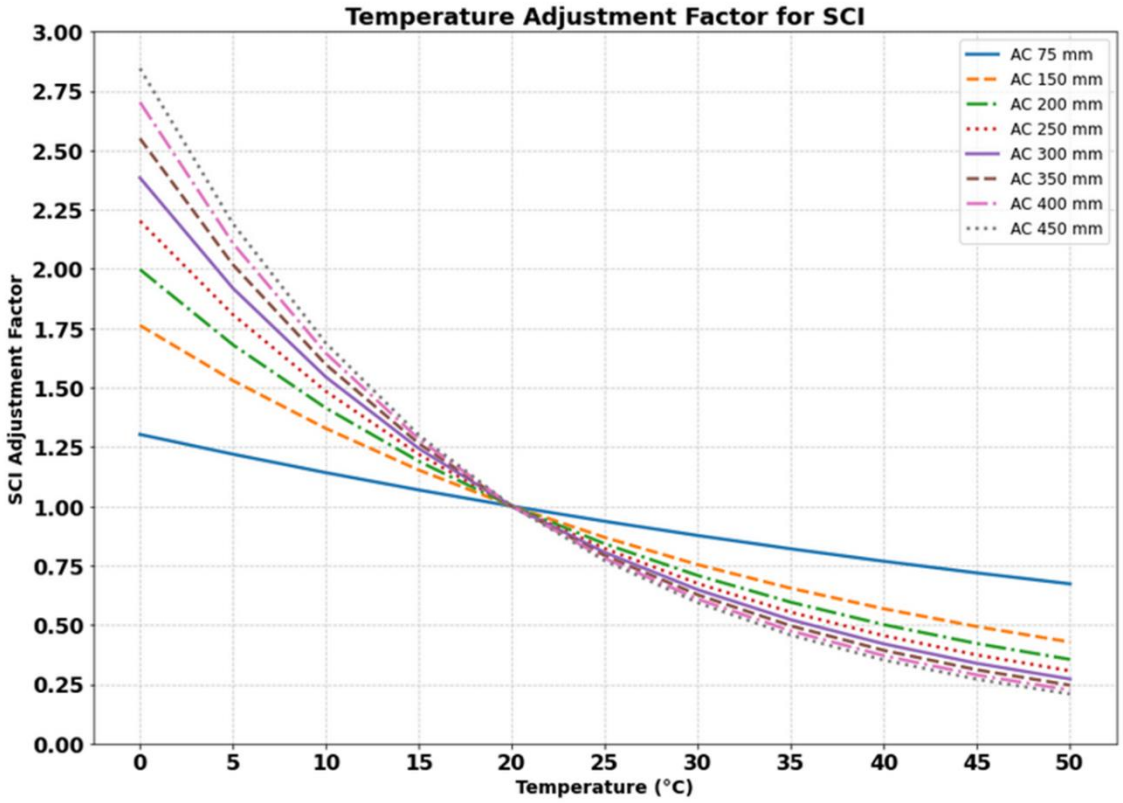

Source: FHWA.

Figure 33. Graph. The temperature adjustment factor curves for SCI under TSDD loading in different AC layer ranges.

When using the temperature adjustment method outlined in this section with reported deflections from TSDD, several factors should be considered:

- The middepth temperature of the AC layer can be calculated from the surface temperature and other relevant parameters using the BELLS2 model (Lukanen, Stubstad, and Briggs 2000), as described in Appendix A.

- The temperature adjustment model shown in the figure 27 formula can be used with any reference temperature.

CHAPTER 7. TEMPERATURE ADJUSTMENT MODELS FOR SURFACE DEFLECTION SLOPES UNDER TSDD LOADING

Figure 34 is proposed to adjust deflection slopes for temperature, following a similar form used for temperature adjustment of surface deflections.

$$\delta_d = 10^{(b_{d1} + b_{d2} \log(h_{AC}))(T_{Ref} - T)}$$

Figure 34. Equation. Deflection slope temperature adjustment factor formula.

Where:

δ_d = deflection slope temperature adjustment factor for the slope at distance "*d*" from the center of the dual tire.
T_{Ref} = reference middepth AC layer temperature (e.g., 20 °C).
T = middepth AC layer temperature at the time of measurement (°C).
h_{AC} = AC layer thickness (mm).
b_{d1} and b_{d2} = model constants and are a function of distance "*d.*"

The research team employed the temperature adjustment factors for deflection across all 257,040 analysis cases to compute the model constants as delineated in figure 34. This equation addresses the temperature-sensitive deflection slopes within the influence zone at 50 mm intervals. The team applied the same optimization method used for adjusting surface deflections to temperature. Table 10 details these model constants.

The deflection slope approaches zero behind the load between 0 and 100 mm from the center of dual tires. In this region, the slopes in all cases are minimal and subject to high variations in temperatures, as depicted in figure 20 and figure 21. Consequently, the model for the slopes in this area demonstrates a considerable degree of variability. Given the relatively small values of slopes, the model constants for slopes at positions such as −50 and −100 mm are not presented in the table.

Table 10. Model constants and associated RMSE for temperature adjustment models for surface deflection slopes under TSDD loading.

Deflection Slope Temperature Adjustment Factor	b_{d1}	b_{d2}	RMSE	Deflection Slope Temperature Adjustment Factor	b_{d1}	b_{d2}	RMSE
$\delta_{-1,500}$	−8.9357E-03	4.0904E-03	0.1393	δ_0	−3.5257E-02	2.3557E-02	0.1212
$\delta_{-1,450}$	−9.9010E-03	4.6500E-03	0.1403	δ_{50}	−3.6349E-02	2.3317E-02	0.1191
$\delta_{-1,400}$	−1.1061E-02	5.3107E-03	0.1407	δ_{100}	−3.5872E-02	2.2431E-02	0.1172
$\delta_{-1,350}$	−1.2201E-02	5.9822E-03	0.1410	δ_{150}	−3.4717E-02	2.1313E-02	0.1148
$\delta_{-1,300}$	−1.3363E-02	6.6666E-03	0.1415	δ_{200}	−3.3202E-02	2.0113E-02	0.1128
$\delta_{-1,250}$	−1.4523E-02	7.3650E-03	0.1425	δ_{250}	−3.1466E-02	1.8878E-02	0.1112
$\delta_{-1,200}$	−1.5597E-02	8.0312E-03	0.1439	δ_{300}	−2.9787E-02	1.7718E-02	0.1104
$\delta_{-1,150}$	−1.6826E-02	8.7728E-03	0.1458	δ_{350}	−2.8235E-02	1.6654E-02	0.1095
$\delta_{-1,100}$	−1.8004E-02	9.5013E-03	0.1481	δ_{400}	−2.6723E-02	1.5640E-02	0.1088
$\delta_{-1,050}$	−1.9262E-02	1.0270E-02	0.1506	δ_{450}	−2.5255E-02	1.4670E-02	0.1077
$\delta_{-1,000}$	−2.0517E-02	1.1061E-02	0.1519	δ_{500}	−2.3812E-02	1.3736E-02	0.1073
δ_{-950}	−2.1839E-02	1.1893E-02	0.1524	δ_{550}	−2.2491E-02	1.2868E-02	0.1079
δ_{-900}	−2.3241E-02	1.2777E-02	0.1528	δ_{600}	−2.1213E-02	1.2045E-02	0.1087
δ_{-850}	−2.4683E-02	1.3698E-02	0.1535	δ_{650}	−2.0056E-02	1.1296E-02	0.1084
δ_{-800}	−2.6248E-02	1.4683E-02	0.1542	δ_{700}	−1.8882E-02	1.0555E-02	0.1067
δ_{-750}	−2.7804E-02	1.5682E-02	0.1530	δ_{750}	−1.7726E-02	9.8278E-03	0.1052
δ_{-700}	−2.9514E-02	1.6773E-02	0.1509	δ_{800}	−1.6689E-02	9.1737E-03	0.1044
δ_{-650}	−3.1395E-02	1.7953E-02	0.1490	δ_{850}	−1.5783E-02	8.5896E-03	0.1037
δ_{-600}	−3.3226E-02	1.9136E-02	0.1478	δ_{900}	−1.4778E-02	7.9748E-03	0.1023
δ_{-550}	−3.5138E-02	2.0373E-02	0.1473	δ_{950}	−1.3904E-02	7.4391E-03	0.0997
δ_{-500}	−3.7193E-02	2.1710E-02	0.1460	$\delta_{1,000}$	−1.2981E-02	6.8878E-03	0.0973
δ_{-450}	−3.9360E-02	2.3120E-02	0.1449	$\delta_{1,050}$	−1.2097E-02	6.3432E-03	0.0956
δ_{-400}	−3.8831E-02	2.3372E-02	0.1444	$\delta_{1,100}$	−1.1256E-02	5.8265E-03	0.0944
δ_{-350}	−4.3545E-02	2.6011E-02	0.1441	—	—	—	—
δ_{-300}	−4.5425E-02	2.7441E-02	0.1459	—	—	—	—
δ_{-250}	−4.6875E-02	2.8741E-02	0.1505	—	—	—	—
δ_{-200}	−4.8350E-02	3.0128E-02	0.1618	—	—	—	—
δ_{-150}	−5.6541E-02	3.5108E-02	0.2404	—	—	—	—

—Not applicable.

Figure 35 illustrates the absolute errors between the temperature adjustment factors for slopes from the model and those in the database. Compared with the errors for deflection temperature adjustment factors, the errors for slope temperature adjustment factors appear higher, likely due to the greater variation of slopes with temperatures. However, the mean and standard deviation of errors displayed in the figure are still relatively small, indicating the appropriateness of the model.

The research team visualized the temperature adjustment factors for some TSDD deflection slopes with higher influence from temperature variations in figure 36. The team derived these adjustment factor curves by using the formula in figure 34, using the model constants outlined in table 10, and by considering different temperatures and AC layer thicknesses. The adjustment factors are comparatively higher than those for deflections, suggesting that slopes are more sensitive to temperature fluctuations. The diagram illustrates consistent trends observed in the database, indicating increased sensitivity of thicker asphalt layers to temperature changes, particularly in deflection slopes occurring behind the loading. In contrast, deflection slopes in thinner asphalt layers (75 mm and below) exhibit minimal sensitivity to temperature fluctuations.

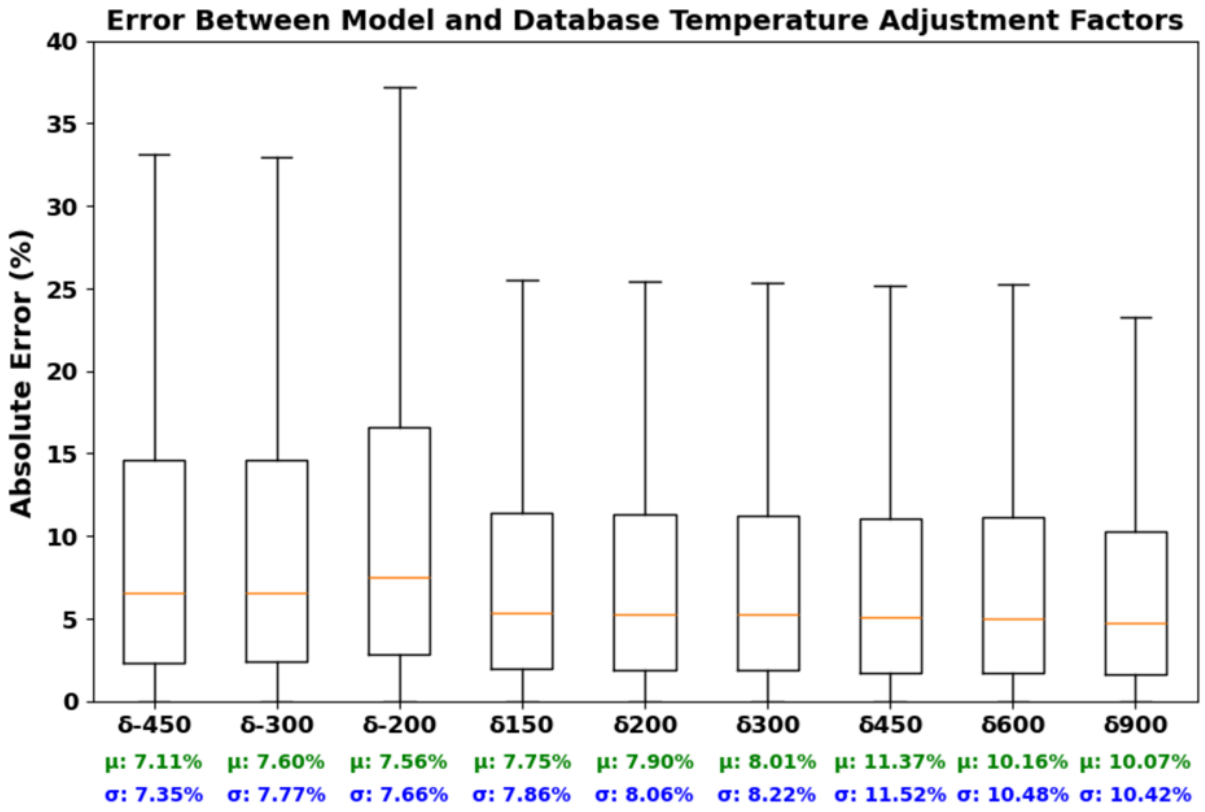

Source: FHWA.

Figure 35. Graph. The box plot illustrating the absolute error between model and database temperature adjustment factors for some TSDD deflection slopes.

When using the temperature adjustment method outlined in this section with reported deflection slopes from TSDD, several considerations should be considered:

- The middepth temperature of the AC layer can be calculated from the surface temperature and other relevant parameters using the BELLS2 model (Lukanen, Stubstad, and Briggs 2000), as described in Appendix A.

- The temperature adjustment model shown in the figure 34 formula can be used with any reference temperature.

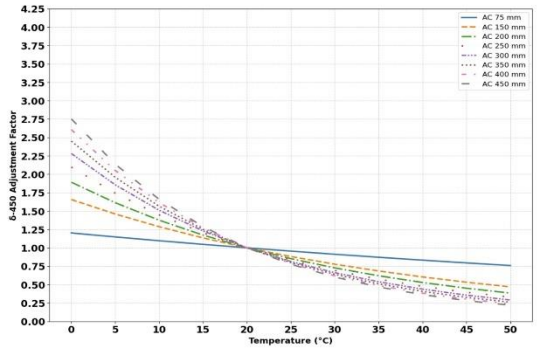

A. Temperature adjustment factor for S_{-450}.

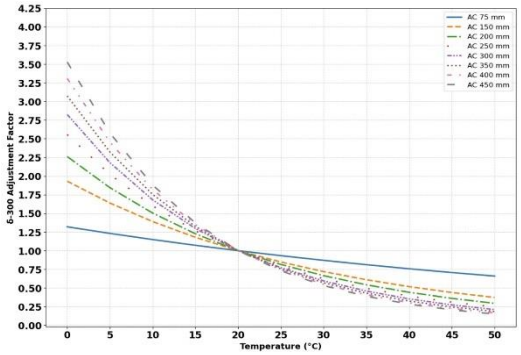

B. Temperature adjustment factor for S_{-300}.

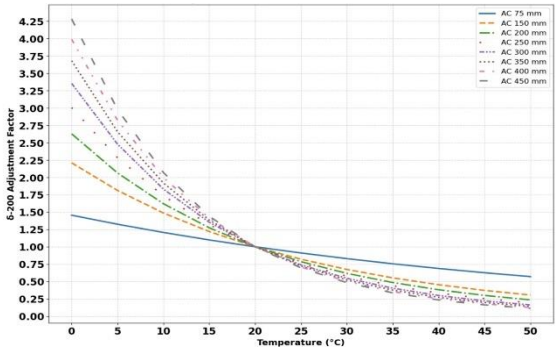

C. Temperature adjustment factor for S_{-200}.

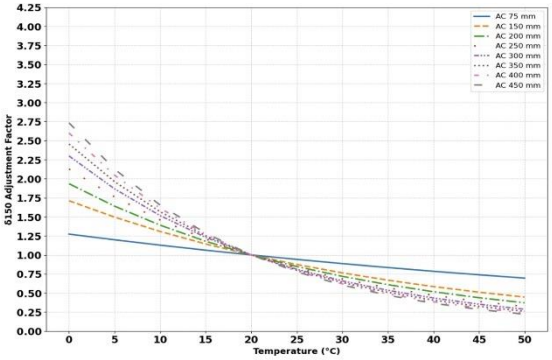

D. Temperature adjustment factor for S_{150}.

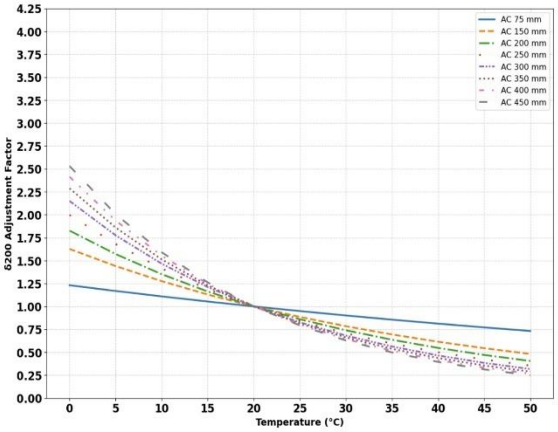

E. Temperature adjustment factor for S_{200}.

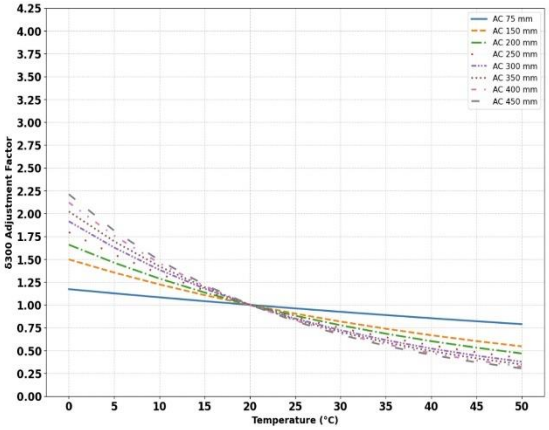

F. Temperature adjustment factor for S_{300}.

All images source: FHWA.

Figure 36. Graphs. The temperature adjustment factor curves for various surface deflection slopes under TSDD loading in different AC layer ranges.

CHAPTER 8. FIELD EVALUATION OF TEMPERATURE ADJUSTMENT MODELS

While the temperature adjustment models developed in this study are generally applicable to data collected by any TSDD that measures deflection and slope along the midline of dual tires, the research team used TSD data for validation purposes. The team based this choice on the availability of field data and the widespread use of TSD devices in practice.

The research team used the TSD data collected in June 2023, along a 50 km loop near Roskilde, Copenhagen, Denmark, to evaluate temperature adjustment models. They conducted three trials on the same day, with average measured surface temperatures of 30.3 ℃, 33.7 ℃, and 37.1 ℃ for trials 1, 2, and 3, respectively. The team selected trials 1 and 3 for a detailed evaluation in this section due to their greater differences in average surface temperatures.

The researchers determined the AC layer thicknesses for pavement sections within the loop from ground-penetrating radar (GPR) data they had collected within the same year. The team calculated the AC middepth temperatures corresponding to each TSD measurement interval by using the BELLS2 equation (see Appendix A). They obtained the previous day's average air temperature, required for the BELLS2 equation, from the nearest weather station for each measurement. After using the BELLS2 equation, the research team calculated the average AC layer middepth temperatures for sections within the loop for trials 1 and 3 as 25.1 ℃ and 29.6 ℃, respectively.

The research team applied the proposed models for the temperature adjustments of deflection slopes and deflections (refer to figure 27 and figure 34) to each measurement to adjust them to a reference temperature of 25 ℃. The team selected the corresponding model constants for each TSD measurement selected from table 9 and table 10. The researchers performed all these processes by using a tool described in Appendix B.

Figure 38-A and figure 38-B through figure 48-A and figure 48-B illustrate the performance of temperature adjustment models on reported TSD deflections and measured deflection slopes at various positions. The top diagrams present reported and measured deflections or deflection slopes in two trials, whereas the bottom diagrams show the temperature adjusted values to 25 ℃. For each diagram, the researchers calculated the standard error of estimate (SEE) by using the equation shown in figure 37, to assess the consistency between two sets of measurements. The SEE quantifies the discrepancies (residuals) between paired measurements, providing a measure of repeatability.

$$SEE = \sqrt{\frac{\sum\left(Y_i - Y_i'\right)^2}{n}}$$

Figure 37. Equation. The standard error of estimate.

Where:

Y_i and Y_i' = paired measurements.

n = number of paired measurements in the database.

The calculated SEE is shown on each diagram. For clarity, the diagrams represent the values as a moving average over 10 measurements.

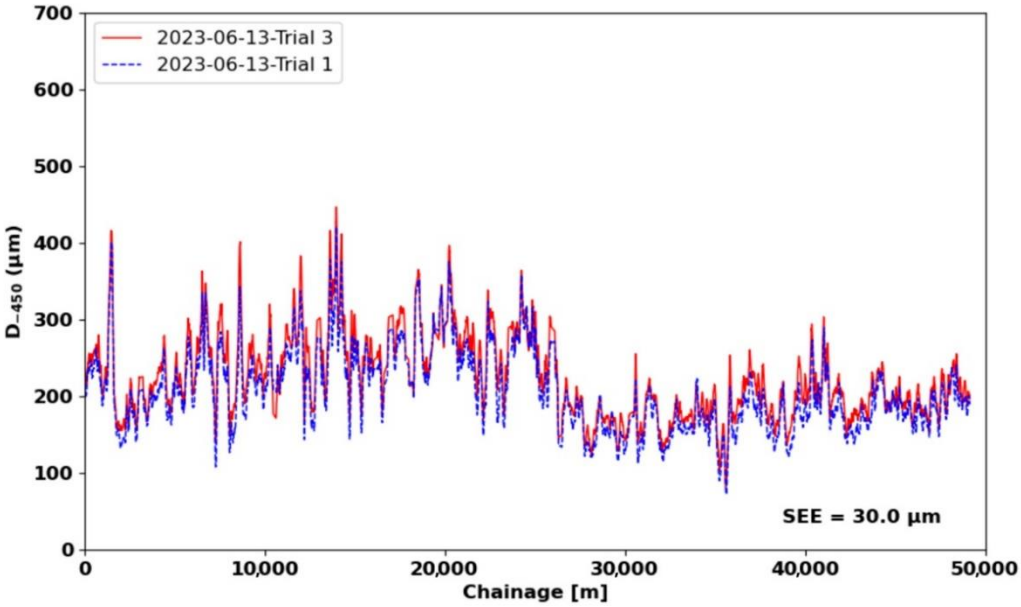

A. Measured D_{-450} at average AC layer middepth temperature of 25.1 °C and 29.6 °C in trials 1 and 3, respectively.

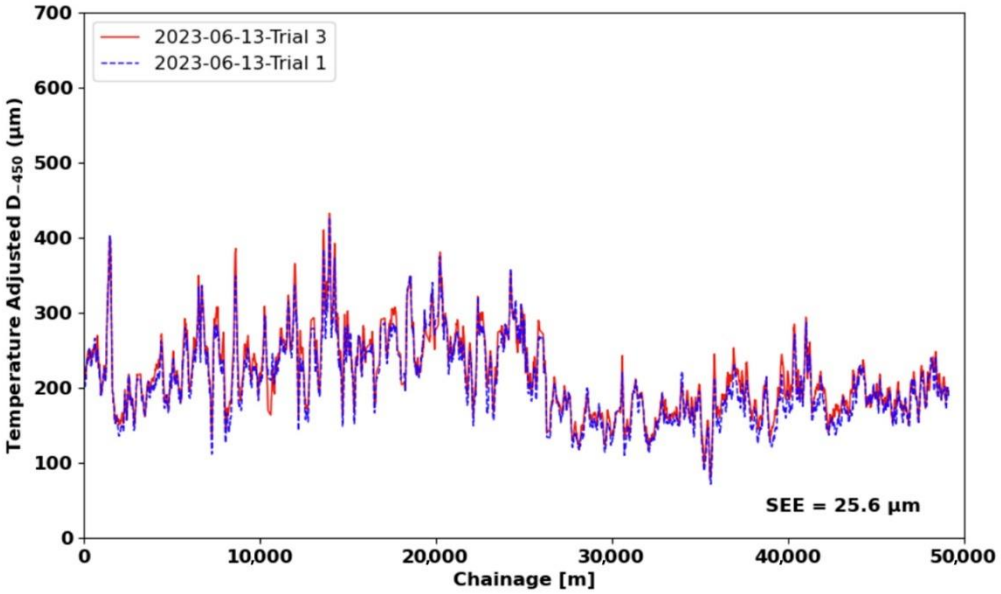

B. Temperature-adjusted D_{-450} in trials 1 and 3 adjusted to 25 °C.

All images source: FHWA.

Figure 38. Graphs. Measured D_{-450} and temperature-adjusted D_{-450} in trials 1 and 3.

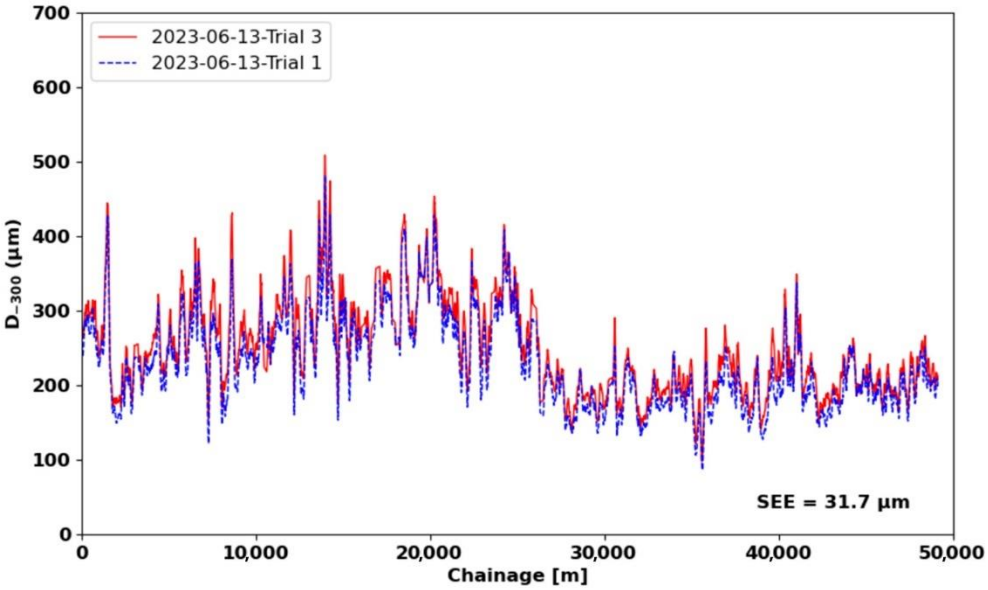

A. Measured D_{-300} at average AC layer middepth temperature of 25.1 °C and 29.6 °C in trials 1 and 3, respectively.

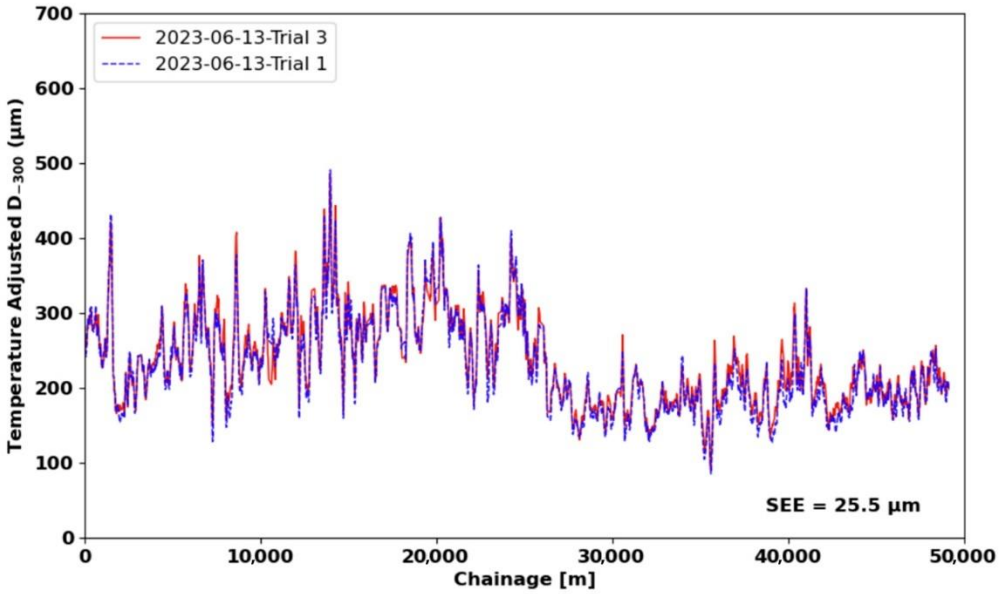

B. Temperature-adjusted D_{-300} in trials 1 and 3 adjusted to 25 °C.

All images source: FHWA.

Figure 39. Graphs. Measured D_{-300} and temperature-adjusted D_{-300} in trials 1 and 3.

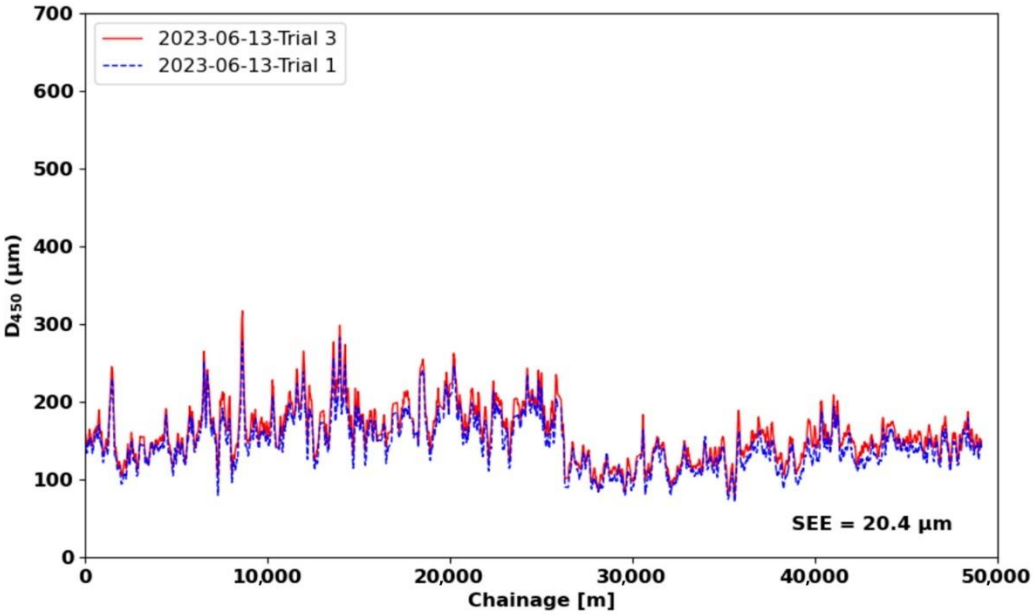

A. Measured D_{-200} at average AC layer middepth temperature of 25.1 °C and 29.6 °C in trials 1 and 3, respectively.

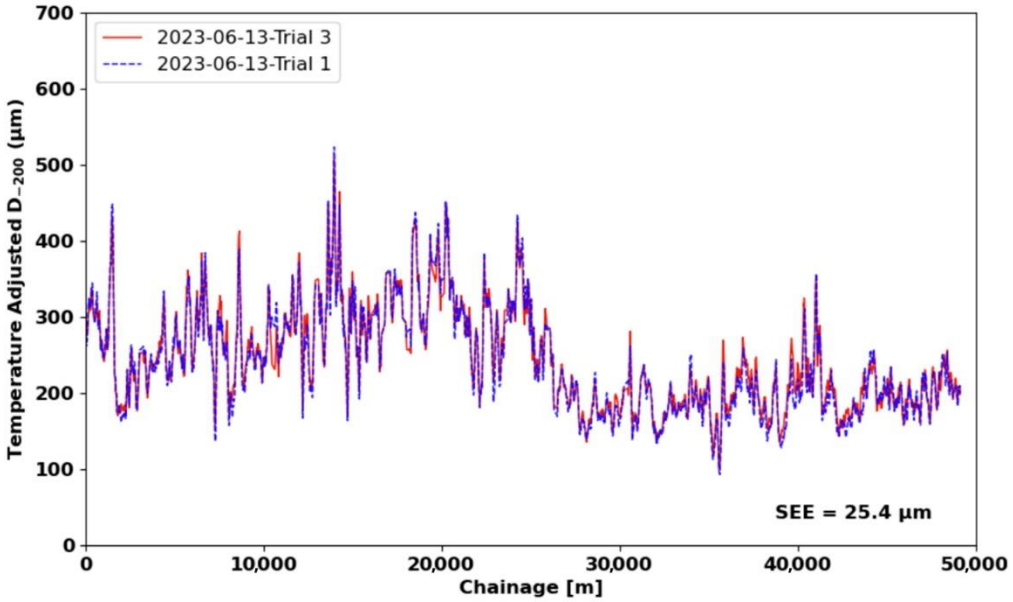

B. Temperature-adjusted D_{-200} in trials 1 and 3 adjusted to 25 °C.

All images source: FHWA.

Figure 40. Graphs. Measured D_{-200} and temperature-adjusted D_{-200} in trials 1 and 3.

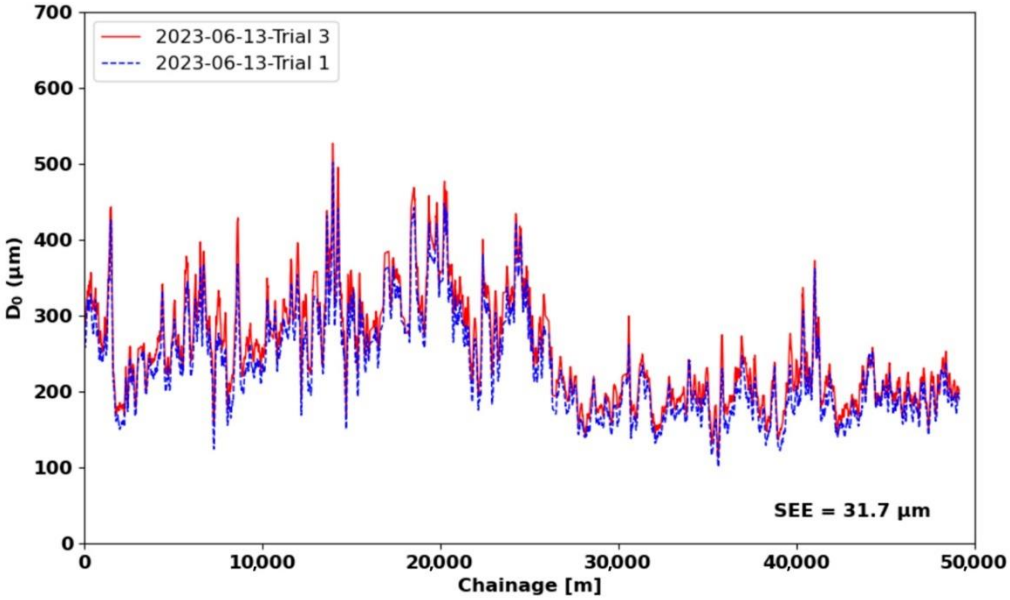

A. Measured D_0 at average AC layer middepth temperature of 25.1 °C and 29.6 °C in trials 1 and 3, respectively.

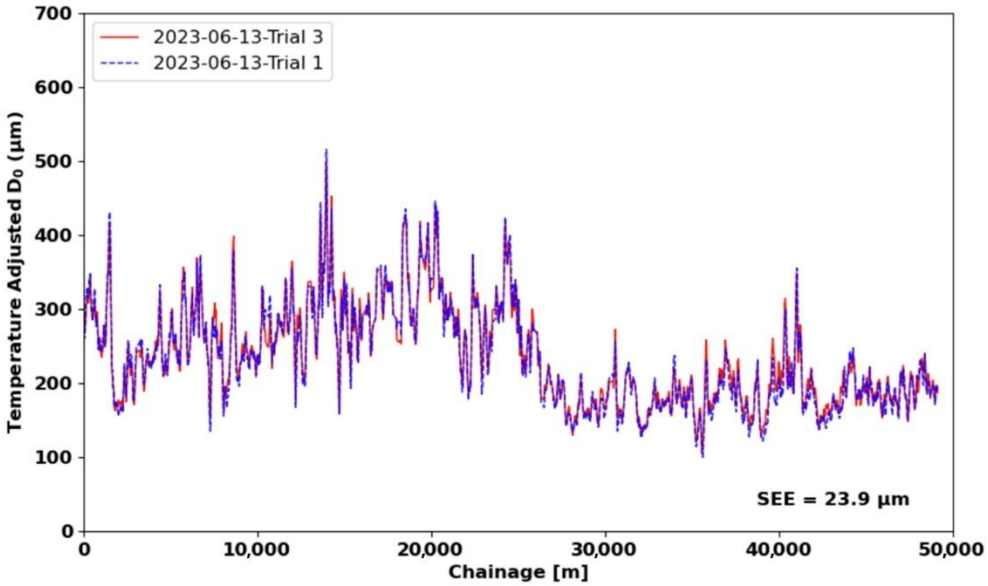

B. Temperature-adjusted D_0 in trials 1 and 3 adjusted to 25 °C.

All images source: FHWA.

Figure 41. Graphs. Measured D_0 and temperature-adjusted D_0 in trials 1 and 3.

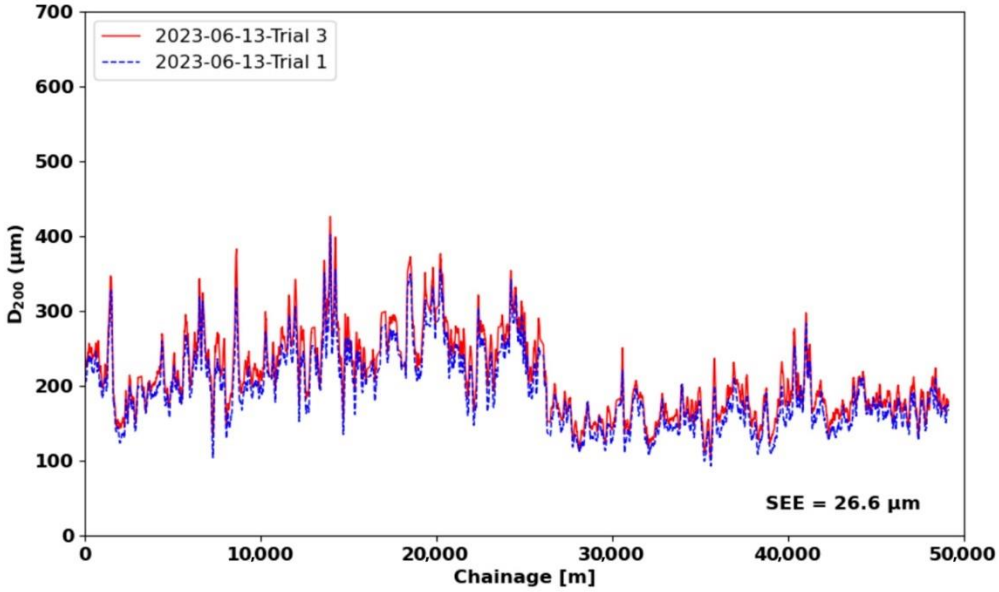

A. Measured D_{200} at average AC layer middepth temperature of 25.1 °C and 29.6 °C in trials 1 and 3, respectively.

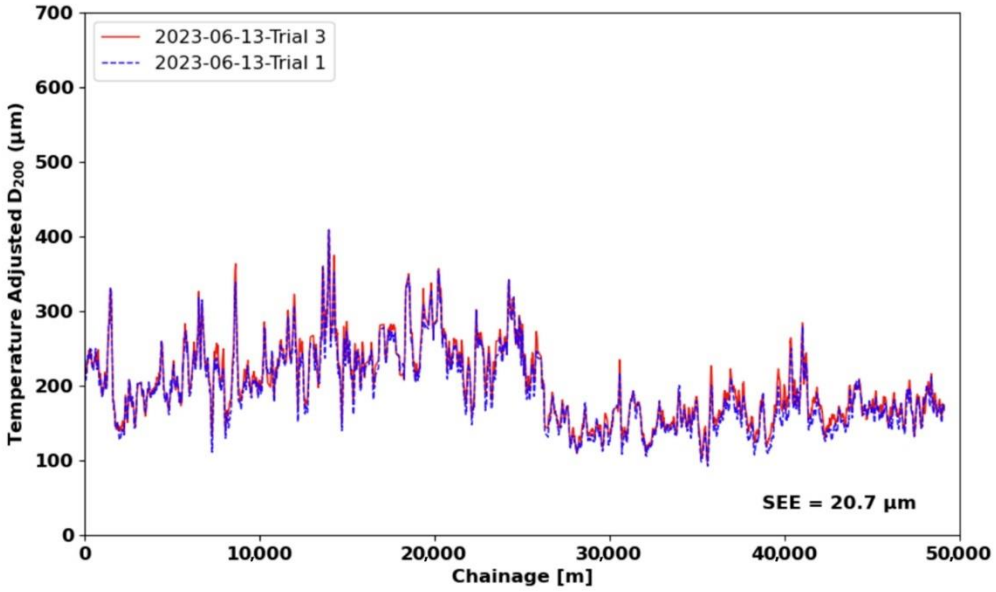

B. Temperature-adjusted D_{200} in trials 1 and 3 adjusted to 25 °C.

All images source: FHWA.

Figure 42. Graphs. Measured D_{200} and temperature-adjusted D_{200} in trials 1 and 3.

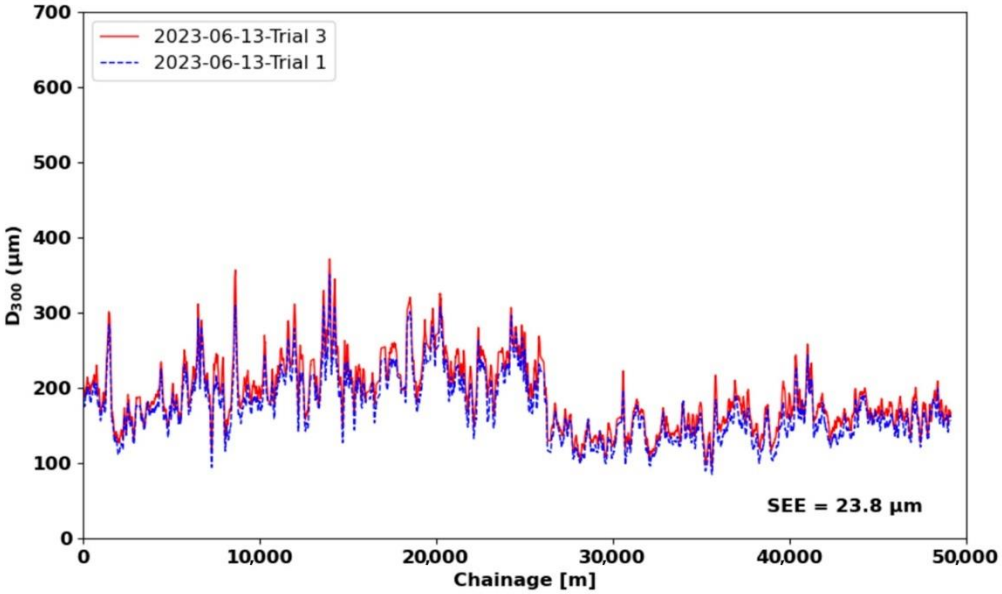

A. Measured D_{300} at average AC layer middepth temperature of 25.1 °C and 29.6 °C in trials 1 and 3, respectively.

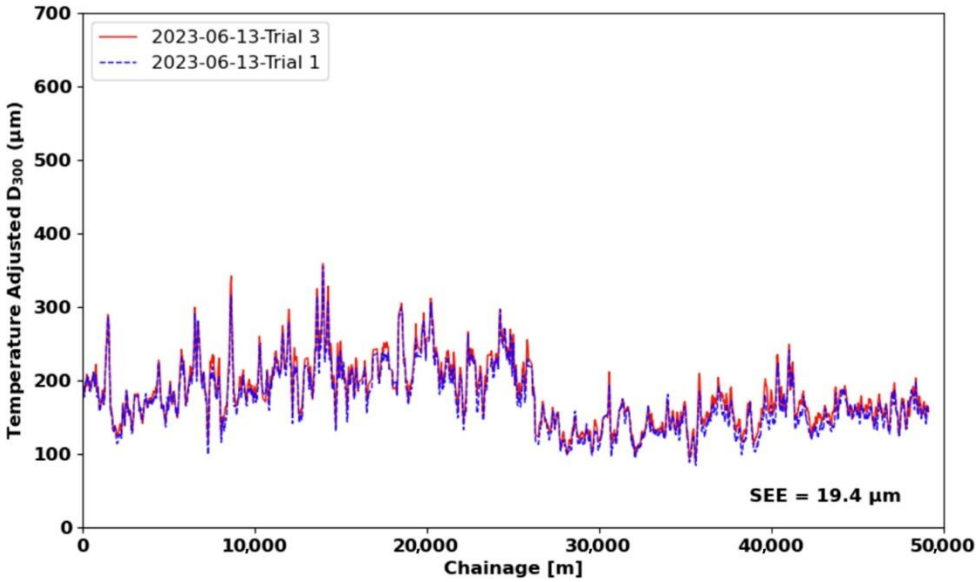

B. Temperature-adjusted D_{300} in trials 1 and 3 adjusted to 25 °C.

All images source: FHWA.

Figure 43. Graphs. Measured D_{300} and temperature-adjusted D_{300} in trials 1 and 3.

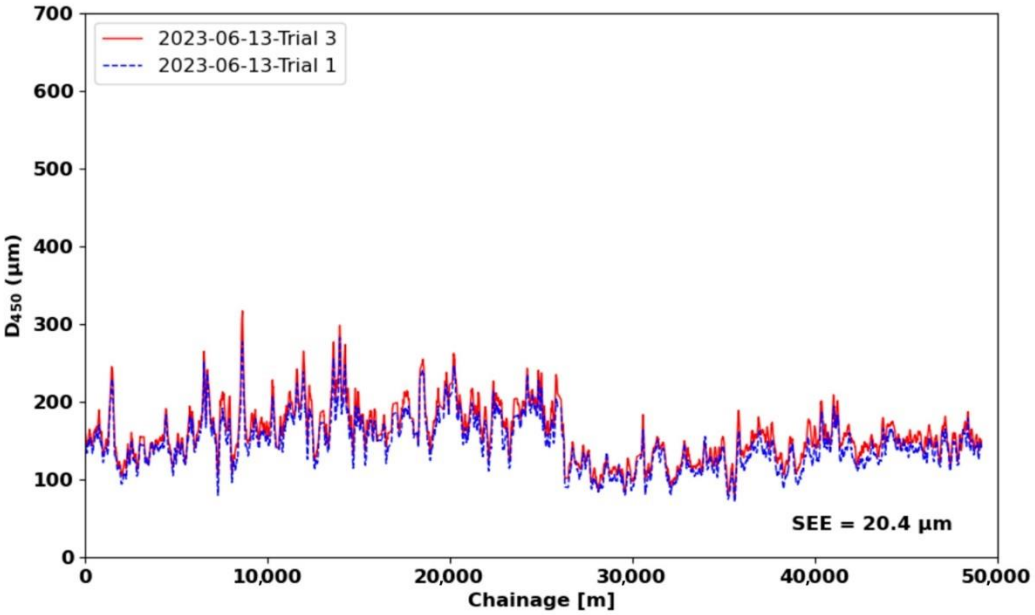

A. Measured D_{450} at average AC layer middepth temperature of 25.1 °C and 29.6 °C in trials 1 and 3, respectively.

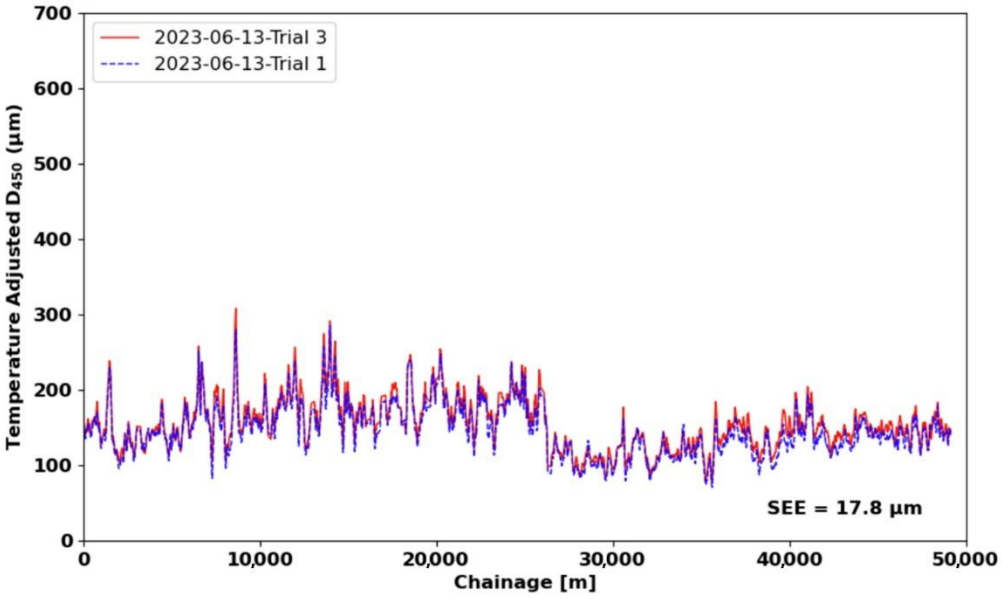

B. Temperature-adjusted D_{450} in trials 1 and 3 adjusted to 25 °C.

All images source: FHWA.

Figure 44. Graphs. Measured D_{450} and temperature-adjusted D_{450} in trials 1 and 3.

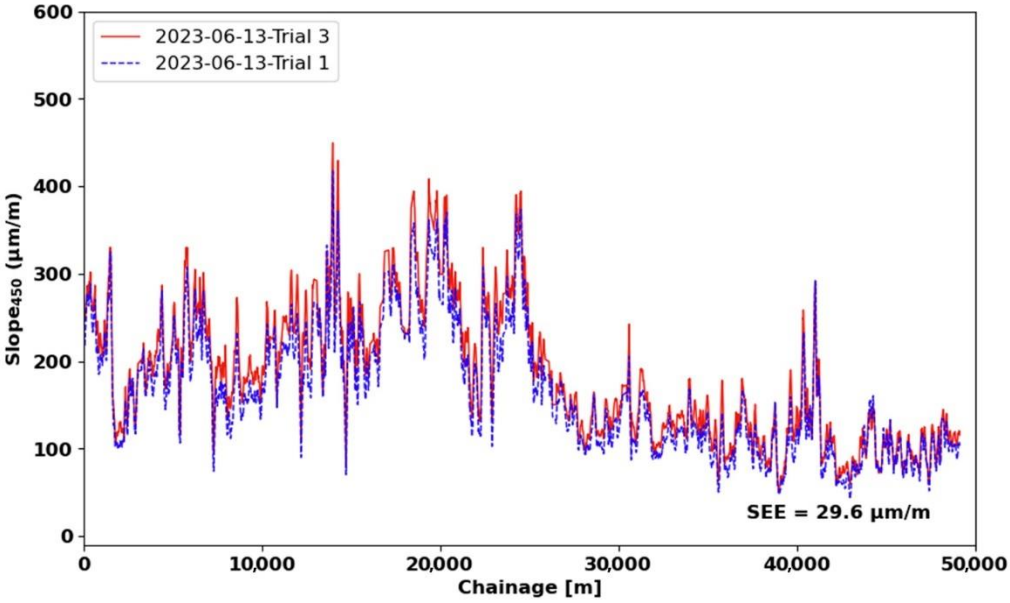

A. Measured S_{450} at average AC layer middepth temperature of 25.1 °C and 29.6 °C in trials 1 and 3, respectively.

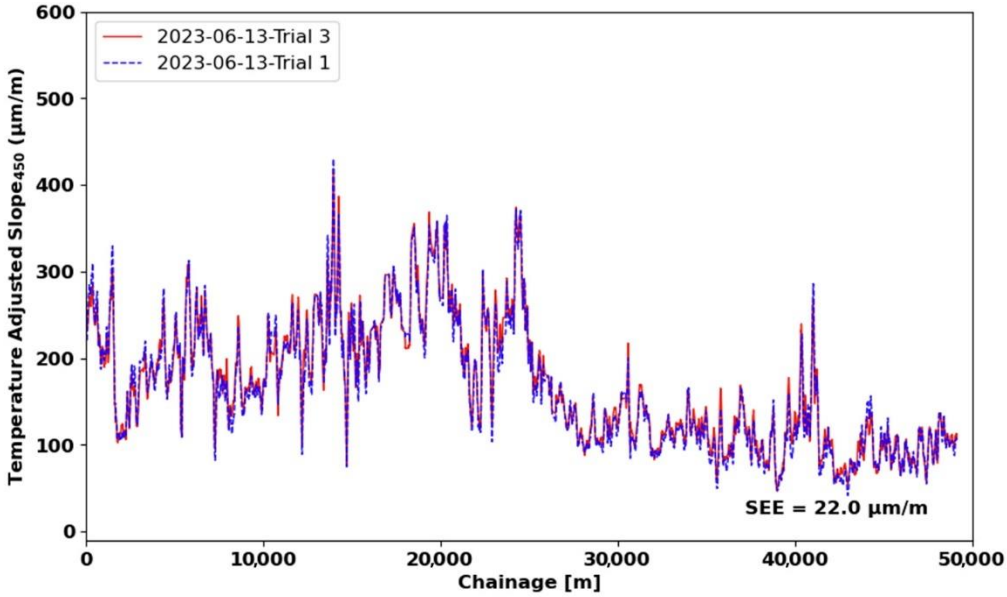

B. Temperature-adjusted S_{450} in trials 1 and 3 adjusted to 25 °C.

All images source: FHWA.

Figure 45. Graphs. Measured S_{450} and temperature-adjusted S_{450} in trials 1 and 3.

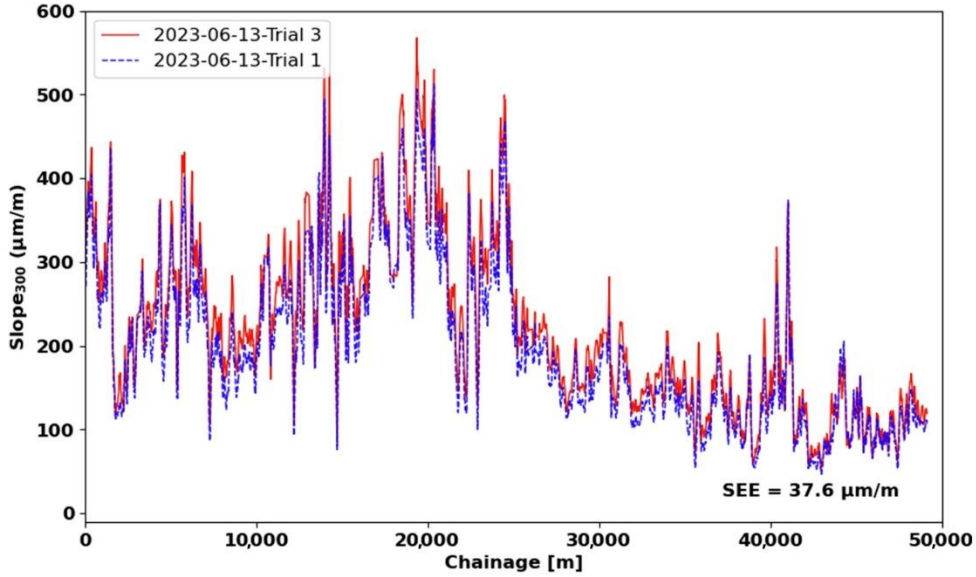

A. Measured S_{300} at average AC layer middepth temperature of 25.1 °C and 29.6 °C in trials 1 and 3, respectively.

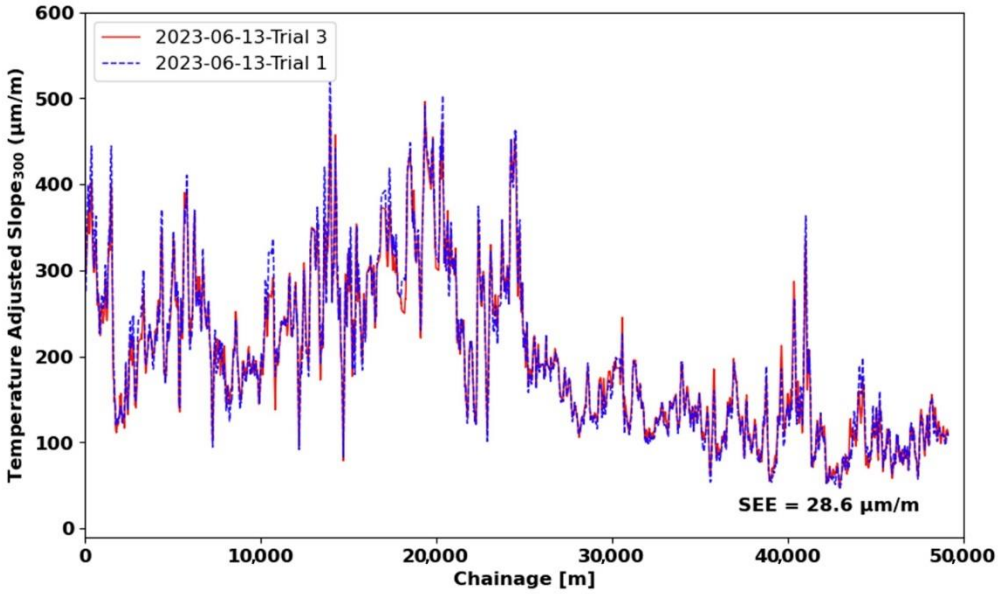

B. Temperature-adjusted S_{300} in trials 1 and 3 adjusted to 25 °C.

All images source: FHWA.

Figure 46. Graphs. Measured S_{300} and temperature-adjusted S_{300} in trials 1 and 3.

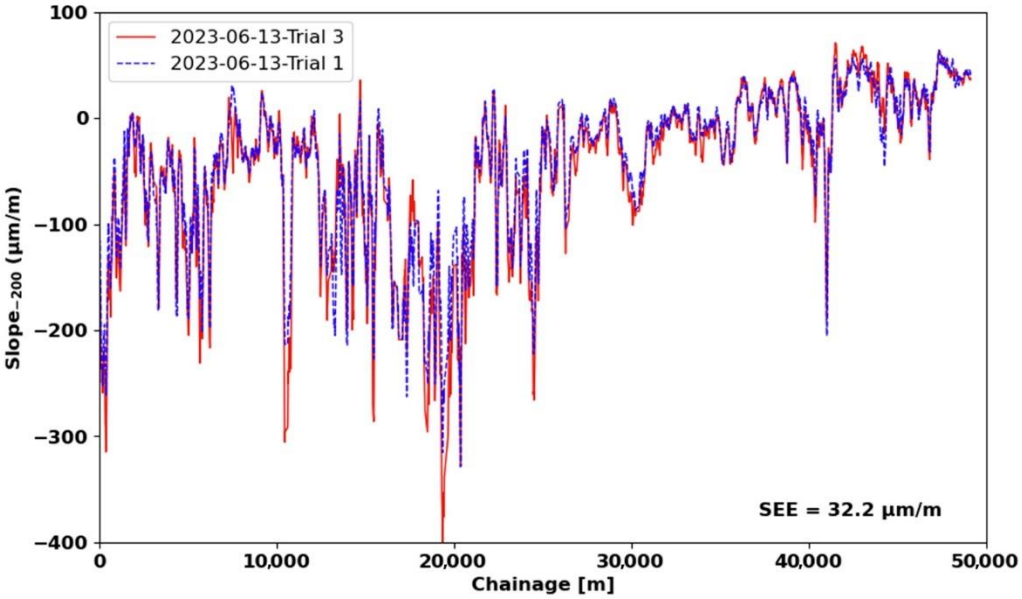

A. Measured S_{-200} at average AC layer middepth temperature of 25.1 ℃ and 29.6 ℃ in trials 1 and 3, respectively.

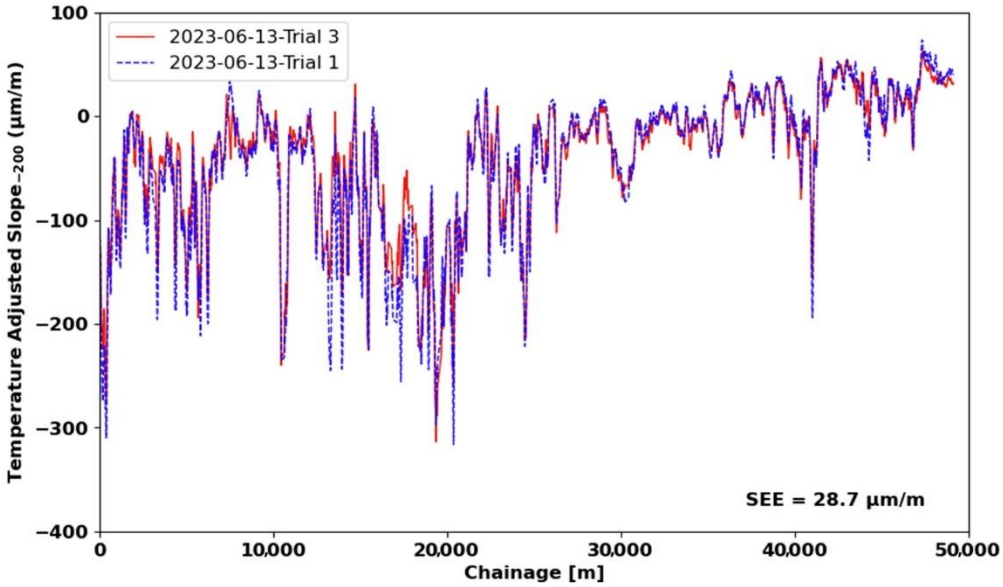

B. Temperature-adjusted S_{-200} in trials 1 and 3 adjusted to 25 ℃.

All images source: FHWA.

Figure 47. Graphs. Measured S_{-200} and temperature-adjusted S_{-200} in trials 1 and 3.

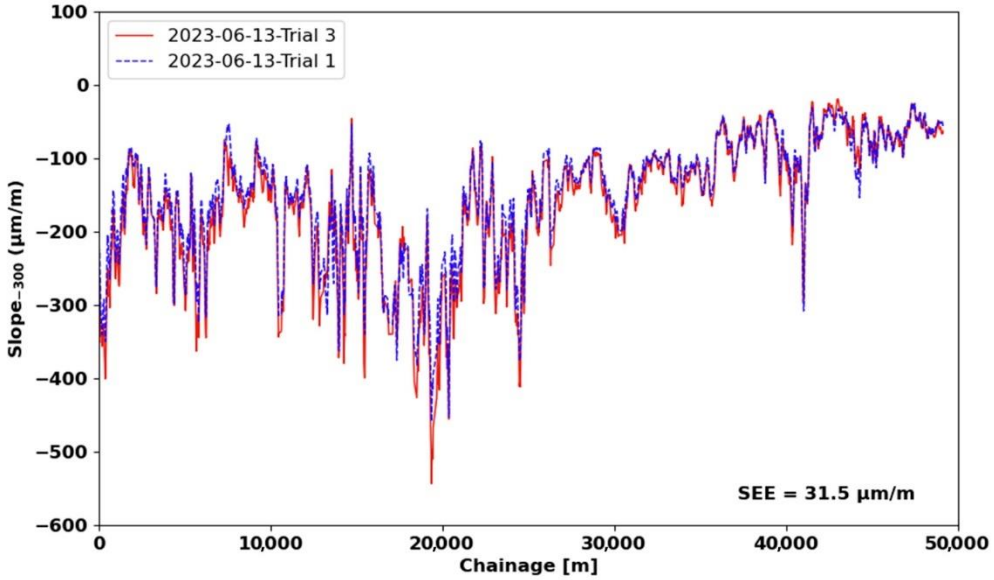

A. Measured S_{-300} at average AC layer middepth temperature of 25.1 °C and 29.6 °C in trials 1 and 3, respectively.

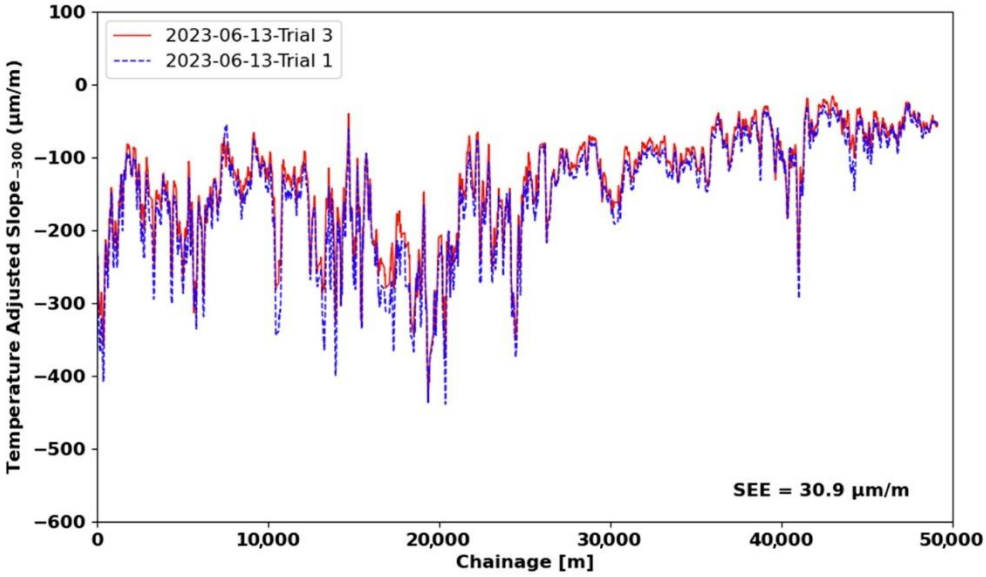

B. Temperature-adjusted S_{-300} in trials 1 and 3 adjusted to 25 °C.

All images source: FHWA.

Figure 48. Graphs. Measured S_{-300} and temperature-adjusted S_{-300} in trials 1 and 3.

Despite a modest difference of 4.5 °C in the average middepth AC layer temperature between the two trials, trial 3, with the higher temperature, generally yielded higher measurements across most sections of the loop. However, following the application of temperature adjustment, the measurements from both trials converged, aligning them to the same reference temperature. Furthermore, SEE values in the temperature-adjusted diagrams are notably reduced compared with those values at the original temperatures. These comparisons provide compelling evidence of the effective performance of the temperature adjustment models.

Figure 49-A and figure 49-B display the measured SCI values from trials 1 and 3, alongside the temperature-adjusted SCI derived from the equation provided in figure 32. As illustrated, the SEE for the temperature-adjusted values is lower, indicating the convergence of data following temperature adjustment.

Within pavement management systems, assessing changes in the structural capacity of pavement over time is crucial. The research team compared TSD data collected from this loop in August 2020 and June 2023 to assess the role of temperature adjustment models in ensuring consistent monitoring of structural changes over time. The team calculated the average middepth temperature of the AC layer at 29.9 °C for TSD data collected in August 2020. They made comparisons between the SCIs measured in 2020 and those from one of the 2023 tests (trial 1), with an average AC layer temperature of 25.1 °C, as depicted in figure 50-A. As expected, traffic over 3 yr likely resulted in some degree of asphalt layer deterioration. However, interpreting structural index changes is challenging due to the compounded effects of temperature and deterioration.

The research team used the equation presented in figure 32 to adjust the SCIs for temperature to a reference temperature of 20 °C, as illustrated in figure 50-B. This adjustment facilitated a clearer assessment of structural index changes. Significantly, for most sections, the SCI values that the team observed in 2023 were higher, indicating increased deterioration. This outcome showcases how an implemented temperature adjustment model assists in interpreting the structural capacity of pavements over time.

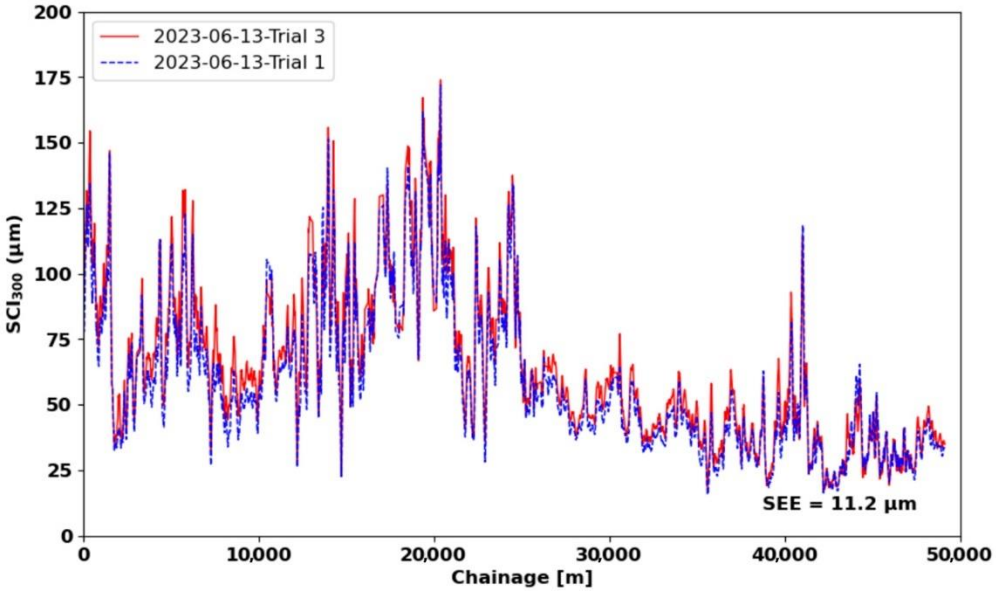

A. Measured SCI at average AC layer middepth temperature of 25.1 °C and 29.6 °C in trials 1 and 3, respectively.

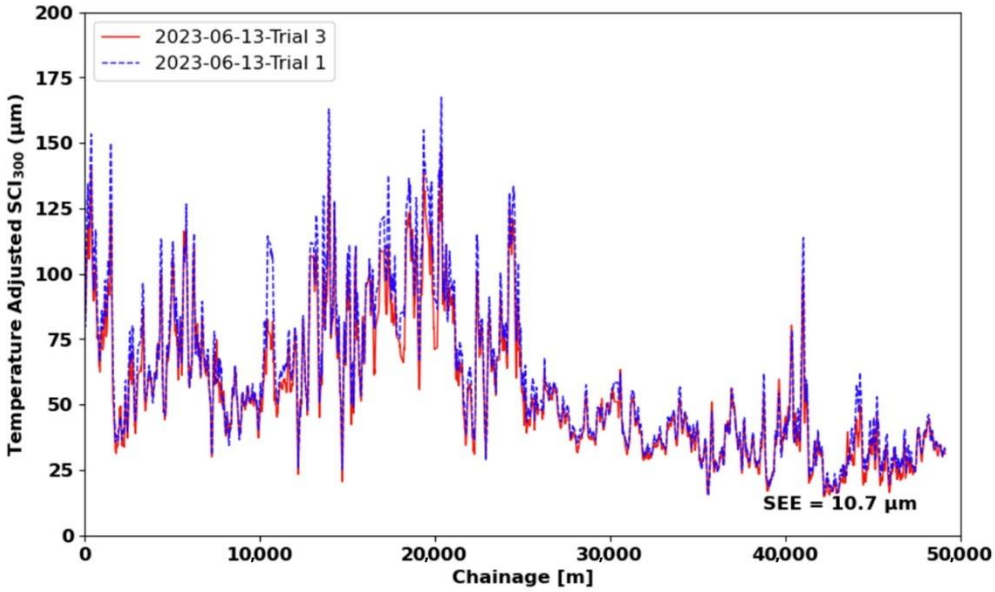

B. Temperature-adjusted SCI in trials 1 and 3 adjusted to 25 °C.

All images source: FHWA.

Figure 49. Graphs. Measured SCI and temperature-adjusted SCI in trials 1 and 3.

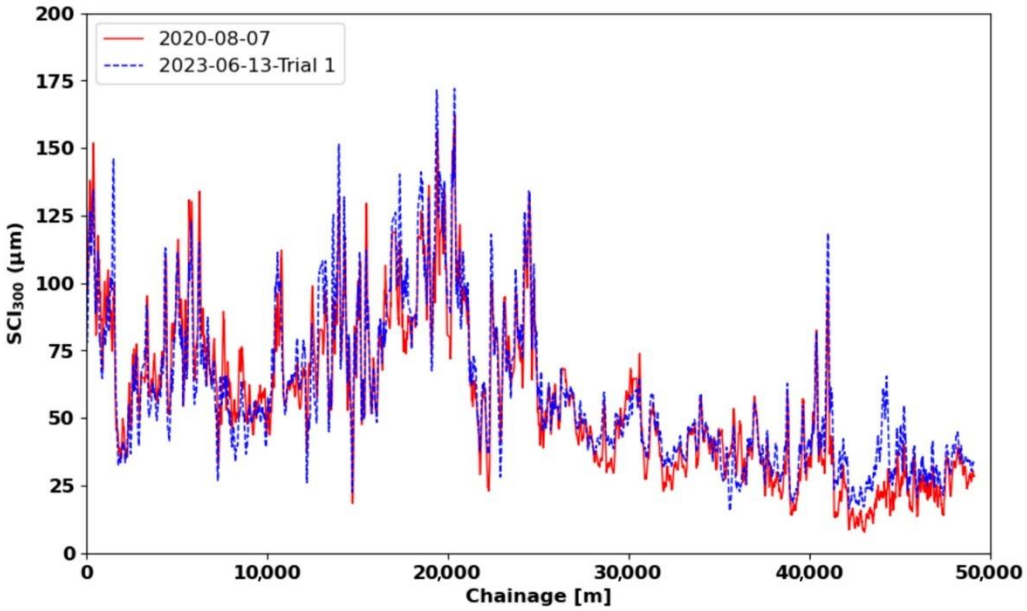

A. Measured SCI from the August 2020 trial and trial 1 (June 2023) with average AC layer middepth temperatures of 29.9 ℃ and 25.1 ℃, respectively.

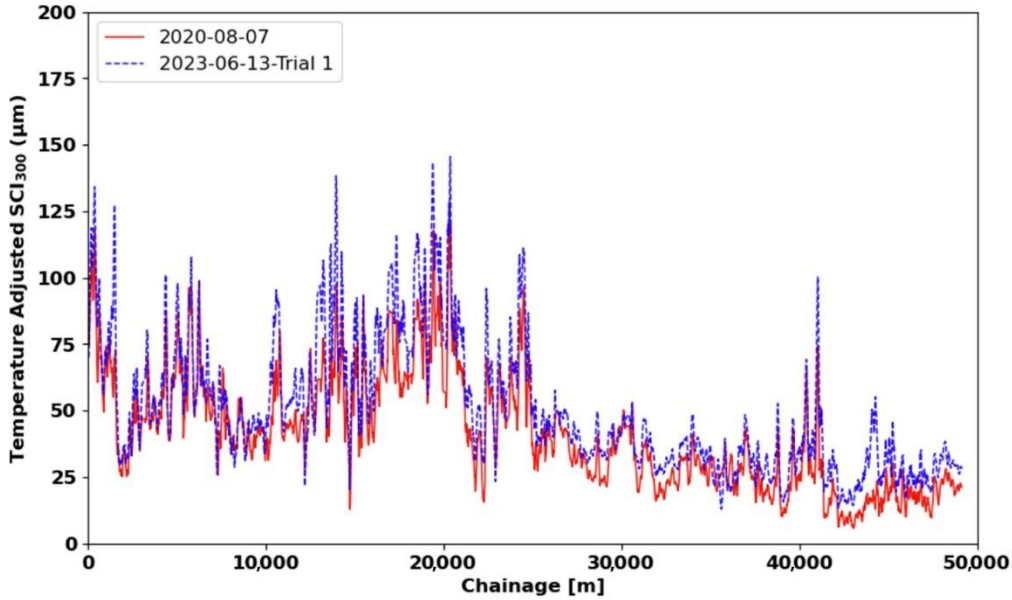

B. Temperature-adjusted SCI from the August 2020 trial and trial 1 (June 2023) adjusted to 20 ℃.

All images source: FHWA.

Figure 50. Graphs. Measured SCI and temperature-adjusted SCI from the August 2020 trial and trial 1 (June 2023).

CHAPTER 9. CONCLUSIONS

In recent years, highway agencies have increasingly shown interest in using TSDD data to gather pavement structural information across their entire networks. The pavement structural responses measured by TSDD, including deflection velocities, deflection slopes, and deflections, are highly sensitive to the temperature of the AC layer. To ensure a consistent interpretation of collected structural data, temperature adjustment needs to be applied to the TSDD measurements.

The researchers chose a wide selection of pavement structures from the FHWA LTPP program across the United States and Canada, and they simulated the TSDD measurements on these sections under various AC layer temperatures and binder types using a validated viscoelastic tool. The analyses yielded more than 250,000 cases, ensuring a broad and wide range of possible scenarios to develop comprehensive models.

The study team evaluated the influence of temperature on TSDD measurements and noted variations based on the thickness of the AC layer. As the AC layer thickness increases, the temperature influence zone widens. Specifically, in thinner AC layers (<100 mm), TSDD deflections within approximately 500 mm on either side of the center of dual tires are primarily affected by temperature. However, in thicker layers (>400 mm), this influence zone expands to approximately 1,500 mm from the center of dual tires.

The team defined temperature adjustment factors as the ratio of deflection slopes or deflections at the reference temperature to those at the measurement temperature. They proposed a functional form for temperature adjustment factors for deflection slopes and deflections and suggested model constants for various measurements at different positions. The model incorporates the temperature at the time of measurement, as well as the reference temperature and the thickness of the AC layer. The middepth AC layer temperature at the time of measurements should be used in the model, which can be estimated from the measured surface temperature and other pertinent parameters using models such as the BELLS2 equation. The AC layer thickness can be determined from coring, GPR, or construction history. Although the research team used only one vehicle speed in creating the database, the effect of vehicle speed on temperature adjustment factors is insignificant. Therefore, the developed models can be used with operational TSDD vehicle speeds.

This report includes a Python script that implements the temperature adjustment of TSDD slopes and deflections. This tool can calculate the AC layer middepth temperature from the GPS location, date and time of measurements, and measured surface temperature. The tool then applies the developed temperature adjustment models to the measurements. Users can modify this script based on their custom requirements and the specific format of the reporting file.

APPENDIX A. EVALUATION OF THE EFFECT OF TEMPERATURE GRADIENT

The temperature adjustment models developed and presented in the previous chapters use the middepth temperature of the AC layer during testing for adjustments, assuming indirectly uniform temperature across the entire layer. While this assumption aligns with similar temperature adjustment approaches reported in the literature (e.g., AASHTO 1993; Lukanen, Stubstad, and Briggs 2000), uniform temperature distribution is not often the case, and this section evaluates how temperature gradients affect the calculated temperature adjustment factors.

The research team chose two distinct structural cases, Structure 1 and Structure 2, each with three middepth AC layer temperatures (10, 20, and 30 °C), for evaluation. Table 11 displays the pavement structures alongside the temperature adjustment factors for SCIs corresponding to each temperature.

Table 11. Selected cases for temperature gradient evaluation.

St. Number	AC Layer Thickness (mm)	Base Layer Thickness (mm)	Base Modulus (MPa)	Subgrade Modulus (MPa)	Binder Type	Uniform AC Layer Temperature (°C)	λ_{sci} from Database (ELLVA Analyses)
1	198	302	108	49	70–16	10	1.6455
1	198	302	108	49	70–16	20	1.0000
1	198	302	108	49	70–16	30	0.6397
2	297	302	108	49	70–16	10	1.7407
2	297	302	108	49	70–16	20	1.0000
2	297	302	108	49	70–16	30	0.6044

St. = structure.

The BELLS2 model (Lukanen, Stubstad, and Briggs 2000) is widely used to determine the temperature at various depths of pavements, as shown in figure 51.

$$T_d = 2.78 + 0.912 \times IR + \{log(d) - 1.25\} \times \{-0.428 \times IR + 0.553 \times (1 - day) + 2.63 \times sin(hr_{18} - 15.5)\} + 0.027 \times IR \times sin(hr_{18} - 13.5)$$

Figure 51. Equation. BELLS2 formula.

Where:

T_d = pavement temperature at depth "*d*" (°C).
IR = pavement surface temperature (°C).
d = depth at which temperature will be predicted (mm).
1-day = average air temperature on the day before to testing (°C).
sin = sine function on an 18-h clock system, where 2π radians equals one 18-h cycle.
hr_{18} = time of day in a 24-h clock system, but calculated using an 18-h AC temperature rise-and-fall time cycle, as illustrated in figure 52.

The BELLS2 equation can be employed during TSDD measurements to estimate the middepth AC layer temperature, which is essential for implementing the temperature adjustment models developed and presented in this report. In this section, the equation is used to determine the temperature gradient within the AC layer for the aforementioned two structures, assuming a middepth temperature of 10, 20, or 30 °C.

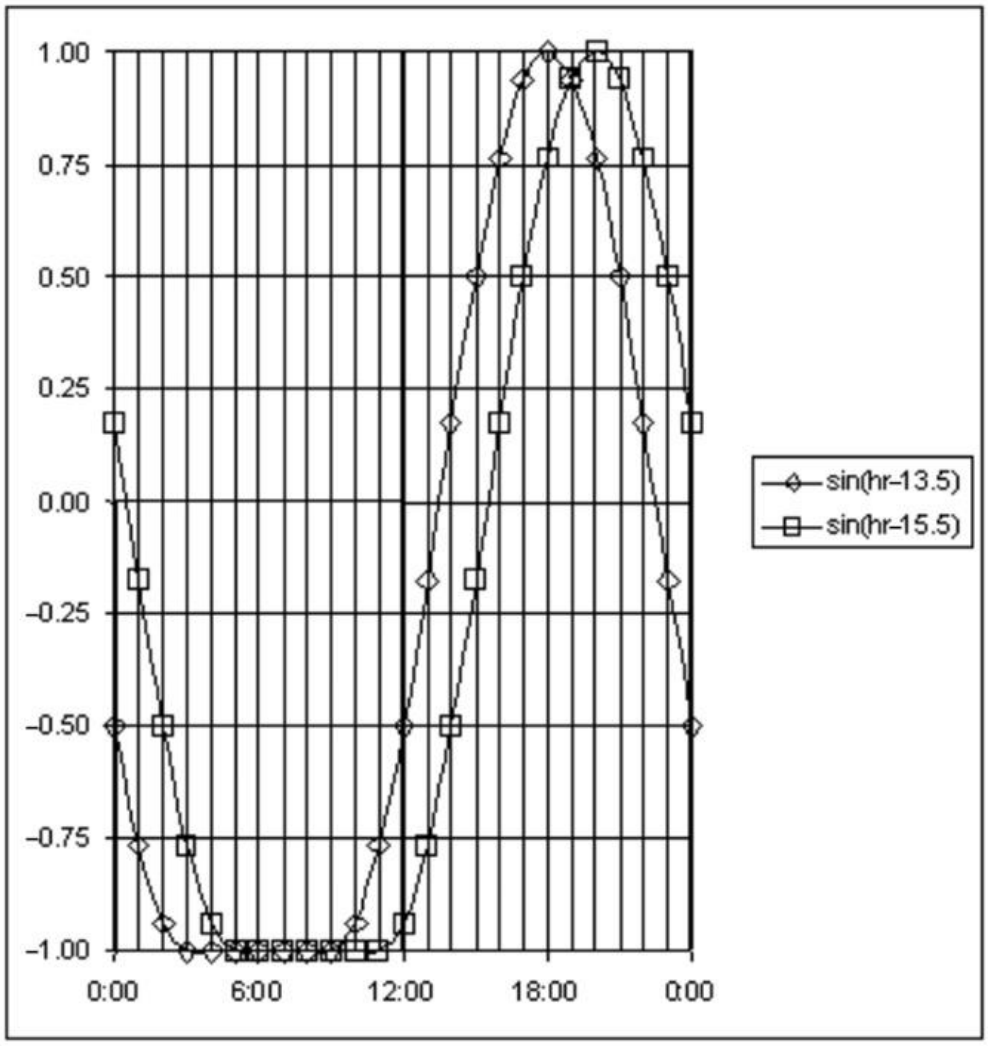

Source: FHWA.

Figure 52. Graph. 18-h sine function used in BELLS equations (Lukanen, Stubstad, and Briggs 2000).

Since temperature gradients vary between morning and afternoon, the research team assessed the temperature gradients for Structure 1 and Structure 2 at two times during the day: 10 a.m. and 4 p.m. Figure 53-A and figure 53-B illustrate the temperature gradients for these structures at these two time points, with middepth temperatures set to 10, 20, and 30 °C. To fulfill this requirement, the research team adjusted the pavement surface temperature (IR) in the equation accordingly. An average air temperature of 18 °C the day before (1 d) was assumed for all gradients. Because temperature gradients in the afternoon exhibit slightly more variability within the AC layer, the team selected them for further analyses.

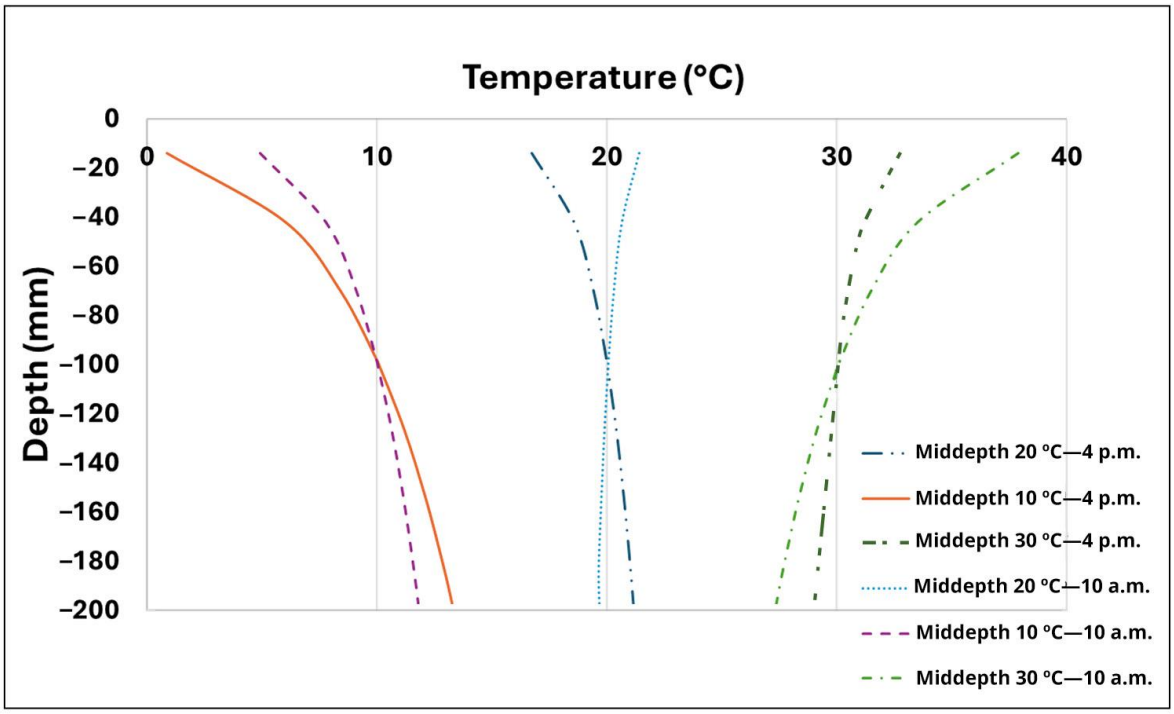

A. Temperature gradients with 198 mm AC layer thickness.

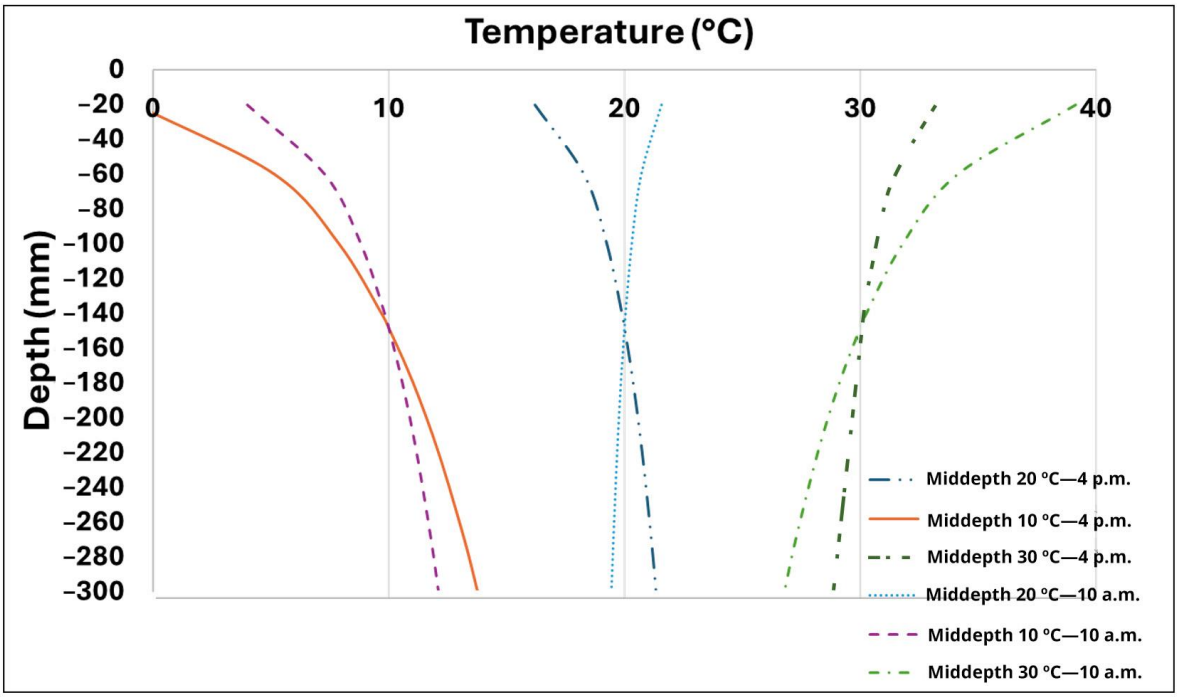

B. Temperature gradients with 297 mm AC layer thickness.

All images source: FHWA.

Figure 53. Graphs. Temperature gradients at two times during the day when middepth temperatures are 10, 20, and 30 °C for two structures with different AC layer thicknesses.

Subsequently, the research team assessed the impact of incorporating temperature gradients instead of assuming a uniform temperature at the middepth of the AC layer on the temperature adjustment factor. This analysis specifically targeted the SCI temperature adjustment factor, which has been shown to be highly sensitive to temperature variations. To conduct this investigation, the team analyzed the structures with temperature gradients, necessitating the division of the AC layer into sublayers, each characterized by its own temperature.

Because the ELLVA software limits the analysis to five layers, it was not suitable for this purpose. Therefore, the researchers used an alternative validated viscoelastic program, known as 3D-Move, which was developed at the University of Nevada, Reno (University of Nevada, Reno 2024). 3D-Move allows for the modeling of up to 10 layers, including 3 underlying layers (base, subgrade, and bedrock), thus accommodating the division of the AC layer into 7 sublayers.

Consequently, the researchers divided the AC layer of Structure 1 and Structure 2 into seven sublayers, and they determined the temperature at the middepth of each sublayer from the temperature gradient.

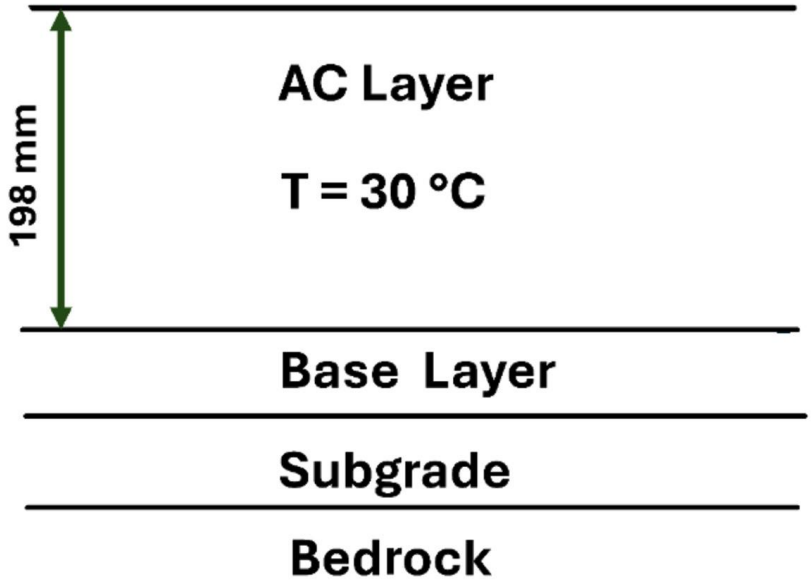

A. Uniform temperature equal to the middepth temperature of 30 °C.

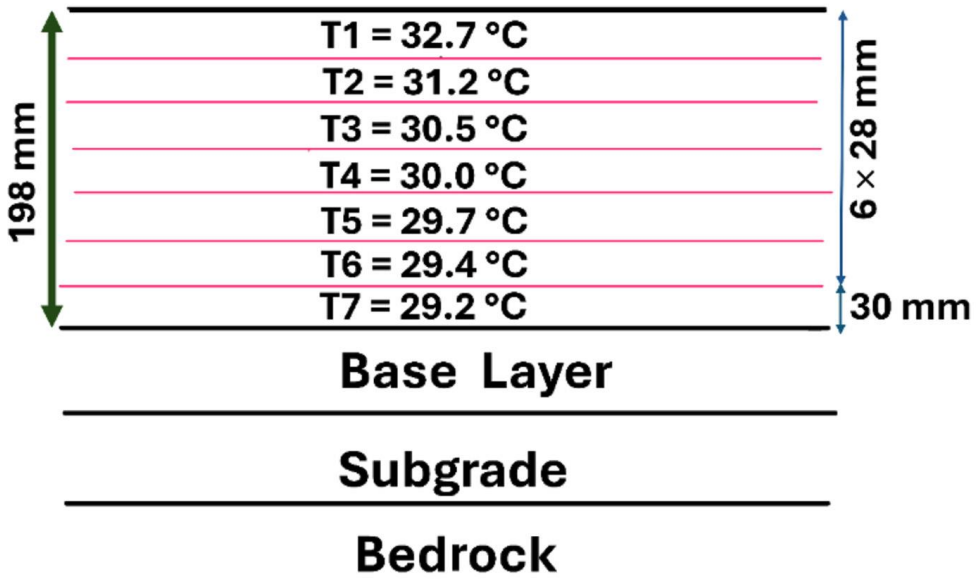

B. Nonuniform temperature distribution with a middepth temperature of 30 °C.
All images source: FHWA.

Figure 54-A illustrates Structure 1 with a 197 mm AC layer, assuming a uniform temperature of 30 °C throughout the AC layer. Figure 54-B depicts the same structure with the AC layer segmented into seven sublayers: six layers of 28 mm each and a final layer of 30 mm. The temperature at the middepth of each sublayer is calculated from the temperature gradient AC layer segmented into seven sublayers: six layers of 28 mm each and a final layer of 30 mm. The temperature at the middepth of each sublayer is calculated from the temperature gradient.

The research team computed the dynamic moduli for each sublayer and used them in the 3D-Move analyses. The team performed two 3D-Move analyses for each of the three selected temperatures (10, 20, and 30 °C) for both structures. In the first analysis, the researchers uniformly set the AC layer temperature to the specific temperature being evaluated. In contrast, the second analysis involved a nonuniform AC layer temperature, adjusting the middepth temperature to correspond to the specified temperature.

Figure 55-A and figure 55-B show the deflection bowls from the 3D-Move analyses. Solid lines represent cases with uniform AC layer temperatures, while dotted lines depict deflection bowls for nonuniform temperature distributions. Across both structures and all three middepth temperatures considered, the team observed minimal differences between the deflection bowls.

Figure 56 compares the SCI temperature adjustment factors (λ_{SCI}) for the two structures, presenting two sets of adjustment factors: one derived from 3D-Move analyses, assuming a uniform temperature distribution, and the other incorporating temperature gradient effects with nonuniform temperature distribution. The diagram visually demonstrates minimal difference in λ_{SCI} values between the two approaches. This observation suggests that assuming a uniform middepth temperature distribution within the AC layer does not notably affect the accuracy of the database or the developed temperature adjustment models.

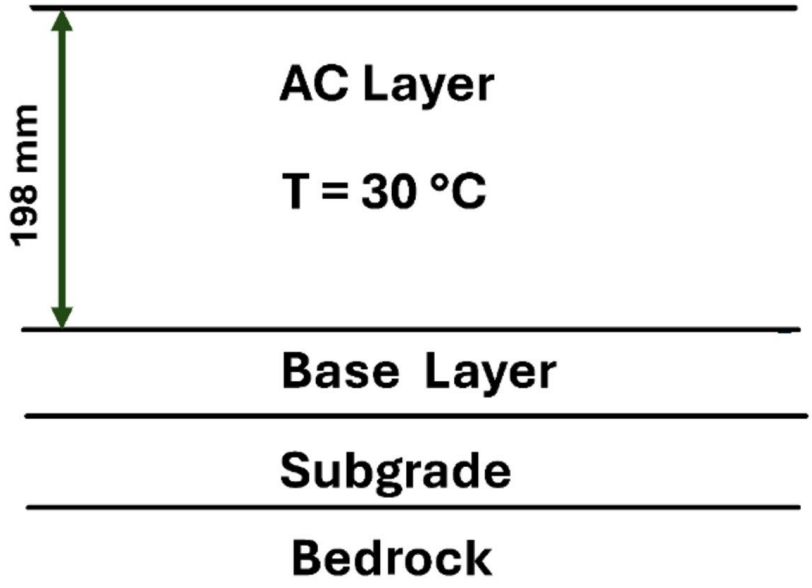

A. Uniform temperature equal to the middepth temperature of 30 °C.

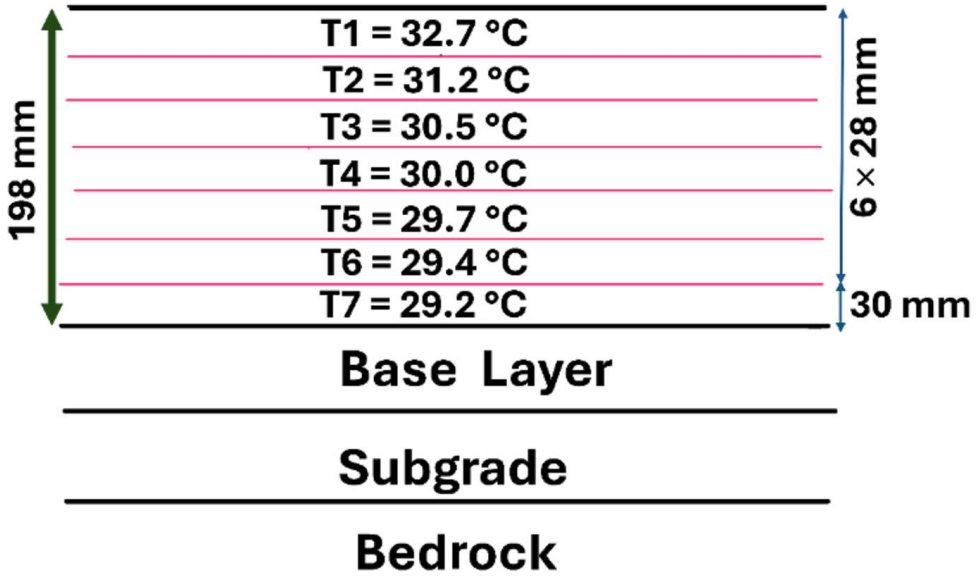

B. Nonuniform temperature distribution with a middepth temperature of 30 °C.

All images source: FHWA.

Figure 54. Illustrations. Structure No. 1 with an AC layer thickness of 198 mm analyzed using 3D-Move.

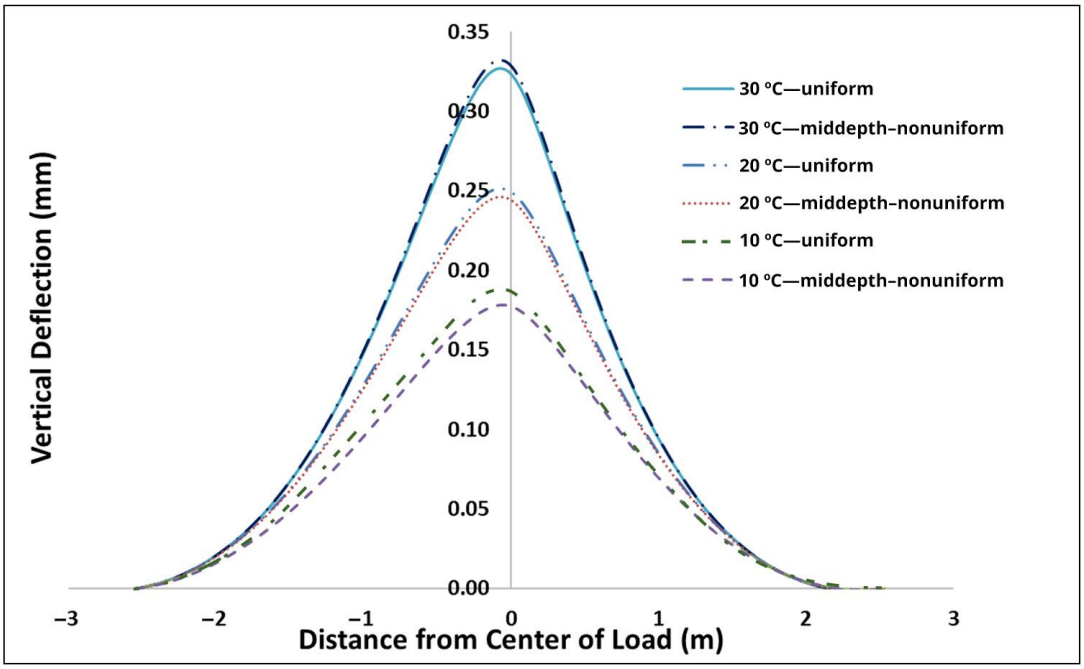

A. AC layer thickness (198 mm).

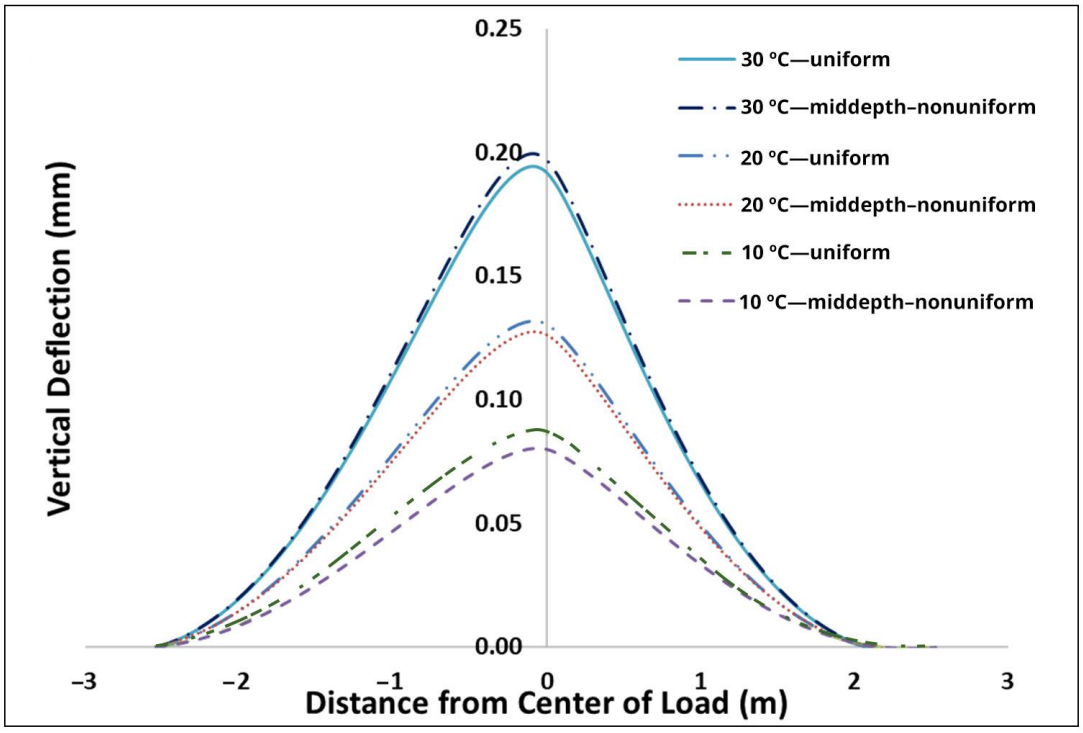

B. AC layer thickness (297 mm).

All images source: FHWA.

Figure 55. Graphs. Deflection bowls from 3D-Move analyses for uniform and nonuniform temperature distribution when middepth temperatures are 10, 20, and 30 °C for two structures with different AC layer thicknesses.

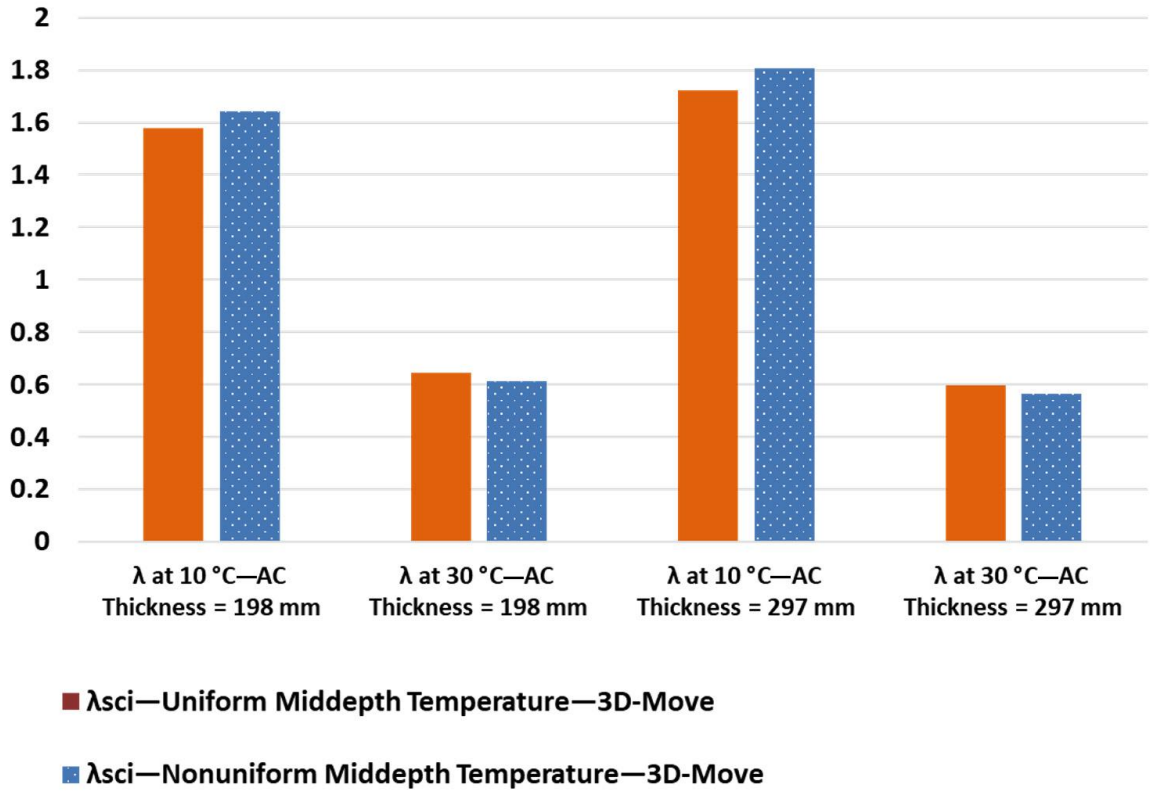

Source: FHWA.

Figure 56. Graph. Comparison of SCI temperature adjustment factors between uniform and nonuniform temperature distributions.

APPENDIX B. EXAMPLE PROGRAM FOR CALCULATING AC LAYER MIDDEPTH TEMPERATURE AND TEMPERATURE-CORRECTED TSDD MEASUREMENTS

The source code presented in figure 57 aims to streamline the implementation of proposed temperature adjustment models in this report. This Python script is tailored to handle data stored in a Microsoft® Excel® file, execute computations using predefined coefficients and mathematical models, and produce output files containing corrected temperature measurements for selected reference temperatures. The following overview depicts its functionality:

1. **Libraries and Modules**: The script imports necessary libraries such as 'tkinter' for creating a GUI, 'pandas' for data manipulation, 'numpy' for numerical calculations, 're' for regular expressions, 'math' for mathematical operations, 'datetime' for handling date and time, 'meteostat' for fetching weather data, and 'dateutil.parser' for parsing dates. The user should ensure that all these libraries are properly installed before running the code.

2. **Model Coefficients**: The script defines two dictionary-named deflection and slope coefficients, which store model coefficients corresponding to specific deflection and deflection slope positions (table 9 and table 10).

3. **Functions**:

    - 'extract_lambda': This function extracts corresponding temperature model coefficients for deflections provided in input files.

    - 'extract_slope': This function extracts corresponding temperature model coefficients for deflection slopes provided in input files.

    - 'BELLS2': This function implements the BELLS2 model (figure 51) for estimating asphalt middepth temperature based on input parameters.

    - 'get_avg_temperature': This function fetches the average previous day air temperature for a given coordinate and date using the meteostat library. This parameter is required in BELLS2 function.

    - 'temperature_correction': This function calculates temperature adjustment factors for deflections and slopes based on model coefficients and input parameters.

    - 'process_excel': This function processes the input Excel file, and generates output files with corrected temperature deflections and derived parameters.

    - 'browse_input_file': This function opens a file dialog to browse and select the input Excel file.

    - 'process_file': This function retrieves the input file path from the graphical user interface (GUI) entry field and initiates the processing of the Excel file.

```
    import tkinter as tk
    from tkinter import filedialog, messagebox
    import pandas as pd
    import numpy as np
    import re
    import math
    from datetime import datetime, timedelta, time
    from meteostat import Point, Daily
    from dateutil.parser import parse, ParserError
    import os

    # --- Coefficients ---
    deflections_coefficients = {
        -1500: [-1.72332931e-03, -6.57981679e-05], -1450: [-1.91547018e-03, 5.97948946e-05],
        -1400: [-0.00224689, 0.00025452], -1350: [-0.00250345, 0.00042317],
        -1300: [-0.00297204, 0.00068735], -1250: [-0.00336346, 0.0009334],
        -1200: [-0.00384288, 0.00121686], -1150: [-0.00431487, 0.00151045],
        -1100: [-0.0049304, 0.0018719], -1050: [-0.00550043, 0.00221944],
        -1000: [-0.00614255, 0.00260812], -950: [-0.00677107, 0.00299249],
        -900: [-0.00751535, 0.00344484], -850: [-0.00821798, 0.00388147],
        -800: [-0.00896932, 0.00435378], -750: [-0.00973622, 0.00483872],
        -700: [-0.01061527, 0.00538097], -650: [-0.01144062, 0.00591624],
        -600: [-0.01235425, 0.00649639], -550: [-0.01322211, 0.00706371],
        -500: [-0.01421658, 0.00769987], -450: [-0.01516518, 0.00832189],
        -400: [-0.01608215, 0.00894385], -350: [-0.01699755, 0.00956582],
        -300: [-0.01780887, 0.01015199], -250: [-0.01841931, 0.01065557],
        -200: [-0.01874189, 0.01102491], -150: [-0.01884194, 0.01127219],
        -100: [-0.01855887, 0.01128425], -50: [-0.01806349, 0.01108676],
        0: [-0.01750139, 0.01073122], 50: [-0.0169511, 0.01028671],
        100: [-0.01629908, 0.00976141], 150: [-0.0154275, 0.00913843],
        200: [-0.01462867, 0.00856224], 250: [-0.01385949, 0.00800235],
        300: [-0.01293665, 0.00739955], 350: [-0.01208462, 0.00683406],
        400: [-0.0113222, 0.00632298], 450: [-0.01055013, 0.00581497],
        500: [-0.00972699, 0.00529723], 550: [-0.00901798, 0.00483751],
        600: [-0.00828696, 0.00437904], 650: [-0.00752683, 0.00391731],
        700: [-0.00685844, 0.00350581], 750: [-0.00619337, 0.00309949],
        800: [-0.00558824, 0.00273055], 850: [-0.00496443, 0.00235541],
        900: [-0.00434607, 0.00198501], 950: [-0.00370838, 0.00162089],
        1000: [-0.00323916, 0.00133687], 1050: [-0.00257091, 0.00095774],
        1100: [-0.00211645, 0.00068621]
    }

    slopes_coefficients = {
        -1500: [-0.00893569, 0.00409044], -1450: [-0.00990098, 0.00465002],
        -1400: [-0.01106082, 0.00531073], -1350: [-0.01220147, 0.00598219],
        -1300: [-0.01336291, 0.00666664], -1250: [-0.01452274, 0.00736497],
        -1200: [-0.01559663, 0.00803121], -1150: [-0.01682631, 0.00877281],
        -1100: [-0.0180045, 0.00950132], -1050: [-0.01926202, 0.0102704 ],
        -1000: [-0.02051682, 0.01106099], -950: [-0.02183936, 0.01189298],
        -900: [-0.02324055, 0.0127769 ], -850: [-0.02468308, 0.01369787],
        -800: [-0.02624796, 0.01468332], -750: [-0.02780398, 0.01568201],
        -700: [-0.02951375, 0.01677303], -650: [-0.03139499, 0.01795264],
        -600: [-0.03322564, 0.01913623], -550: [-0.03513801, 0.0203727 ],
        -500: [-0.03719341, 0.02171005], -450: [-0.03936045, 0.02311982],
        -400: [-0.03883139, 0.02337173], -350: [-0.04354467, 0.026011  ],
        -300: [-0.0454247, 0.02744091], -250: [-0.04687461, 0.02874101],
        -200: [-0.04835013, 0.03012772], -150: [-0.05654052, 0.03510831],
        -100: [ 0.27000436, -0.09720482], -50: [-0.03445901, 0.02914409],
        0: [-0.03525687, 0.02355705], 50: [-0.03634881, 0.023317  ],
        100: [-0.03587244, 0.02243099], 150: [-0.03471666, 0.02131283],
        200: [-0.03320223, 0.02011345], 250: [-0.03146552, 0.01887794],
        300: [-0.02978668, 0.0177181 ], 350: [-0.0282354, 0.01665362],
        400: [-0.0267234, 0.01563969], 450: [-0.02525537, 0.01467039],
        500: [-0.02381247, 0.01373621], 550: [-0.02249098, 0.0128683 ],
        600: [-0.02121317, 0.01204483], 650: [-0.02005622, 0.01129616],
        700: [-0.01888153, 0.01055463], 750: [-0.01772607, 0.00982778],
        800: [-0.01668869, 0.00917372], 850: [-0.01578334, 0.0085896 ],
        900: [-0.01477796, 0.00797485], 950: [-0.01390433, 0.00743915],
        1000: [-0.01298104, 0.00688781], 1050: [-0.01209667, 0.00634325],
```

```
        1100: [-0.01125608, 0.0058265 ]
    }

    # --- Date/Time Parsing (Inlined from date_parser.py) ---
    def safe_parse_date(value):
        """
        Attempts to parse a date from string, timestamp, or other formats.
        Returns a date object or None if parsing fails.
        """
        try:
            return parse(str(value)).date()
        except (ParserError, ValueError, TypeError):
            return None

    def safe_parse_time(value):
        """
        Converts a time value into decimal hours.
        Accepts time strings ("HH:MM:SS"), datetime.time objects, datetime objects,
        pandas Timestamps, or Excel float values (e.g., 0.5 = 12:00).
        Returns float or None.
        """
        try:
            if isinstance(value, (datetime, pd.Timestamp)):
                time_val = value.time()
                return time_val.hour + time_val.minute / 60 + time_val.second / 3600
            elif isinstance(value, time):
                return value.hour + value.minute / 60 + value.second / 3600
            elif isinstance(value, str):
                if not value.strip():
                    return None
                parsed = datetime.strptime(value.strip(), "%H:%M:%S").time()
                return parsed.hour + parsed.minute / 60 + parsed.second / 3600
            elif isinstance(value, (int, float)):
                if 0 <= value < 1:
                    total_seconds = value * 24 * 3600
                    return total_seconds / 3600
                else:
                     return None
            else:
                return None
        except Exception:
            return None

    # --- Coefficient Interpolation  ---
    def interpolate_or_pass(x, coef_dict):
        """
        Interpolates coefficients for a given position 'x' using the provided dictionary.
        Returns a list [c0, c1] or None if x is outside the range of keys.
        """
        if x is None:
            return None
        keys = sorted(coef_dict.keys())
        if not keys or x < keys[0] or x > keys[-1]:
            return None
        c0 = np.interp(x, keys, [coef_dict[k][0] for k in keys])
        c1 = np.interp(x, keys, [coef_dict[k][1] for k in keys])
        return [c0, c1]

    # --- Position Extraction ---
    def extract_lambda(col_name):
        """Extracts the integer offset from deflection column names like 'D-200 [µm]' or 'D300 [µm]'."""
        col_parts = re.findall(r'D(-?\d+) \[.*?\]', col_name)
        if col_parts:
            try:
                return int(col_parts[0])
            except ValueError:
                return None
        return None
```

```
    def extract_slope(col_name):
        """Extracts the offset (as integer * 1000) from slope column names like 'Slope 0.300 [µm/m]'."""
        col_parts = re.findall(r'Slope (-?\d+\.\d+) \[.*?\]', col_name)
        if col_parts:
            try:
                # Convert to float first, then multiply and convert to int
                return int(float(col_parts[0]) * 1000)
            except ValueError:
                return None
        return None

    def get_avg_temperature(latitude, longitude, date_value):
        """Fetches previous day's average air temperature using Meteostat."""
        if pd.isna(latitude) or pd.isna(longitude) or pd.isna(date_value):
            print(f"Skipping weather fetch: Invalid input detected - Lat: {latitude}, Lon: {longitude},
    Date Value: {date_value}")
            return np.nan
        try:
            date_obj = parse(str(date_value))
            point = Point(latitude, longitude)
            previous_day_dt = date_obj - timedelta(days=1)
            data = Daily(point, start=previous_day_dt, end=previous_day_dt).fetch()
            if not data.empty and 'tavg' in data and pd.notna(data['tavg'].iloc[0]):
                return data['tavg'].iloc[0] # Return scalar value
            else:
                print(f"Warning: No weather data found or 'tavg' missing for {latitude}, {longitude} on
    {previous_day_dt.date()}")
                return np.nan # Return NaN if no data or temp is missing
        except Exception as e:
            print(f"ERROR fetching weather for Lat: {latitude}, Lon: {longitude}, Raw Date: {date_value}:
    {type(e).__name__} - {e}")
            return np.nan

    def BELLS2(sIR, sTime, sDepth, sPrevDayAir):
        """
        BELLS2 Model for estimation of asphalt temperature at sDepth.
        Returns temperature in Celsius or np.nan on error.
        """
        try:
            if pd.isna(sIR) or pd.isna(sTime) or pd.isna(sDepth) or pd.isna(sPrevDayAir) or sDepth <= 0:
                return np.nan
            sDecHrs = float(sTime)
            cPI = math.pi
            time_for_sin155 = sDecHrs + 24 if sDecHrs < 5 else sDecHrs
            sSin155 = math.sin(2 * cPI * (time_for_sin155 - 15.5) / 18) if 11 <= time_for_sin155 < 29 else
    -1

            time_for_sin135 = sDecHrs + 24 if sDecHrs < 3 else sDecHrs
            sSin135 = math.sin(2 * cPI * (time_for_sin135 - 13.5) / 18) if 9 <= time_for_sin135 < 27 else
    -1

            sTd = 2.78 + 0.912 * sIR
            log_depth_term = math.log10(sDepth) - 1.25
            sFirstBracket = -0.428 * sIR + 0.553 * sPrevDayAir + 2.63 * sSin155
            sLastTerm = 0.027 * sIR * sSin135
            result = sTd + log_depth_term * sFirstBracket + sLastTerm

            return result

        except (ValueError, TypeError, OverflowError):
            return np.nan

    def process_excel(input_file_path):
        """
        Reads an Excel file, performs temperature normalization, and saves the results.
        """
        output_file_path = filedialog.asksaveasfilename(
            defaultextension=".xlsx",
            filetypes=[("Excel files", "*.xlsx")],
```

```
            title="Save Processed File As"
        )
        if not output_file_path:
            messagebox.showinfo("Cancelled", "File processing cancelled.")
        try:
            try:
                df = pd.read_excel(input_file_path, sheet_name='Data')
                print("Read data from sheet 'Data'.")
            except ValueError: # Sheet 'Data' not found
                 print("Sheet 'Data' not found. Reading the first sheet.")
                 df = pd.read_excel(input_file_path, sheet_name=0)
            # --- Input Validation ---
            required_cols = [
                'SURVEY_DATE', 'SURVEY_TIME', 'Latitude [dd.dddd]', 'Longitude [dd.dddd]',
                'Temp Road (°C)', 'AC thickness (mm)', 'Ref Temp (°C)' # Assuming Ref Temp is a column
            ]
            print(f"Checking for required columns: {required_cols}")
            missing_cols = [col for col in required_cols if col not in df.columns]
            if missing_cols:
                messagebox.showerror("Error", f"Missing required columns in the input file:\n{',
'.join(missing_cols)}")
                return
            print("All required columns found.")

            # Identify deflection and slope columns using the extraction functions
            deflection_cols = [c for c in df.columns if extract_lambda(c) is not None]
            slope_cols = [c for c in df.columns if extract_slope(c) is not None]
            print(f"Found {len(deflection_cols)} deflection columns and {len(slope_cols)} slope columns.")

            if not deflection_cols and not slope_cols:
                 messagebox.showerror("Error", "No deflection or slope columns found matching expected
patterns (e.g., 'D0 [µm]', 'Slope 0.300 [µm/m]'). Check column names.")
                 return

            # --- Data Preparation ---
            print("Parsing dates and times...")
            df['Decimal Time'] = df['SURVEY_TIME'].apply(safe_parse_time)
            time_errors = df['Decimal Time'].isnull().sum()
            error_messages = []
            if time_errors > 0:
                 error_messages.append(f"Could not parse SURVEY_TIME for {time_errors} rows.")
            if error_messages:
                 messagebox.showwarning("Parsing Warnings", "\n".join(error_messages) + "\nThese rows may
have issues during processing.")

            # --- Calculations ---
            print("Fetching previous day air temperatures...")
            df['prev_day_air Temperature'] = df.apply(
                lambda row: (
                    get_avg_temperature( # Call the function
                        row['Latitude [dd.dddd]'], row['Longitude [dd.dddd]'], row['SURVEY_DATE']
                    )
                ),
                axis=1
            )
            nan_weather_count = df['prev_day_air Temperature'].isnull().sum()
            if nan_weather_count > 0:
                warning_msg = f"Could not retrieve previous day air temperature for {nan_weather_count}
out of {len(df)} rows."
                if nan_weather_count == len(df):
                    warning_msg += " Check coordinates, dates, internet connection, or Meteostat service."
                else:
                    warning_msg += " Check specific rows for invalid coordinates/dates or network issues
during fetch."
                warning_msg += " Proceeding without this data might lead to errors."
                messagebox.showwarning("Weather Data Warning", warning_msg)
                print(warning_msg)

            print("Calculating mid-depth temperatures...")
```

```
            df['AC_mm_numeric'] = pd.to_numeric(df['AC thickness (mm)'], errors='coerce')
            df['Mid_Depth_mm'] = df['AC_mm_numeric'] / 2
            df['Mid_Depth_mm'] = df['Mid_Depth_mm'].apply(lambda x: x if pd.notna(x) and x > 0 else
    np.nan)

            df['MID-DEPTH Temp (°C)'] = df.apply(
                lambda row: BELLS2(row['Temp Road (°C)'], row['Decimal Time'], row['Mid_Depth_mm'],
    row['prev_day_air Temperature']),
                axis=1
            )
            nan_mid_depth_count = df['MID-DEPTH Temp (°C)'].isnull().sum()
            if nan_mid_depth_count > 0:
                warning_msg = f"Could not calculate MID-DEPTH Temp (°C) for {nan_mid_depth_count} out of
    {len(df)} rows."
                if nan_mid_depth_count == len(df):
                     warning_msg += " Check input temperatures, AC thickness, time, and previous day air
    temp."
                warning_msg += " Correction might fail for these rows."
                messagebox.showwarning("Mid-Depth Temp Warning", warning_msg)
                print(warning_msg)
            print("Applying temperature correction...")
            correction_errors = 0
            total_points = len(df) * (len(deflection_cols) + len(slope_cols))

            output_df = df.copy()
            # Add "Original" columns first
            for col in deflection_cols + slope_cols:
                 if col in output_df.columns:
                     output_df[f"Original {col}"] = output_df[col]
                 else:
                     print(f"Warning: Column '{col}' identified for correction but not found in DataFrame
    during copy.")
            for col in deflection_cols + slope_cols:
                if col not in df.columns: continue

                is_slope = col.startswith("Slope")
                new_col_name = f"Temp-Corrected {col}"
                coef_dict = slopes_coefficients if is_slope else deflections_coefficients
                extract_func = extract_slope if is_slope else extract_lambda

                corrected_values = []
                for index, row in df.iterrows():
                    original_value = row[col]
                    mid_temp = row['MID-DEPTH Temp (°C)']
                    ref_temp = row['Ref Temp (°C)']
                    ac_thk  =  row['AC_mm_numeric']
                    pos_val = extract_func(col)

                    corrected_val = np.nan if pd.isna(original_value) else original_value

                    if pd.notna(original_value) and pd.notna(mid_temp) and pd.notna(ref_temp) and
    pd.notna(ac_thk) and ac_thk > 0:
                        coef = interpolate_or_pass(pos_val, coef_dict)
                        if coef:
                            try:
                                log_ac = np.log10(ac_thk)
                                exponent_ref = coef[0] * ref_temp + coef[1] * ref_temp * log_ac
                                exponent_mid = coef[0] * mid_temp + coef[1] * mid_temp * log_ac

                                if np.isfinite(exponent_ref) and np.isfinite(exponent_mid):
                                    term_ref = 10 ** exponent_ref
                                    term_mid = 10 ** exponent_mid
                                    if np.isfinite(term_ref) and np.isfinite(term_mid) and term_mid != 0:
                                        factor = term_ref / term_mid
                                        if np.isfinite(factor):
                                            corrected_val = original_value * factor
                                        else:
                                            corrected_val = np.nan; correction_errors += 1
                                    else:
```

```
                                    corrected_val = np.nan; correction_errors += 1
                            else:
                                corrected_val = np.nan; correction_errors += 1
                        except (ValueError, OverflowError, ZeroDivisionError):
                            corrected_val = np.nan; correction_errors += 1
                    else:
                        corrected_val = np.nan; correction_errors += 1
                elif pd.notna(original_value):
                    correction_errors += 1
                    corrected_val = np.nan # Set to NaN as correction failed

                corrected_values.append(corrected_val)

            output_df[new_col_name] = corrected_values # Add corrected column to output_df
        output_df = output_df.drop(columns=deflection_cols + slope_cols, errors='ignore')

        # --- Final Output ---
        print("Saving results...")
        if correction_errors > 0:
            successful_corrections = total_points - correction_errors

            warning_detail = (
                f"Temperature correction applied successfully for {successful_corrections} data
points.\n\n"
                f"Calculation was skipped for {correction_errors} out of {total_points} data
points.\n\n"
                "Common reasons for skips/failures include:\n"
                "- Sensor position is outside the range covered by the coefficients.\n"
                "- Invalid inputs (e.g., missing temps, AC thickness ≤ 0).\n" # Using ≤ symbol
                "- Math errors during calculation.\n\nResult set to NaN in affected cells.")
            messagebox.showwarning("Correction Warnings", warning_detail)

        # Write results to Excel
        with pd.ExcelWriter(output_file_path) as writer:
            output_df.to_excel(writer, index=False, sheet_name='Processed Data')
            # Write coefficients used
            used_deflection_coeffs_df = pd.DataFrame.from_dict(deflections_coefficients,
orient='index', columns=['Coefficient 1', 'Coefficient 2'])
            used_deflection_coeffs_df.index.name = 'Lambda'
            used_slope_coeffs_df = pd.DataFrame.from_dict(slopes_coefficients, orient='index',
columns=['Coefficient 1', 'Coefficient 2'])
            used_slope_coeffs_df.index.name = 'Delta_x1000' # More descriptive name
            used_deflection_coeffs_df.to_excel(writer, sheet_name='Used Deflection Coefficients')
            used_slope_coeffs_df.to_excel(writer, sheet_name='Used Slope Coefficients')

        messagebox.showinfo("Success", f"File processing completed!\nOutput saved
to:\n{output_file_path}")

    except FileNotFoundError:
        messagebox.showerror("Error", f"Input file not found:\n{input_file_path}")
    except KeyError as e:
         messagebox.showerror("Error", f"Processing error: A required column is missing or named
incorrectly: {e}")
    except PermissionError:
         messagebox.showerror("Error", f"Permission denied. Cannot save the file
to:\n{output_file_path}\nPlease check if the file is open or if you have write permissions.")
    except Exception as e:
        # Catch-all for other unexpected errors
        messagebox.showerror("Error", f"An unexpected error occurred during
processing:\n{type(e).__name__}: {e}")
        print(f"Detailed error: {e}")

# --- Tkinter GUI Setup ---
def browse_input_file():
    """Opens a dialog to select the input Excel file."""
    file_path = filedialog.askopenfilename(
        title="Select Input Excel File",
        filetypes=[("Excel files", "*.xlsx *.xls")]
    )
```

```
        if file_path:
            input_file_entry.delete(0, tk.END)
            input_file_entry.insert(0, file_path)

    def process_file_wrapper():
        """Gets the input file path and calls the main processing function."""
        input_file_path = input_file_entry.get()
        if not input_file_path:
            messagebox.showerror("Error", "Please select an input Excel file first.")
            return
        if not os.path.exists(input_file_path):
             messagebox.showerror("Error", f"Input file not found:\n{input_file_path}")
             return
        process_button.config(state=tk.DISABLED, text="Processing...")
        app.update_idletasks() # Update UI to show disabled button
        process_excel(input_file_path)
        process_button.config(state=tk.NORMAL, text="Process File")

    # --- Create the main application window ---
    app = tk.Tk()
    app.title("Pavement Temperature Correction Tool")
    app.geometry("550x120")

    # Configure grid layout
    app.columnconfigure(1, weight=1)

    # Input File Section
    input_file_label = tk.Label(app, text="Input Excel File:")
    input_file_label.grid(row=0, column=0, padx=10, pady=10, sticky="w")

    input_file_entry = tk.Entry(app, width=50)
    input_file_entry.grid(row=0, column=1, padx=5, pady=10, sticky="ew") # Use ew for horizontal expansion

    browse_input_button = tk.Button(app, text="Browse...", command=browse_input_file)
    browse_input_button.grid(row=0, column=2, padx=10, pady=10, sticky="e")

    # Process Button
    process_button = tk.Button(app, text="Process File", command=process_file_wrapper, width=15, height=1)
    process_button.grid(row=1, column=0, columnspan=3, pady=(10, 15)) # Span across columns and add
    padding

    # --- Start the application ---
    app.mainloop()
```

Source: FHWA.

Figure 57. Python script. Source code listing for application of proposed temperature adjustment models.

USER INTERFACE

The script creates a GUI window with input fields for selecting the input Excel file, as shown in figure 58. It provides a button to browse and select the input file and includes another button to initiate the processing of the input file.

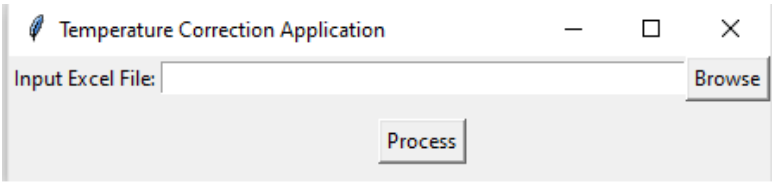

Source: FHWA.

Figure 58. Screenshot. Temperature adjustment application.

The input file should be in Excel format, and figure 59 shows a screenshot of a sample file. When preparing the sample file, consider the following guidelines:

- Ensure the Excel sheet is named 'Data.' However, the user has the option to modify the sheet name directly in the code.
- The column order can be flexible.
- Make sure the column headings align with the provided sample file: Latitude [dd.dddd], Longitude [dd.dddd], SURVEY_DATE, SURVEY_TIME, AC thickness (mm), Temp Road (°C), Ref Temp (°C). The user has the option to modify the name of the columns directly in the code. (Note: Ref = reference; Temp = temperature).
- The number of deflection columns and their units may vary, but the headings of the deflection columns must match those in the example input file. The unit inside the bracket is optional.
- The number of deflection slope columns and their units may vary, but the headings of the deflection slope columns must match those in the example input file. The unit inside the bracket is optional.

A	B	C	D	E	F	G	H	I	J	K	L	M	N	O	P	Q	R	S	T	U	V	W	X	Y	Z	AA	AB	AC
Latitude [dd.dddd]	Longitude [dd.dddd]	SURVEY_DATE	SURVEY_TIME	AC thickness (mm)	Temp Road (°C)	Ref Temp (°C)	D-450 [Âµm]	D-300 [Âµm]	D-200 [Âµm]	D0 [Âµm]	D200 [Âµm]	D300 [Âµm]	D450 [Âµm]	D600 [Âµm]	D900 [Âµm]	D1200 [Âµm]	D1500 [Âµm]	D1800 [Âµm]	Slope 1.500 [Âµm/m]	Slope 0.900 [Âµm/m]	Slope 0.600 [Âµm/m]	Slope 0.450 [Âµm/m]	Slope 0.300 [Âµm/m]	Slope 0.215 [Âµm/m]	Slope 0.130 [Âµm/m]	Slope - 0.200 [Âµm/m]	Slope - 0.300 [Âµm/m]	Slope - 0.450 [Âµm/m]
55.651542	12.118488	6/13/2023	10:00:00	160	29.429	25	324.6	385.6	423.1	428.6	321.6	268.3	209	168.5	119.1	90.4	72.1	59	-8.20407	141.54992	215.70225	320.77106	474.17151	559.25672	595.60984	-310.2385	-417.0537	-413.1645
55.651632	12.118492	6/13/2023	10:00:00	160	29.695	25	233.2	284.4	314.2	316.2	233.1	193.5	148.2	114.8	69	41.5	25	15.2	17.98286	143.14712	174.29006	258.11892	358.10422	424.95622	453.5115	-242.4584	-342.0884	-332.195
55.651722	12.118494	6/13/2023	10:00:00	160	28.899	25	243.3	282.6	301.3	294.4	231.6	198.5	155	119.3	67.9	37.5	20.5	11.2	2.14385	169.03017	192.44172	261.0932	323.46418	340.70566	337.34334	-126.0477	-240.8646	-276.4499
55.651811	12.118496	6/13/2023	10:00:00	160	29.048	25	223.6	248	257.3	247	207.1	185.5	154.7	126.8	82	51.2	31.8	19.7	20.69183	156.97697	150.26983	194.64847	219.85601	225.92377	198.56649	-32.2633	-141.0225	-196.506
55.651901	12.118498	6/13/2023	10:00:00	160	28.583	25	200	227.5	240.4	236.1	197	175.6	145.3	118.1	75.2	46	27.9	16.7	18.46245	152.95251	142.82216	182.63035	216.02853	225.96414	197.59174	-75.84228	-169.3397	-212.5237
55.651991	12.1185	6/13/2023	10:00:00	152.76	28.043	25	211.9	244.8	259.8	256	214.2	190.2	155.5	124.3	75.9	44.9	26.4	15.5	10.64696	161.53847	169.29564	214.18936	246.89559	243.67867	216.60106	-87.35303	-197.166	-253.8015
55.652081	12.118503	6/13/2023	10:00:00	141.9	28.128	25	221.5	259.9	278.9	275.9	223.4	194.1	154.3	120.5	70.4	39.9	22.6	12.6	10.32226	161.80071	185.57464	239.77009	290.21301	298.62144	281.20785	-128.0448	-240.3078	-275.7484
55.652171	12.118507	6/13/2023	10:00:00	141.9	28.713	25	210.8	250.4	270	267.5	213.1	183.6	145.3	113.8	68.1	39.9	23.3	13.3	12.40763	154.28862	165.22464	225.89024	288.05832	307.81733	290.9614	-136.9789	-246.9196	-278.4212
55.65226	12.118511	6/13/2023	10:00:00	141.9	28.593	25	226.4	256.6	269.1	260.9	217	192.2	157.7	127.3	79.4	48.2	28.8	17.2	20.73264	162.53883	166.48326	209.1561	255.31347	253.10661	226.4752	-62.941	-176.791	-231.3043

Source: FHWA.

Figure 59. Screenshot. Sample input file.

PROCESS DATA

After selecting the input file, the user clicks the *process* button and chooses the path and name for the output file. The code will then conduct the following calculations:

- Based on deflections and deflection slopes provided in input, the code selects the corresponding temperature model constants as detailed in table 9 and table 10.

- The code retrieves the average air temperature from the previous day's measurements for each row based on the provided latitude and longitude in the input file. This parameter is essential for the BELLS2 equation, which calculates the middepth temperature of the AC layer. The code uses the Meteostat Python Library (Meteostat n.d.) to retrieve the average previous air temperature used in the BELLS2 equation for each measurement point. The library accesses a wide range of meteorological data, combining information from multiple sources such as airports, weather stations, and other meteorological networks. The library then uses spatial queries to find the closest weather station to the specified latitude and longitude, retrieving the temperature from the closest station to each measuring point. The first three columns shown in figure 59 are used for extracting this parameter.

- Using the time-of-day data (column 'Time'), the AC layer thickness (column 'AC thickness (mm)'), pavement surface temperature (column 'Temp Road (°C)'), and the average air temperature from the previous day, calculated in the previous step, the BELLS2 equation is applied to estimate the middepth temperature of the AC layer for each row in the database.

- The proposed temperature adjustment model for deflections and deflection slopes (shown in figure 27 and figure 34) is then applied to each deflection and deflection slope in the input file to adjust them to the selected reference temperature. As previously mentioned, the model is designed to function with any reference temperature, which is specified in the 'Ref Temp (°C)' column.

- After processing the input file, the output file will be generated. This output file will contain the data provided in the input file along with the following parameters for each row of data:

    - The extracted average air temperature on the previous day of data collection.
    - The estimated middepth temperature of the AC layer.
    - The temperature-corrected deflections to the provided reference temperature.
    - The temperature-corrected deflection slopes to the provided reference temperature.

ACKNOWLEDGMENTS

Sincere gratitude is expressed to Susanne Baltzer from the Danish Road Department for generously collaborating in sharing the field data TSD in Denmark.

REFERENCES

AASHTO. 1993. *Guide for Design of Pavement Structures*, 4th ed. Washington, DC: AASHTO.

AASHTO. 1998. *Specification for Performance Graded Asphalt Binder,* Interim ed. MP1. Washington, DC: AASHTO.

AASHTO. 2012. *Standard Method of Test for Determining the Rheological Properties of Asphalt Binder Using a Dynamic Shear Rheometer (DSR)*. T 315-22. Washington, DC: AASHTO.

ASTM International. 1998. *Standard Practice for Viscosity-Temperature Chart for Asphalt Binders*. ASTM D2493/D2493M-16. West Conshohocken, PA: ASTM International.

FHWA. n.d. "LTPP InfoPave™" (Web portal). https://infopave.fhwa.dot.gov/, last accessed February 21, 2025.

Habbouche, J., E. Y. Hajj, P. E. Sebaaly, and N. E. Morian. 2018. "Damage Assessment for ME Rehabilitation Design of Modified Asphalt Pavements: Challenges and Findings." *Transportation Research Record* 2672, no. 40: 228–241.

Kim, Y. R., B. Underwood, M. S. Far, N. Jackson, and J. Puccinelli. 2011. *LTPP Computed Parameter: Dynamic Modulus*. Report No. FHWA-HRT-10-035. Washington, DC: Federal Highway Administration.

Levenberg, E. 2013. "Inverse Analysis of Viscoelastic Pavement Properties Using Data From Embedded Instrumentation." *International Journal for Numerical and Analytical Methods in Geomechanics* 37: 1016–1033.

Levenberg. E. 2016. "Viscoelastic Pavement Modeling With a Spreadsheet." In *Proceedings of the Eighth International Conference on Maintenance and Rehabilitation of Pavements*. Singapore, Republic of Singapore: Research Publishing Services.

Lukanen, E., R. Stubstad, and R. Briggs. 2000. *Temperature Predictions and Adjustment Factors for Asphalt Pavement*. Report No. FHWA-RD-98-085. Washington, DC: Federal Highway Administration.

Meteostat. n.d. "Python Library" (Web portal). https://dev.meteostat.net/python/#installation, last accessed May 16, 2025.

Nasimifar, M., S. Chaudhari, S. Thyagarajan, and N. Sivaneswaran. 2020. "Temperature Adjustment of Surface Curvature Index From Traffic Speed Deflectometer Measurements." *International Journal of Pavement Engineering* 21, no. 11: 1408–1418.

Nelder, J. A., and R. Mead. 1965. "A Simplex Method for Function Minimization." *Computer Journal* 7, no. 4: 308–313.

Park, S. W., and R. A. Schapery. 1999. “Methods of Interconversion Between Linear Viscoelastic Material Functions. Part I—A Numerical Method Based on Prony Series.” *International Journal of Solids and Structures* 36, no. 1: 1653–1675.

Smith, T. 1971. “Empirical Equations for Representing Viscoelastic Functions and for Deriving Spectra.” *Journal of Polymer Science Part C: Polymer Symposia* 35, no. 1: 39–50.

Spearman, C. 1904. “The Proof and Measurement of Association Between Two Things.” *The American Journal of Psychology* 15, no. 1: 72–101.

University of Nevada, Reno. 2024. *3D-Move* (software). Version 2.1. http://www.arc.unr.edu/Software.html, last accessed April 17, 2025.

Recommended citation: Federal Highway Administration,
A Study on the Influence of Asphalt Layer Temperature on TSDD-Measured Deflection Slopes and Deflections
(Washington, DC: 2026) https://doi.org/10.21949/y3fe-jw58

HRDI-1/04-26(WEB)E